AD_____

Award Number: DAMD17-98-1-8579

TITLE: Novel RNA- or Antibody-Based Strategies Targeting Growth Factors in Prostate Cancer

PRINCIPAL INVESTIGATOR: Yoko Fujita-Yamaguchi, Ph.D.

CONTRACTING ORGANIZATION: The Beckman Research Institute
Duarte, California 91010-3000

REPORT DATE: March 2001

TYPE OF REPORT: Final

PREPARED FOR: U.S. Army Medical Research and Materiel Command
Fort Detrick, Maryland 21702-5012

DISTRIBUTION STATEMENT: Approved for Public Release;
Distribution Unlimited

The views, opinions and/or findings contained in this report are those of the author(s) and should not be construed as an official Department of the Army position, policy or decision unless so designated by other documentation.

20010531 035

REPORT DOCUMENTATION PAGE

Form Approved
OMB No. 074-0188

Public reporting burden for this collection of information is estimated to average 1 hour per response, including the time for reviewing instructions, searching existing data sources, gathering and maintaining the data needed, and completing and reviewing this collection of information. Send comments regarding this burden estimate or any other aspect of this collection of information, including suggestions for reducing this burden to Washington Headquarters Services, Directorate for Information Operations and Reports, 1215 Jefferson Davis Highway, Suite 1204, Arlington, VA 22202-4302, and to the Office of Management and Budget, Paperwork Reduction Project (0704-0188), Washington, DC 20503

1. AGENCY USE ONLY (Leave blank)	2. REPORT DATE	3. REPORT TYPE AND DATES COVERED
	March 2001	Final (1 Sep 98 - 28 Feb 01)

4. TITLE AND SUBTITLE
Novel RNA- or Antibody-Based Strategies Targeting Growth Factors in Prostate Cancer

5. FUNDING NUMBERS
DAMD17-98-1-8579

6. AUTHOR(S)
Yoko Fujita-Yamaguchi, Ph.D.

7. PERFORMING ORGANIZATION NAME(S) AND ADDRESS(ES)
The Beckman Research Institute
Duarte, California 91010-300

E-Mail: yyamaguchi@coh.org

8. PERFORMING ORGANIZATION REPORT NUMBER

9. SPONSORING / MONITORING AGENCY NAME(S) AND ADDRESS(ES)
U.S. Army Medical Research and Materiel Command
Fort Detrick, Maryland 21702-5012

10. SPONSORING / MONITORING AGENCY REPORT NUMBER

11. SUPPLEMENTARY NOTES

12a. DISTRIBUTION / AVAILABILITY STATEMENT
Approved for Public Release; Distribution Unlimited

12b. DISTRIBUTION CODE

13. ABSTRACT ***(Maximum 200 Words)***

PC-3 cells expressing active IGF-II ribozymes do not grow or are prone to die under the serum-free or low serum whereas PC-3 cells expressing the inactive ribozyme or vector only grew and survived. Inhibition of IGF-II/IGFIR signaling by intracellular expression of IGF-II ribozyme only reduced endogenous IGF-II levels to ~40% of control levels. Their results not only confirmed our hypothesis that IGF-II plays a critical role in prostate cancer growth, but also suggested that complete inhibition of the IGF-II/IGFIR signaling cannot be achieved since this signaling is absolutely required for PC-3 cell growth. This is most likely the reason why we were not able to isolate stable clones.

Thus, as alternative, we tried inducible expression system and retrovirus-mediated transfer of ribozymes or αIGFIR scFvs. Inducible or transient expression, which we planned to do, did not result in good outcomes. Stable clones expressing active and inactive ribozymes from prostate cancer PC-3, LNCaP, DU145, and M12 infected by retrovirus were then isolated and characterized (manuscript in preparation). Prostate cancer cells expressing αIGFIR scFvs have been studied by a new collaborator, Dr. Sikes.

14. SUBJECT TERMS	15. NUMBER OF PAGES
Prostate Cancer	49
	16. PRICE CODE

17. SECURITY CLASSIFICATION OF REPORT	18. SECURITY CLASSIFICATION OF THIS PAGE	19. SECURITY CLASSIFICATION OF ABSTRACT	20. LIMITATION OF ABSTRACT
Unclassified	Unclassified	Unclassified	Unlimited

FOREWORD

Opinions, interpretations, conclusions and recommendations are those of the author and are not necessarily endorsed by the U.S. Army.

____ Where copyrighted material is quoted, permission has been obtained to use such material.

____ Where material from documents designated for limited distribution is quoted, permission has been obtained to use the material.

____ Citations of commercial organizations and trade names in this report do not constitute an official Department of Army endorsement or approval of the products or services of these organizations.

_X_ In conducting research using animals, the investigator(s) adhered to the "Guide for the Care and Use of Laboratory Animals", prepared by the Committee on Care and Use of Laboratory Animals of the Institute of Laboratory Resources, National Research Council (NIH Publication NO. 86-23, Revised 1985).

N/A for the protection of human subjects, the investigator(s) adhered to the policies of applicable Federal Law 45 CFR 46.

N/A In conducting research utilizing recombinant DNA, the investigator(s) adhered to the NIH Guidelines for Research Involving Recombinant DNA Molecules.

N/A In the conduct of research involving hazardous organisms, the investigator(s) adhered to the CDC-NIH Guide for Biosafety in Microbiological and Biomedical Laboratories.

Yoko Fujita Yam. 9/21/00

PI - Signature **Date**

TABLE OF CONTENTS

I INTRODUCTION

1. Overview of Work Accomplished during the 2-Year Funding Period

PC-3 cells expressing active IGF-II ribozymes do not grow or are prone to die under the serum-free or low serum whereas PC-3 cells expressing the inactive ribozyme or vector only grew and survived. Inhibition of IGF-II/IGFIR signaling by intracellular expression of IGF-II ribozyme reduced endogenous IGF-II levels only to ~40% of control levels. Their results not only confirmed our hypothesis that IGF-II plays a critical role in prostate cancer growth, but also suggested that complete inhibition of the IGF-II/IGFIR signaling cannot be achieved since this signaling is absolutely required for PC-3 cell growth. This is most likely the reason why we were not able to isolate stable clones.

Thus, as alternative, we tried inducible expression system and retrovirus-mediated transfer of ribozymes or αIGFIR scFvs. Inducible or transient expression, which we planned to do, did not work out well. Stable clones expressing active and inactive ribozymes from prostate cancer PC-3, LNCaP, DU145, and M12 infected by retrovirus were then isolated and characterized (maniscript in preparation). Prostate cancer cells expressing αIGFIR scFvs have been studied by a new collaborator, Dr. Sikes.

2. Hypothesis and Its Supporting Rationale

Prostate cancer cells could escape hormonal control by constitutively expressing growth factors such as insulin-like growth factors (IGFs). This proposal is to test the hypothesis that IGF-II/IGF receptor signaling plays an important role in prostate growth and progression.

3. Objectives and Specific Aims of the Study

RNA- or antibody-based strategies may provide novel strategies for inhibiting the expression of specific gene products that may be involved in prostate cancer cell growth and progression. To prove the proposed hypothesis, IGF-II ribozymes and single-chain antibodies against the IGF-I receptor (αIGFIR scFvs) were used. **Aim 1** tested our hypothesis using already available PC-3 prostate cancer cell transfectants and control cells. **Aim 2** took alternative approaches towards testing our hypothesis and developing novel gene and/or immunotherapy approaches for prostate cancer treatment.

4. Research Design, Study Methods, and Number of Subjects or Samples Studied

We have used stable, inducible, and transient expression systems to characterize the effect of IGF-II ribozyme or αIGFIR scFvs expression in prostate cancer cells.

Prostate cancer cells that we used included PC-3, DU145, LNCaP, M12, and others.

5. Relevance of the Proposed Work to Prostate Cancer Research

RNA- or antibody-based strategies targeting growth factors in prostate cancer have never been evaluated. The proposed studies should thus lay the foundation for the development of novel strategies for prostate cancer treatment.

II BODY

Task 1. **To evaluate the effect of intracellular expression of IGF-II ribozyme and αIGFIR scFvs on cell growth, tumorigenesis, and apoptosis in cell culture and athymic mice (Months 1-24)**

- **To test the efficacy of the ribozyme expression on prostate cancer cell growth and apoptosis (Months 1-12)**

  We evaluated the effect of the IGF-II ribozyme expression on PC-3 cell growth, which demonstrated that PC-3 cells expressing the ribozyme do not grow but tend to die under the serum-free or low serum conditions while PC-3 cells expressing the inactive ribozyme or vector only grew or survive. This demonstrated that IGF-II ribozymes were able to lower endogenous IGF-II mRNA and protein levels, thereby blocking IGF-II/IGFIR signaling and inhibiting cell growth, which has been published (1)(Xu *et al.*, Endocrinology, **140**, 2134-2144, 1999; see Enclosure Appendix 1).

  We tried to evaluate whether PC-3 cells expressing the IGF-II ribozyme are prone to apoptosis. The experiments to measure apoptosis in general, however, did not work well in our laboratory. Thus, we stopped pursuing this research direction.

- **To test the efficacy of the αIGFIR scFvs expression on prostate cancer cell growth and apoptosis (Months 1-12)**

  We lost the stable PC-3 clones expressing αIGFIR scFvs such as clones 19 and 26 shown in Fig. 3 of the original proposal. We attempted to isolate new stable PC-3 clones expressing αIGFIR scFvs, but failed to do so. Thus, we switched our strategy from stable transfection to transient transfection. During the 2nd year, we ceased working towards this aim due to the insufficiently low titer of our packaged retrovirus.

- **To purify and characterize soluble αIGFIR scFv-Fc (Months 1-6)**

  A manuscript describing purification and characterization of αIGFIR scFv-Fc has been published (Appendix 2). Briefly, αIGFIR scFv-Fc containing the human IgG_1 Fc domain was stably expressed in NSO myeloma cells using a gluytamine synthase selection system, and purified from the conditioned medium of stable clones by protein A-agrarose chromatography. Levels of αIGFIR scFv-Fc expression ranged from 40 mg/l to 100 mg/l of conditioned media. To date, we have purified nearly 600 mg of the soluble αIGFIR scFv-Fc, which has been used to characterize the effect of IGF signaling in cancer growth *in vitro* and *in vivo*. SDS-PAGE analysis under reducing and nonreducing conditions indicated that αIGFIR scFv-Fc is a dimeric antibody (2). αIGFIR scFv-Fc retained general characteristics of the parental 1H7 monoclonal antibody except that its binding affinity for IGFIR was estimated to be ~10^8 M^{-1}, which was one-order of magnitude lower than that of 1H7 monoclonal antibody.

- **To test the effect of the intracellular ribozyme expression on tumorigenesis and apoptosis in athymic mice (Months 6-24)**

  Effects of intracellular ribozyme expression on tumorigenesis have been measured using PC-3 cells expressing ribozymes, control vector, and parental PC-3 cells in athymic nude mice. Of those described in our ribozyme paper, we found that R4 and R6 lost the ribozyme expression while R39 was still expressing the ribozyme.

  Tumor growth of PC-3 cells expressing Rz or vector and parental PC-3 cells is shown in Figures 1 and 2 (Appendix 4 and 5). The results repeatedly indicated that Rz-expressing PC-3 clones, especially Rz, appear to grow *in vivo* more aggressively than control vector or parental PC-3 cells. These results are contrary to those of the *in vitro* cell growth experiments in which we showed that Rz-expressing PC-3 clones do not grow well as control PC-3 cells (1). In order to investigate this unexpected result we obtained, we are collaborating with Dr. Daisy De Leon, Loma Linda University.

To test the effect of the intracellular αIGFIR scFvs expression on tumorigenesis and apoptosis in athymic mice (Months 6-24)

Since we were not able to obtain stable PC-3 transfectants expressing αIGFIR scFvs to evaluate the effect of the intracellular αIGFIR scFvs expression on tumorigenesis and apoptosis, we first examined the effect of extracellular addition of αIGFIR scFv-Fc on PC-3 tumor growth in athymic mice. We did not find the significant effect of extracellular addition of αIGFIR scFv-Fc on PC-3 tumor growth in athymic mice (Fig. 8 in Appendix 2) while breast cancer MCF-7 tumor growth was significantly inhibited *in vivo* under the same conditions (Fig. 7 in Appendix 2). We reason that this difference is due to the level of IGFIR expression which influences IGF dependency of the cancer cells.

Task 2. **To construct and evaluate alternative ribozymes and scFvs (Months 13-30)**

- **To construct and express alternative IGF-II ribozymes (Months 13-24)**
  Retrovirus-mediated transfer to three prostate cancer cell lines PC-3, LNCaP, and M12 has been carried out to compare the effect of Rz or inactive Rz expression on prostate cancer cell growth (manuscript in preparation).

- **To construct and express additional αIGFIR scFvs (Months 13-30)**
  Retrovirus-mediated transfer of prostate cancer cell lines has been carried out to compare the effect of scFvs expression on prostate cancer cell growth. However, we did not get good results (See Alternative Task).

- **To evaluate alternative IGF-II ribozymes in cell culture (Months 18-30)**
  This part has not been started.

Alternative task

Collaboration with Dr. Robert Sikes of University of Virginia Health System, Molecular Urology and Therapeutics Program, Dept. of Urology has begun. Dr. Sikes has transduced LNCaP, C4-2, PC-3, PC-3M, DU145, and P69 cells. He will evaluate the effect of ER-retained form of αIGFIR scFv on prostate cancer progression.

III CONCLUSIONS

Intracellular expression of an active IGF-II ribozyme suppressed endogenous IGF-II mRNA and protein levels, and thereby inhibited prostate cancer PC-3 cell growth. This result is consistent with our hypothesis that IGF-II plays a critical role in prostate cancer cell growth.

We have thus far failed to obtain stable PC-3 cell transfectants expressing αIGFIR scFvs. In addition, inhibition of IGF-II/IGFIR signaling by intracellular expression of IGF-II ribozyme reduced endogenous IGF-II levels only to ~40% of the control levels, which resulted in cell growth inhibition. The results not only confirmed our hypothesis, but also suggested that complete inhibition of the IGF-II/IGFIR signaling cannot be achieved since this signaling is absolutely required for PC-3 cell growth.

Our focus for the 2nd year was the retrovirus-mediated transient expression of IGF-II ribozyme and αIGFIR scFvs to three prostate cancer cell lines in order to test the effect of IGF-II ribozyme or αIGFIR scFvs expression on cell growth. As described above, this part of the project was ongoing when P.I. made the decision to accept the offered position at Tokai University in Japan. Thus, a new collaboration with Dr. Sikes has started. As of August 2000, this project is still ongoing and making progress (Appendix 6).

IV REPORTABLE OUTCOMES

Appendix 1. Xu, Z.D., Oey, L., Mohan, S., Kawachi, M.H., Lee, N-S., Rossi, J.J., and Fujita-Yamaguchi, Y. Hammerhead ribozyme-mediated cleavage of the human insulin-like growth Factor-II Ribonucleic Acid *in vitro* and in prostate cancer cells. *Endocrinology* **140**, 2134-2144, 1999

Appendix 2. Li, S.L., Liang, S.J., Guo, N., Wu, A.M., and Fujita-Yamaguchi, Y. Single chain antibodies against human insulin like growth factor-I receptor: Expression, purification, and effect on tumor growth. *Cancer Immunol. Immunother.* **49**, 243-252, 2000

Appendix 3. Fichera, E., Liang, SJ., Xu, Z.D., Guo, N., Mineo, R., and Fujita-Yamaguchi, Y. A quantitative reverse transcription and polymerase chain reaction assay for human IGF-II allows direct comparison of IGF-II mRNA levels in cancerous breast, bladder, and prostate tissues. *Growth Hormone & IGF Res.* **10**, 61-70, 2000

Appendix 4. Mineo, R., Fichera, E., Liang, S.J., and Fujita-Yamaguchi, Y. Promoter usage for insulin-like growth Factor-II in cancerous and benign human breast, prostate, and bladder tissues, and confirmation of a 10th exon. *Biochem. Biophys. Res. Comm.* **268**, 886-892, 2000

Oral and Poster Presentations:

- 11th International Conference of Women Engineers and Scientists. Science and Technology for Global Ecology, "Application of biotechnology to the treatment of cancer." Chiba, Japan, July 24-27, 1999.
- Fujita-Yamaguchi,Y., Guo, N., Wu, A.M., Rossi, J.J., and Li, S.L. Biochemistry and Molecular Biology '99 (ASBMB). "Inhibition of breast and prostate cancer cell growth by IGF-II ribozymes and IGF-I receptor single chain antibodies". San Francisco, CA, May 16-20, 2000.
- Mineo, R., Xu, Z.D., Liang, S.J., and Fujita-Yamaguchi, Y. ENDO 81st Annual Meeting, San Diego, CA. "IGF-II levels and promoter usage in malignant and benign human breast, prostate, and bladder tissues." June 12-15, 1999.
- Fichera, E., Mineo, R., Liang, S.J., and Fujita-Yamaguchi, Y. 5th International Symposium on Insulin-like Growth Factors, Brighton, UK. "Insulin-like growth factor-II promoter usage and utilization of an additional exon 4b in malignant and benign human breast, prostate, and bladder tissues.

V REFERENCES

1. Xu, Z.D., Oey, L., Mohan, S., Kawachi, M.H., Lee, N.S., Rossi, J.J., and Fujita-Yamaguchi, Y. (1999) Hammerhead ribozyme-mediated cleavage of the human insulin-like growth factor-II RNA *in vitro* and in prostate cancer cells. *Endocrinology*, **140**, 2134-2144.

2. Li, S.L., Kato, J., Paz, B.I., Kasuya, J., and Fujita-Yamaguchi, Y. (1993) Two new monoclonal antibodies against the α subunit of the human insulin-like growth factor-I receptor. *Biochem. Biophys. Res. Comm.* **196**:92-98.

VI GRANT PERSONNEL LIST

The following is a list of the individuals who worked on grant DAMD17-98-1-8579.

Shu-Lian Li
Ning Guo
JingJing Ye
Shu-Jian Liang
Epifanio Fichera

VII APPENDICES

Appendix 1. Xu, Z.D., Oey, L., Mohan, S., Kawachi, M.H., Lee, N.S., Rossi, J.J., and Fujita-Yamaguchi, Y. Hammerhead ribozyme-mediated cleavage of the human insulin-like growth Factor-II Ribonucleic Acid *in vitro* and in prostate cancer cells. *Endocrinology* **140**, 2134-2144, 1999

Appendix 2. Li, S.L., Liang, S.J., Guo, N., Wu, A.M., and Fujita-Yamaguchi, Y. Single chain antibodies against human insulin like growth factor-I receptor: Expression, purification, and effect on tumor growth. *Cancer Immunol. Immunother.* **49**, 243-252, 2000

Appendix 3. Fichera, E., Liang, S.J., Xu, Z.D., Guo, N., Mineo, R., and Fujita-Yamaguchi, Y. A quantitative reverse transcription and polymerase chain reaction assay for human IGF-II allows direct comparison of IGF-II mRNA levels in cancerous breast, bladder, and prostate tissues. *Growth Hormone & IGF Res.* **10**, 61-70, 2000

Appendix 4. Mineo, R., Fichera, E., Liang, S.J., and Fujita-Yamaguchi, Y. Promoter usage for insulin-like growth Factor-II in cancerous and benign human breast, prostate, and bladder tissues, and confirmation of a 10^{th} exon. *Biochem. Biophys. Res. Comm.* **268**, 886-892, 2000

Appendix 5. Figures 1-2

Appendix 6. E-Mail message from Dr. Sikes

0013-7227/99/$03.00/0
Endocrinology
Copyright © 1999 by The Endocrine Society
Vol. 140, No. 5
Printed in U.S.A.

Hammerhead Ribozyme-Mediated Cleavage of the Human Insulin-Like Growth Factor-II Ribonucleic Acid *in Vitro* and in Prostate Cancer Cells*

ZHAO-DONG XU, LILY OEY, SUBBURAMAN MOHAN, MARK H. KAWACHI, NAN-SOOK LEE, JOHN J. ROSSI, AND YOKO FUJITA-YAMAGUCHI

Department of Molecular Biology (Z-D.X., L.O., N.-S.L., J.J.R., Y.F.-Y.) Beckman Research Institute of the City of Hope and Department of Urology (L.O., M.H.K.), City of Hope Medical Center, Duarte, California 91010; and Department of Biochemistry, Physiology, and Medicine (S.M.), Loma Linda University, Jerry L. Pettis Veterans Affairs Medical Center, Loma Linda, California 92357

ABSTRACT

Insulin-like growth factor (IGF)-II plays an important role in fetal growth and development. IGFs are potent mitogens for a variety of cancer cells. A paracrine/autocrine role of IGF-II in the growth of breast and prostate cancer cells has been suggested. To test the role of IGF-II in cancer cell growth, hammerhead ribozymes targeted to human IGF-II RNA were constructed. Single (R)- and double (RR)-ribozymes were catalytically active *in vitro* whereas mutant ribozymes (M or MM) did not cleave IGF-II RNA. RR was more active than R. In human prostate cancer PC-3 cells, both R and RR similarly suppressed IGF-II messenger RNA (mRNA) levels (~40%) compared with the level in parental or M-expressing PC-3 cells. Polymerase II and III promoter-driven R similarly suppressed IGF-II mRNA levels. Suppression of IGF-II mRNA levels by R was associated with suppression of IGF-II protein levels. R- (or RR-) expressing PC-3 cells did not grow under serum-starved conditions and showed prolonged doubling times in the presence of 10% FCS compared with those of parental or M-expressing cells. These results substantiated that IGF-II plays a critical role in prostate cancer cell growth. (*Endocrinology* **140:** 2134–2144, 1999)

CANCER arises as a result of a series of molecular alterations in normal cells including up-regulation of growth factors that could facilitate uncontrolled cell growth. Insulin-like growth factor (IGF)-I and -II are important mitogens for a variety of cancer cells (1). The mitogenic actions of both IGF-I and -II are mediated via the IGF-I receptor (2–4). IGF-II also binds to the IGF-II/mannose-6 phosphate receptor and insulin receptor with high affinity while IGF-I binds to these receptors with low affinity. In addition, IGF-binding proteins bind IGFs with high affinity (5) and modulate IGF actions in both a positive and negative manner. Thus, the activity of IGFs in the local tissues depend, not only on the amount of IGFs produced, but also on the type and amount of IGF system components present.

IGF-II is a 7.5-kDa single-chain polypeptide of 67 amino acid residues, which is processed from its precursor (6). Previous studies suggested that an incompletely processed form of 15-kDa IGF-II is expressed more abundantly than the 7.5-kDa form in many cancers (1, 7–9). The 15-kDa form of human IGF-II was shown to have a mitogenic potency greater than that of 7.5 kDa (10). We showed that of 36 prostate, 17 breast, 10 bladder cancers, and 9 paraganglioma tissues examined, IGF-II was expressed in more than 50% of prostate, breast, and bladder tumors, and in 100% of paraganglioma tumors (9). Greater expression of the 15-kDa IGF-II relative to the 7.5-kDa IGF-II form was clearly demonstrated in all six prostate cancers and in one of the two breast and two of the four bladder cancers examined (9). The results are consistent with the hypothesis that the 15-kDa form of IGF-II expressed in cancerous cells contributes to autocrine cancer cell growth *in vivo*.

Evidence is accumulating that an enhanced IGF/IGF-I receptor (IGFIR) signaling leads to increased cancer cell proliferation and tumorigenesis as well as antiapoptotic effects (11, 12). For example, it has been demonstrated in experimental systems that overexpression of human IGFIR promotes ligand-induced neoplastic transformation (13) and tumorigenesis (14) in the presence of an active protein tyrosine kinase. An important role of IGFIR in mediating c-Myc-induced apoptosis of fibroblasts in low serum medium was first reported (15). Since then, a series of studies supporting the antiapoptotic role of IGFIR in cancer cells have been published (16–18). In brief, reduction of the number of IGFIR by introduction of antisense IGFIR cDNA caused extensive apoptosis *in vivo* in several transplantable human or rodent tumors (16).

In the case of prostate cancer, it was originally reported that IGF-I is responsible for autocrine growth of human prostate cancer cell lines including androgen-dependent LNCaP as well as hormone-independent DU145 and PC-3 cells (19). We and others more recently showed that IGF-II, but not IGF-I, is produced in those established human prostate cancer cell lines and suggested an autocrine regulation

Received August 27, 1998.
Address all correspondence and requests for reprints to: Yoko Fujita-Yamaguchi, Ph.D., Department of Molecular Biology, Beckman Research Institute of the City of Hope, 1450 East Duarte Road, Duarte, California 91010. E-mail: yyamaguchi@coh.org.
* Supported in part by NIH Grants, CA-65767, AI-38592, and AI-29329 and DOD Grant PC-970432. This work was a part of Ph.D. dissertation of Loma Linda University graduate school for Zhao-Dong Xu, and has been presented at 80th Annual Meeting of The Endocrine Society, New Orleans, Louisiana, June 24–27, 1998.

of DU145 and PC-3 cell growth by IGF-II (20–22). Furthermore, recent studies using *in situ* hybridization and immunohistochemistry indicated that epithelial cells rather than stromal cells in prostate tumors express IGF-II *in vivo* (9, 23). These data provided the basis for using prostate cancer as a model to test the hypothesis that cancer cell growth may be regulated by IGF-II in an autocrine manner.

Blockage of IGF-II/IGFIR signaling and subsequent effects on cell growth, transformation, and tumorigenicity have been reported. Examples of strategies to block IGF-II/IGFIR signaling include 1) inhibition of IGF-II expression by antisense oligonucleotides or RNAs (24–26); 2) inhibition of IGFIR expression by antisense oligonucleotides or RNAs (19, 27–28); 3) blockage of IGFIR by IGFIR monoclonal antibody such as αIR-3 (29, 30); and 4) blockage of IGF-mediated growth by IGF-binding proteins (20, 31). In addition, a number of anticancer drug agents have been shown to work, at least in part, by suppression of IGFIR action. For instance, suramin administration to breast, lung, and prostate cancer patients significantly reduced IGF-I and -II serum levels (32). Similarly, the antiestrogen tamoxifen has a powerful cytostatic effect in breast cancer cells, which in part is due to its inhibitory effect on the IGF-I/IGFIR axis (33).

Ribozymes (RZs) are RNA enzymes that specifically cleave their respective target RNAs, thereby inhibiting the expression of specific gene products. Hammerhead-type RZs work in *cis* (intramolecularly) in nature, but separation of *cis*-acting RZs into two RNA fragments can convert them into *trans*-acting RNAs capable of site-specific cleavage of substrate RNAs. In the last 15 yr, RZs have progressed from an intriguing subject of scientific study to therapeutic agents for the potential treatment of both acquired and inherited diseases (34). It is becoming increasingly evident that RZs can serve the duel function of a tool to elucidate the functional roles of many gene products as well as therapeutic agents designed to functionally destroy deleterious RNAs. Suppression of IGF-II expression by IGF-II-specific RZs in cells has never been reported. We thus constructed catalytically active IGF-II RZs and expressed them intracellularly in human prostate cancer PC-3 cells.

Materials and Methods

Design and construction of IGF-II RZs

Two hammerhead RZs were designed and constructed to be complementary to the sequence near the translation initiation site of human prepro-IGF-II mRNA at nucleotides 16–30 and 16–46, respectively (35) (Fig. 1). As controls, activity of RZ was inactivated by introducing a point mutation of G to A in the catalytic core as shown in Fig. 1. Template DNAs for RZs and mutant RZs were prepared by filling in the opposite strands of two overlapping oligonucleotides by PCR. The oligonucleotides used for construction of the single ribozyme were 5′-ACGCGTCGACCAGCATCCT(A/G)ATGAGTCCGTGAGG-3′ (34 bases) and 5′-GCTCTAGAGCGGGGAAGTTTCGTCCTCACGGACTC-3′ (35 bases), which contained restriction enzyme *Sal*I and *Xba*I sites, respectively. The primers for the double RZs were 5′-ACGCGTCGACAGAAGGTCT(A/G)ATGAGTCCGTGAGGACGAAAGAAGCACCAGCAT-3′ (53 bases) and 5′GCTCTAGAGCGGGAAGTTT CGTCCTCACGGACTCAT(C/T)AGGATGCTGGTGCTT-3′ (52 bases), which contained restriction enzyme *Sal*I and *Xba*I sites, respectively. For both single and double RZs, the sequences that are complementary are *underlined*. Note that the position indicated as (/) represents equal ratios of both nucleotides incorporated to generate both active and inactive (mutant) RZ at the same time. The template DNAs for single and double RZ were prepared by five cycles of PCR of 94 C for 1 min, 37 C for 1.5 min, and 72 C for 1.5 min, and five cycles of PCR of 94 C for 1 min, 33 C for 1.5 min, and 72 C for 0.5 min, respectively. After the PCR, the quality of PCR products was examined by PAGE. The PCR products were cleaned up, digested with *Sal*I and *Xba*I, and subcloned into the *Sal*I/*Xba*I sites of pTZU6 + 27 vector, which contained the human U6 promoter and pUC19 multiple cloning site (36). After the ligation reaction was carried out, the ligation products were electroporated into *Escherichia coli* XL-1 blue cells. The bacteria were plated on the LB agar containing ampicillin, X-gal, and isopropyl-β-D-thiogalactopyranoside. Plasmids were prepared from white colonies, and colonies containing the correct inserts were identified by *Sal*I/*Xba*I digestion and gel electrophoresis. To confirm authenticity of the RZs, plasmid DNAs were prepared and subjected to Southern blot analysis and DNA sequencing. Clones expressing single RZ (R) and its mutant (M, an inactive RZ in which a point mutation of G5 to A is introduced), and double RZ (RR), its mutant (MM), and double RZ with one mutant, RM or MR, were isolated. These plasmids, pTZU6+27/RZ, were used for both *in vitro* transcription of RZ as well as RNA polymerase (pol) III-driven expression of the RZ in mammalian cells.

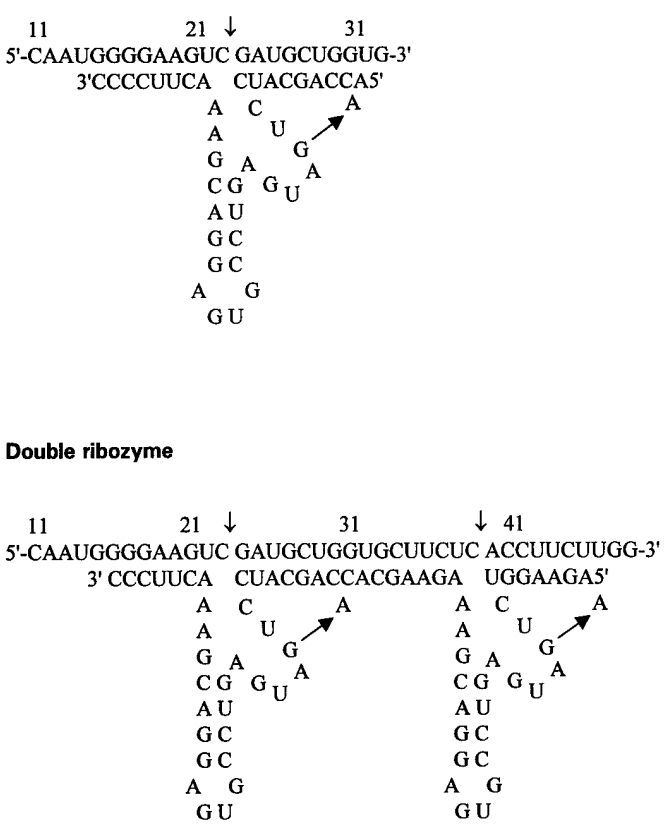

FIG. 1. Structure of the hammerhead RZ and target human IGF-II RNA. Secondary structures of single and double RZs and IGF-II substrate RNA are illustrated. Cleavage of the IGF-II substrate occurs at 3′ of the GUC or CUC as indicated with ↓. To produce an inactivated RZ, a highly conserved base, G5, in the catalytic domain, which is required for cleavage, was mutated to A as shown (G → A).

Overlapping oligonucleotides that contained *Hin*dIII or *Xba*I sites were used to produce R or M, which was subcloned into *Hin*dIII/*Xba*I sites of pcDNA3 (pcDNA3/RZ). The primers used were; 5′-GCTCTAGAGCGGGGAAGTTTCGTCCTCACGGACTC-3′ and 5′-CCCAAGCTTGGGCAGCATCCT(A/G)ATGAGTCCGTGAGG-3′, in which complementary sequences are *underlined*. The template DNAs for R or M were prepared as described for pTZU6 + 27.

Subcloning of IGF-II substrate

To test the *in vitro* cleavage efficiencies of the RZs, a substrate human IGF-II RNA [−6 to +74, 80 nucleotides (nt)] was prepared by subcloning

a small fragment of IGF-II cDNA into pBluescriptII KS(+) (Stratagene, San Diego, CA). A DNA template for the IGF-II RNA was prepared by PCR from the full-length IGF-II cDNA (9). The primers used for the PCR were: 5′-CGGAATTCCGACACCAATGGGAATCCC-3′ and 5′-CGGGATCCCGGCAGGC AGCAATGCAGCACGA3-′, which contained a restriction enzyme site, *Bam*HI and *Eco*RI, respectively. PCR was performed as follows: 95 C for 3 min, and then 30-cycle amplification of 95 C for 1 min (denaturing), 55 C for 1 min (annealing), and 72 C for 1 min (extension).

The PCR product, digested with *Bam*HI and *Eco*RI, was ligated into pBluescript KS. Transformation of the ligation mixture was achieved by electroporation. Briefly, 3 μl of the ligation mixture were electroporated into *E. coli* XL1 blue cells. After LB was added, the bacteria were incubated at 37 C for 1 h to allow the antibiotic-gene express, and then plated on LB/1.5% agar containing 100 μg/ml Ampicillin, which had been layered with 100 μl of 0.05% X-gal and 75 mM IPTG, and grown at 37 C overnight. Plasmids were prepared from white colonies and their inserts were examined by *Bam*HI/*Eco*RI double digestion and gel electrophoresis. Colonies containing the right-size insert were selected. To confirm the authenticity of the IGF-II substrate sequence, plasmid DNAs were subjected to DNA sequencing.

Preparation of IGF-II mRNA substrate by in vitro transcription

The plasmids that contained the IGF-II substrate (−6 to +74) and the full-length IGF-II were linearized by *Bam*HI digestion and used as templates for *in vitro* transcription. Transcription reactions were carried out at 37 C for 1 h in 40 mM Tris-HCl buffer, pH 7.9, containing ~0.2 μg DNA template, 0.5 U/μl of T3 RNA pol, 20 mM $MgCl_2$, 10 mM NaCl, 10 mM dithiothreitol, 0.5 mM each of ATP, GTP, and uridine triphosphate, 0.05 mM cytidine triphosphate (CTP), 10 μCi of [α-^{32}P]CTP, and 1 U/μl of RNasin (Promega Corp., Madison, WI). After transcription, the RNAs were treated with RNase-free DNase I for 15 min and purified by electrophoresis in a 6% denaturing polyacrylamide gel for 1 h at 200 V. Before purification, a small aliquot of RNAs was removed to use for calculation of the specific activity. After electrophoresis, the gel was exposed to a Kodak XRP film (Eastman Kodak Co., Rochester, NY) for 1 min and the film was developed. The region of the gel containing the desired RNA band was excised and crushed into fine pieces. The IGF-II substrate RNA was eluted in an elution buffer overnight. The aqueous phase was removed and mixed with phenol-chloroform-isoamyl alcohol (25:24:1) to extract the RNA. The substrate RNA was precipitated with ethanol, redissolved in 20 μl diethyl pyrocarbonate-treated H_2O, and stored at −75 C.

In vitro transcription of RZs

The pTZU6+27/RZ plasmids were linerarized by *Xba*I digestion and used as templates for transcription of IGF-II RZ as described for substrate RNA preparation with two exceptions: only a trace amount of the radioisotope was used and T7 RNA pol was used instead of T3 RNA pol.

In vitro RZ cleavage assays

RZ assays were performed according to the methods previously described (37, 38). Briefly, RZs and substrate were heated independently for 1 min at 90 C in 10 μl of water. After cooling to 25 C, the reaction buffer was added to a final concentration of 10 mM $MgCl_2$, 140 mM KCl, and 50 mM Tris-HCl, pH 7.5. RZs and substrate were then combined and incubated at 37 C. The reaction was stopped by adding an equal volume of stop solution (0.5% of SDS/25 mM EDTA) and then 100 μl of phenol. The aqueous phase was brought to 100 μl. After vortexing, the aqueous phase was removed and the RNAs were precipitated with ethanol. The RNAs were analyzed by 6% polyacrylamide/8 M urea gel electrophoresis. Radioactive bands were visualized by autoradiography and quantitated by a PhosphorImager (Molecular Dynamics, Inc.).

The single turnover experiments using RZ excess over substrate were carried out to determine the first-order rate constant for cleavage of the substrate (39). The initial cleavage velocities under single-turnover conditions were determined at a constant substrate concentration of 1 nM and varying RZ concentrations. Reaction mixtures (10 μl) containing 0, 2.5, 5, 10, 20, 30, and 40 nM RZ and the substrate RNA (at a final concentration of 1 nM) were incubated at 37 C for 2 h. The reaction was stopped by the addition of 10 μl of the stop solution and analyzed by PAGE as described above. K_{cat}/K_m values were obtained by plotting the remaining fraction of the ^{32}P-labeled substrate RNA (Frac S) against the ribozyme concentration ([RE]) according to the following equation $k = -\ln(\text{FracS})/t = [RE] \times k_{cat}/K_m$ where k is the observed reaction rate and t is the reaction time of 2 h.

Cell culture and transfections

Human prostate cancer PC-3 cells were transfected with pTZU6+27/RZ or pcDNA3/RZ. The calcium-phosphate precipitation method was used to cotransfect PC-3 cells with pTZU6+27/RZ expression and neo vectors (40). Briefly, 24 h before transfection, exponentially growing cells were harvested by trypsinization and replated into 90-mm tissue culture dishes. Ten milliliters of RPMI 1640 medium with 10% FCS were added, and cells were incubated overnight at 37 C in a humidified incubator in an atmosphere to 5% CO_2. To those cells, were added 0.5 ml of 0.25 M $CaCl_2$ containing 18 μg of superhelical plasmid RZ DNA, 2 μg neo Vector DNA, and 0.5 ml of 2× PBS-buffered saline. The cells were incubated for 15 min at room temperature. RPMI 1640 medium with 10% FCS was added dropwise to the cells in the dishes, which were gently swirled. The cells were incubated for 16 h at 37 C in a humidified incubator in an atmosphere of 3% CO_2. The medium was removed by aspiration, and cells were rinsed twice with medium. Ten milliliters of fresh medium were added, and cells were incubated for 24 h at 37 C in a humidified incubator in an atmosphere of 5% CO_2. After 24 h incubation in nonselective medium to allow expression of the transferred genes to occur, the cells were trypsinized and replated in medium containing 600 μg/ml of G418. The medium was changed every 3 days for 4 weeks to remove the debris of dead cells and to allow colonies of G418-resistant cells to grow.

For the RNA pol II-driven RZ expression system, PC-3 cells were transfected by electroporation. Cells were grown to 70% confluence, trypsinized for 2 min, centrifuged in the table-top centrifuge, and resuspended in PBS buffer at a cell density of 5×10^6 cells per ml. This suspension was preincubated with 5–20 μg of DNA in 800 μl of PBS buffer on ice for 10 min with mixing, transferred to a cuvette, and immediately pulsed with the following settings: capacitance, 800 μFarads; resistance (R4), R4 (72 ohm); and charging voltage, 350 V. A 4-mm gap chamber was used in a BTX electroporator (San Diego, CA). After pulsing, the cells were left in ice for 10 min, transferred into the Petri dish, and cultured in the medium containing 600 μg/ml of G418 for at least 1 month.

Detection of IGF-II RZs expressed in PC-3 cells

RZ expression in G418-resistant clones was confirmed by RT-PCR. A set of primers for detection of RZ prepared were 5′-primer, 5′-TCGCTTCGGCAGCACGTCGAC-3′, containing a sequence corresponding to the junction between U6 promoter and the RZ, and 3′-primer, 5′-GGGAAGTTTCGTCCTCACGGA-3′, containing a sequence of the catalytic stem *underlined*. RT reaction was performed at 37 C for 45 min by mixing 4 μg of total RNA from the PC-3 transformants with 10 pmol of the 3′-primer in 50 mM Tris-HCl, pH 7.5, containing 10 mM dithiothreitol, 75 mM KCl, 3 mM $MgCl_2$, 1 mM of each deoxynucleoside triphospate, 800 U of Moloney murine leukemia virus reverse transcriptase, and 20 U of RNasin. RT reaction products, equivalent to 1 μg of total RNA from each clone, were processed through 30 cycles of PCR with denaturation at 94 C for 1 min, annealing at 47 C for 2 min, and synthesis at 72 C for 3 min, in a final volume of 20 μl. One half of the reaction product was analyzed in 2% agarose gel, stained with EtBr, and blotted onto a nylon membrane. The blot was hybridized with a specific ^{32}P-labeled oligonucleotide probe, 5′-TGGTC GTAGGACTACTCA-3′ (*underline and bold* indicate the complementary sequence to the catalytic stem and the position mutated in M, respectively) at 54 C for 16 h in 6× SSC, 5× Denhardt's solution, 1% SDS, and 100 μg/ml herring-sperm DNA. The membrane was washed three times in 2× SSC and 0.1% SDS for 30 min at 51 C. The bands hybridized with the ribozyme-specific probe were visualized by autoradiography. For detection of RZ in pcDNA3/RZ clones, PT-PCR was performed under the same conditions as above using 5′-primer, 5′-CCCACTGCTTACTGGCTTATCGA-3′, and 3′-primer, 5′-GGACAGTGGGAGTGGCACCTTC-3′.

Quantitation of IGF-II mRNA levels in PC-3 cells by quantitative competitive (QC)-PCR

The 5′- and 3′-primers used to detect RZ-mediated cleavage of IGF-II RNA in cells were 5′-CCAGCACCAATGGGAAT CCCAATGGGGAAG-3′ (−10 to +21) and 5′-GTATCTGGGGAAGTTGTCCGGAAGCAC GGTC-3′ (+294 to +324), respectively. pBluescript KS/IGF2, pBluescriptII KS(+) (Stratagene, La Jolla, CA) containing approximately 1 kb *Eco*RI fragment encoding the human precursor IGF-II (911–2067 nt) (9) was used to generate a new plasmid that encodes a competitor IGF-II sequence. Detailed methods will be published elsewhere (Xu, Z.-D., R. Mineo, S.-J. Liang, and Y. Fujita-Yamaguchi, manuscript in preparation). Briefly, a 110-bp *SalI*/*SalI* fragment was inserted into the IGF-II sequence between the PCR primers so that when the competitor IGF-II RNA was transcribed, it would provide a template for a PCR product that is 110 bp longer than that derived from the authentic IGF-II mRNA. In the presence of the competitor RNA, a 444- bp band, which was therefore produced in addition to the 334-bp band derived from an endogenous IGF-II RNA.

Conditioned medium

PC-3 cells and transfectants were seeded in 25-cm^2 flasks in the regular medium. The next day, cells were washed with PBS three times and grown for 2 days in 4 ml of RPMI 1640 containing 0.1% BSA. Condition media were collected and analyzed for IGF-II and -I as previously described (22). At the time of conditioned medium collection, cell numbers were determined with a hemocytometer, and the IGF-II protein level was expressed as nanograms/ml/10^5 cells.

Determination of cell proliferation

Cell growth was determined by the 3-(4,5-Dimethylthiazol-2-yl)-2,5-diphenyltetrazolium bromide (MTT) method, which measures mitochondrial dehydrogenase activity that is active only in living cells. Cells (10^4 cells per well) were plated in 96-well plates containing 100 μl of medium and cultured 37 C for 4 days. At days 1, 2, 3, and 4, 20 μl of 0.5% MTT were added to the wells in triplicate. After incubation at 37 C for 4 h, the medium was removed and 100 μl of isopropyl alcohol supplemented with 0.05 N HCl were added. The color developed was quantitated by measuring absorbance at 540 nM.

Doubling times of parental PC-3 cells and transfectants were determined by time-lapse microscopy. Approximately 10^5 cells of each clone were seeded in medium supplemented by 10% FCS in a T-25 flasks and incubated at 37 C overnight. The flasks were placed under a phase contrast microscope (Nikon, Melville, NY) in a warm room. A good view of isolated cells was selected and video-recorded for 4 days. Doubling time for each clone was averaged from those of five to eight cell divisions.

Results

In vitro RZ cleavage reactions

Catalytic activity of the RZs constructed was examined using the shorter IGF-II RNA (−6 to +74) as a substrate unless otherwise stated.

Time course. The substrate, 7.7 nM, was incubated with 12.3 nM RZ, R or M, at 37 C for 10 to 210 min (substrate-RZ ratio of 0.6:1). As shown in Fig. 2, only the active RZ cleaved the substrate in a time-dependent manner. After incubation for 210 min, all the substrate was apparently digested by R.

Substrate-RZ ratio. RZ cleavage reactions were carried out under different substrate-RZ ratio conditions. After incubation at 37 C for 210 min, more than 80% of the substrate was cleaved by single RZ, R, at the substrate-RZ ratio of 1.2 or 0.6. In contrast, percent cleavage was markedly reduced at the substrate-excess condition.

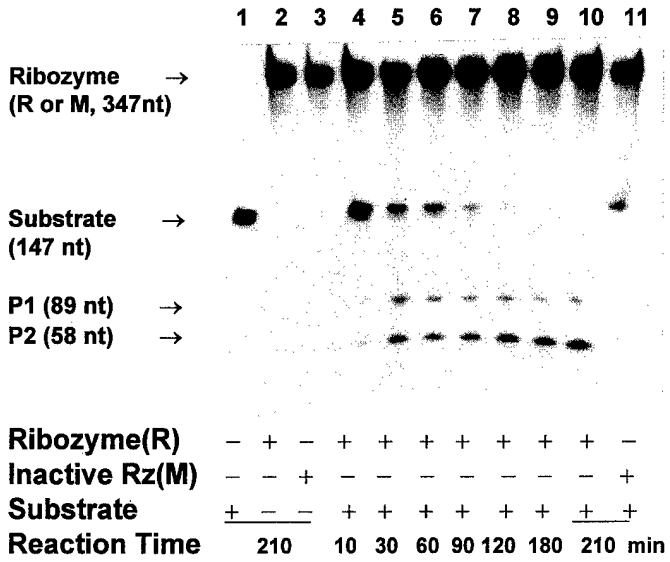

FIG. 2. Time course of RZ cleavage reaction by single RZs *in vitro*. Both RZs and substrate were ^{32}P labeled. A substrate-RZ ratio of 0.6:1 was incubated at 37 C for indicated time, 0–210 min. After cleavage reactions, RZ, substrate, and products were separated by 6% polyacrylamide/8 M urea gel electrophoresis. Nucleotide (nt) sizes of ribozymes, substrate, and products contain additional 5′-sequences derived from the vectors (see Figs. 1 and 3C for schematic illustrations). Note that the free substrate concentration after incubation for 3 h with M (lane 11) seems to become lower than the substrate only (lane 1), probably due to formation of a stable substrate/M RZ complex, which is resistant to denaturation conditions used in these studies.

In vitro cleavage reactions of single and double RZs. RZ activities of single RZ (R), double RZ (RR), its mutant (MM), and double RZs with one mutant (RM and MR) were analyzed. Figure 3A demonstrates that *in vitro* cleavage reactions of both single and double RZs produced the expected sizes of cleavage products as illustrated in Fig. 3C. Mutant double RZ (MM) did not cleave the substrate RNA at all. To compare relative cleavage efficiencies among various RZ constructs, the intensity of the product, either P1 or P1′, was quantitated. Figure 3B clearly indicates that R and RM are equally active whereas MR is less effective in cleaving the substrate IGF-II RNA than RM or R. The double RZ, RR, appeared the most active RZ of the four RZs that we constructed to target IGF-II RNA.

Comparison of RZ cleavage reactions by single and double RZs. Since the results of *in vitro* cleavage reactions suggested that RR is more active than R (Fig. 3), catalytic efficiencies of single and double RZs were further compared.

Kinetic analysis for the two RZs, R and RR, were performed under single-turnover conditions using the short IGF-II RNA substrate. The results summarized in Fig. 4 revealed K_{cat}/K_m = 1546 and 4772 $M^{-1}s^{-1}$, respectively. This indicates that the double RZ is approximately 3-fold more efficient in cleaving the substrate IGF-II RNA than the single RZ *in vitro* ($P < 0.05$).

The catalytic efficiencies of single and double RZs were also examined using the precursor IGF-II RNA (1157 nt) as a substrate. Both RZs cleaved the IGF-II RNA substrate after incubation for 16 h (Fig. 5A, lanes 11 and 12). The time course

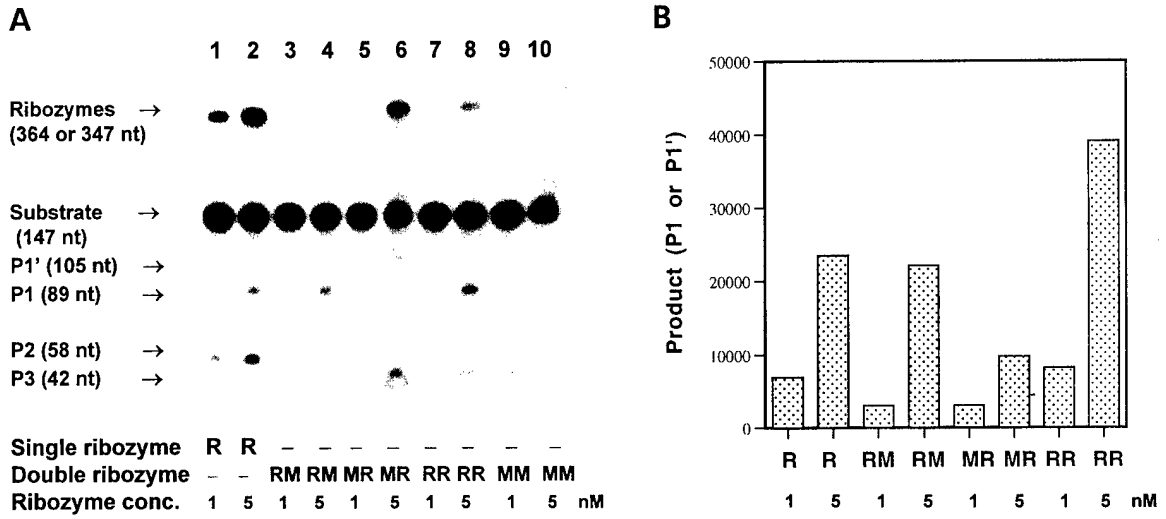

C

Ribozymes	Substrate ~~~~~~~~~~ −6 IGF-II RNA 76	Products (nt)
R	↑	89 + 58
M		147
RM	↑	89 + 58
MR	↑	105 + 42
RR	↑↑	89 + 16 + 42
MM		147

FIG. 3. Comparison of RZ cleavage reaction by single and double RZs *in vitro*. A, Autoradiogram. Cleavage reactions by single RZ (R), double RZ (RR), its mutant (MM), and double RZs with one mutant, RM or MR, were compared. Both RZs and substrate were ^{32}P labeled. Note that RZs were ^{32}P labeled with only trace amounts of radioactivity while the substrate was fully ^{32}P labeled. The differing intensities of RZs are due to differences in the levels of radioactivity incorporated during *in vitro* transcription of template encoding different RZ constructs. RZ reactions were carried out at 37 C for 210 min at a substrate concentration of 5 nM in the presence of 1 or 5 nM RZ (R, RM, MR, RR, or MM). After cleavage reactions, RZ, substrate, and products were separated by 6% polyacrylamide/8 M urea gel electrophoresis. Nucleotide (nt) sizes of the RZ, substrate, and products are indicated. B, Relative intensity of the RZ product, P1 or P1′. Cleavage efficiencies of the RZs shown in lanes 1–8 in panel A were determined by quantitating the intensity of the products, P1 or P1′. C, Schematic illustration of IGF-II RNA substrate and RZ products. The IGF-II substrate and RZ cleavage sites are presented schematically to show nt sizes of the products derived from each RZ or inactive RZ. An additional 5′-sequence which is attached to the substrate is shown as ~~~~~.

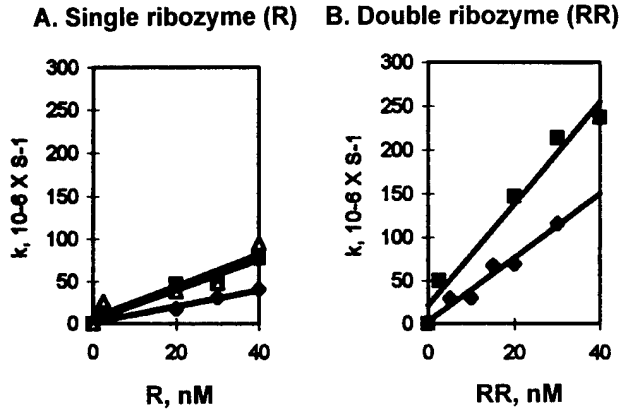

	Kcat/Km, M^{-1} s^{-1}	
	R	RR
Experiment 1 ■	1803	5840
Experiment 2 ◆	965	3704
Experiment 3 Δ	1870	
Mean ± SD*	1546 ± 411	4772 ± 1068

*P<0.05

FIG. 4. Comparison of single and double RZs *in vitro* by single-turnover experiments. Single turnover experiments with RZ in excess over substrate were carried out and K_{cat}/K_m values were calculated as described in *Materials and Methods*. In Exps 1 and 2, R and RR were assayed in parallel.

experiment, however, revealed that during the first 3 h of incubation, RR cleaved the substrate in a time-dependent manner whereas R did not appear significantly to cleave the substrate (Figs. 5A, lanes 1–8, and Fig. 5B). This result is consistent with that of the kinetic analysis that indicated that RR is more active than R *in vitro*.

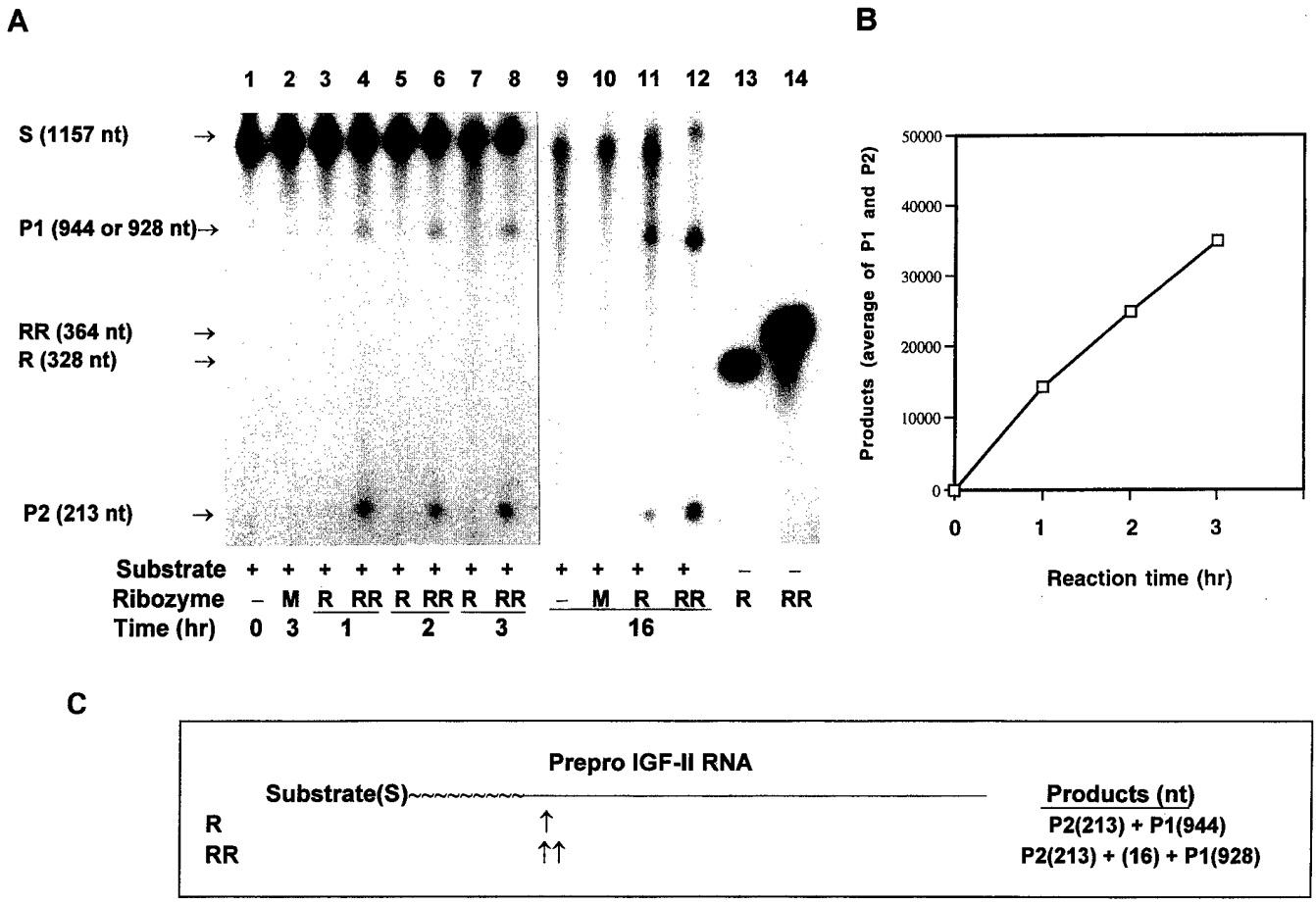

FIG. 5. RZ cleavage reaction by single and double RZs *in vitro* using the precursor IGF-II RNA as a substrate. A, Autoradiogram. Prepro-IGF-II RNA (1157 nt) was synthesized from BluescriptII KS encoding the prepro-IGF-II cDNA. Both RZs and substrate were ^{32}P labeled. RZ reactions were carried out 37 C for 1–16 h at a substrate concentration of 15 nM with 1.2 mM single or double RZ. The results of two independent experiments are shown; lanes 1–8 and lanes 9–14 are from Exp 1 and 2, respectively. B, Relative intensity of the RZ products. Cleavage reaction by RR was shown as average of P1 and P2 produced after incubation of 1, 2, and 3 h. C, Schematic illustration of IGF-II RNA substrate and RZ products. RZ cleavage sites and expected products are schematically presented.

Intracellular cleavage of IGF-II mRNA by RZs

Intracellular activity of the RZs was determined in PC-3 cells that were stably expressing RZs. Two expression systems that use RNA pol III and II were used in this study. While RNA pol II expression systems have been developed for years and widely used for the expression of proteins, RNA pol III expression systems have been suggested to be advantageous for stable, high steady-state expression of short chimeric RNAs since RNA pol III-driven chimeric transcripts are more abundant than poly(A)$^+$ RNAs in mammalian cells (41).

Stable expression of RZs in PC-3 cells driven by RNA Pol III promoter (pTZU6+27 vector).

Detection of RZ mRNA in PC-3 cell transfectants. Expression of R, M, and RR in four, two, and two transfectants, respectively, was confirmed by EtBr-stained agarose gel electrophoresis of RT-PCR products prepared from DNase I-treated RNA (data not shown). No PCR amplification was made when PCR was performed from the corresponding RNA preparations without RT (data not shown). RT-PCR products derived from single and double RZs migrated at the same positions as PCR controls for R and RR, respectively, prepared from the plasmids encoding R and RR (data not shown). The authenticity of R, M, and RR was confirmed by Southern blot analysis using an oligonucleotide probe complementary to the R sequence (data not shown). The mutant RZ did not hybridize with the R-specific probe at 54 C due to a one-base mismatch in the probe sequence.

Quantitation of IGF-II mRNA levels in PC-3 cell transfectants. IGF-II mRNA levels in parental and transfected PC-3 cells were determined by QC-PCR using a competitive IGF-II RNA as a control (Fig. 6A). Endogenous IGF-II mRNA levels in PC-3 cells expressing R or RR were suppressed by 62% or 68%, on average, compared with that of parental PC-3 cells, whereas cells expressing M had little effect (12% suppressed) on the IGF-II mRNA levels (Fig. 6, A and B) as determined by quantitative RT-PCR.

Effect of RZ expression on PC-3 cell growth. The effect of intracellular expression of RZs and the subsequent reduction of IGF-II mRNA and protein levels on cell growth was eval-

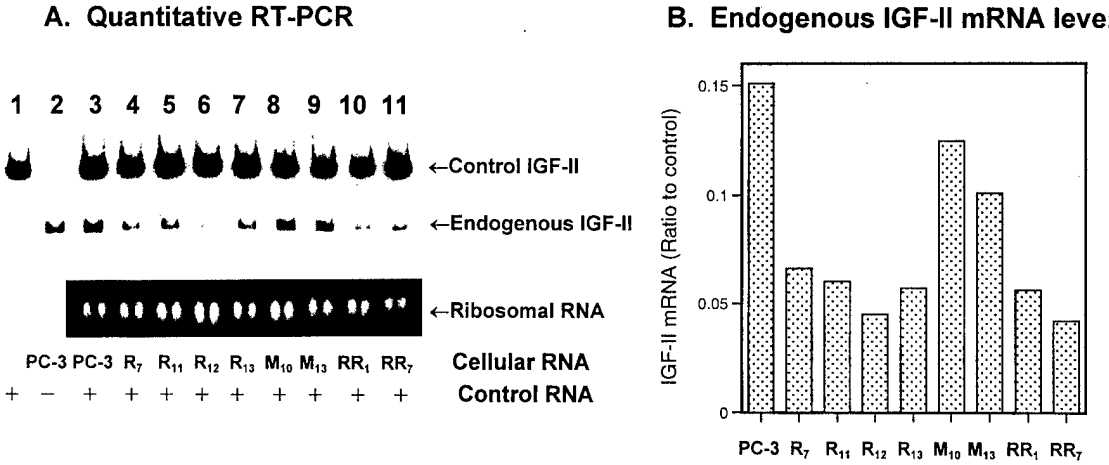

FIG. 6. PC-3 transfectants expressing single (R), double (RR) or inactive single (M) RZ under the control of Pol III promoter. A, Endogenous IGF-II mRNA levels as determined by QC-PCR. Quantitative RT-PCR was performed using IGF-II-specific primers and 1 μg of total RNA prepared from parental PC-3 cells (lane 3) and transfectants (lanes 4–11) in the presence of a competitor IGF-II RNA (110 bp longer than the authentic IGF-II mRNA). Lanes 1 and 2 show PCR products from control IGF-II and PC-3 RNA, respectively. B, Endogenous IGF-II mRNA levels in parental PC-3 cells and R-, RR-, or M-expressing PC-3 cells. Endogenous IGF-II mRNA was expressed as the ratio to control RNA, which is further normalized by 18S ribosomal levels shown in panel A.

TABLE 1. Effect of RZ expression on PC-3 cell growth

	Relative cell growth after 2 days in SFM (mean ± SE)[a]
Parental PC-3 cells	1.23 ± 0.02 (n = 2)
R-expressing PC-3 cells	0.58 ± 0.13 (n = 5)[b]
RR-expressing PC-3 cells	0.4 (n = 1)
M-expressing PC-3 cells	1.61 ± 0.33 (n = 2)

PC-3 cells and transfectants were plated in 24-well plates (1.3×10^4 cells per well), and cell numbers were counted after 2 day-culture in serum-free medium. Cell growth is expressed as a ratio of the cell number at day 2 to the original cell number seeded.

[a] The relative cell growth values are mean values of those of independently isolated stable clones. Numbers of clonally selected transfectants are indicated in *parentheses*. For parental PC-3 cells, n = 2 means two independent measurements of the cell line.

[b] Significantly different ($P < 0.01$) by Newman-Keuls post hoc test compared with parental PC-3 cells.

uated under serum-free conditions. Parental PC-3 and transfectants were grown in serum-free medium (SFM) for 2 days. While cell numbers of parental PC-3 cells or M-expressing cells increased, those of R- or RR-expressing cells decreased (Table 1), indicating that catalytically active RZ expression is inhibitory for PC-3 cell growth. These results suggest that cleavage of IGF-II mRNA by R or RR, but not the potential antisense effect of M *per se*, is required for inhibition of PC-3 cell growth.

Stable expression of RZs in PC-3 cells driven by RNA Pol II (pcDNA vector). While the transcripts expressed by the RNA pol III U6 + 27 system are nuclear (36), capped, polyadenylated RNA pol II transcripts are more likely to direct RZ transcripts to the same intracellular compartment as the targeted IGF-II mRNA in the cytoplasm. To compare RZ activity under the control of RNA pol II promoter, PC-3 cells were transfected with pcDNA3/RZ.

Detection of RZ mRNA in PC-3 cell transfectants. Of 10 transfectants examined, expression of R was confirmed in 4 independent clones by RT-PCR (Fig. 7A). EtBr-stained agarose gel electrophoresis of the RT-PCR product also identified six G418-resistant clones that do not express R. They were used as vector-control cells below.

Measurements of IGF-II mRNA and protein levels in PC-3 cell transfectants. IGF-II mRNA levels in parental and transfected cells were determined by QC-PCR (Fig. 7B). Endogenous IGF-II mRNA levels for parental, R-expressing, and vector-transfected PC-3 cells were 0.2 (n = 1), 0.045 ± 0.005 (n = 4), and 0.122 ± 0.018 (n = 6), respectively. Endogenous IGF-II mRNA levels in R-expressing PC-3 cells were thus reduced to approximately 40% level when compared with those of six transfectants that do not express R (vector-control), and to about 20% level when compared with that of parental PC-3 cells. In parallel to the IGF-II mRNA levels, IGF-II protein levels secreted into conditioned media by R-expressing PC-3 cells were significantly lower than those of parental or vector clones, while that of the vector-transfected cells was modestly reduced (Table 2)[1].

Effect of RZ expression on PC-3 cell growth as measured by the MTT method. The growth of parental PC-3 cells and the vector- or R-transfectants, shown in Fig. 7, were analyzed in SFM (Fig. 8A) or in the presence of 2% FCS (Fig. 8B). The results clearly demonstrate that PC-3 cells expressing the IGF-II RZ do not grow well under serum-free or 2% FCS conditions. The results are similar to the observation we had for R- or RR-expressing PC-3 cells under the control of RNA pol III promoter. Since the R-expressing PC-3 cells were isolated after culturing those transfectants in the medium containing 10% FCS, they must have been able to grow in the presence of 10% FCS (see time-lapse microscopy experiments below).

[1] IGF-I protein levels secreted into conditioned media by parental and PC-3 cell transfectants were determined. The IGF-I levels measured, however, were too low to be informative given that PC-3 cell IGF-I levels are below accurate levels of detection (22).

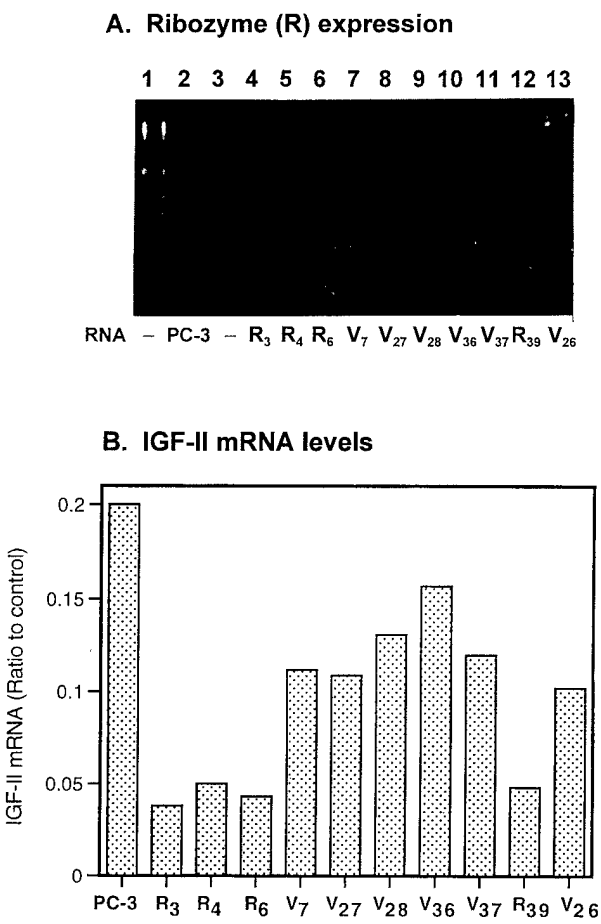

FIG. 7. Expression of RZ under the control of Pol II promoter. A, Detection of RZ expression by RT-PCR. Experiments were performed as described in Fig. 6A. B, Endogenous IGF-II mRNA levels in parental PC-3 cells, R-expressing PC-3 cells, and vector-controls as determined by QC-PCR. Experiments were performed as described in Fig. 6B. C, IGF-II protein levels in conditioned media. IGF-II protein levels in conditioned media harvested from parental cells and PC-3 cell transfectants were measured in duplicate.

Effect of RZ expression on PC-3 cell growth as measured by time-lapse microscopy. Analysis of cell division of parental PC-3 cells, vector-transfected cells (V37), and R-expressing PC-3 cells (R4, R6, and R39) revealed doubling times (mean ± SEM) of 28.3 ± 0.39 (n = 8), 32.3 ± 1.0 (n = 3), 37 ± 1.1 (n = 6), 38.6 ± 2.3 (n = 5), and 42.5 ± 2.8 (n = 2) h, respectively (Table 3). This result indicates that PC-3 cells expressing the IGF-II RZ showed a significantly prolonged doubling times compared with parental PC-3 cells, while the doubling times of vector-transfected PC-3 cells are not significantly different from those of the parental cells.

Discussion

Hammerhead RZs against human IGF-II RNA, which we have constructed, were catalytically active *in vitro*. The catalytic efficiencies, however, varied among differently designed IGF-II RZs. The results can be summarized as follows; RR > R ~ RM > MR. This indicates that the first RZ cleavage site may be a better target than the second RZ cleavage site since the cleavage of the former by R, RM, or RR was more

TABLE 2. IGF-II protein levels secreted into conditioned media

	Exp	IGF-II protein level (ng/ml/10^5 cells)
Parental PC-3 cells	1	6.22
	2	5.85
Vector-transfected PC-3 cells	1	4.07
	2	4.5
R-expressing PC-3 cells (R3)	1	2.07
	2	2.91
R-expressing PC-3 cells (R4)	1	2.95
	2	2.5
R-expressing PC-3 cells (R6)	1	2.31
	2	2.06
R-expressing PC-3 cells (R39)	1	1.07
	2	3.68

IGF-II protein levels in conditioned media harvested from parental PC-3 cells and transfectants were measured in duplicate. IGF-II protein levels in the pooled data of R-expressing PC-3 cells were significantly different ($P < 0.01$) by Newman-Keuls post hoc test compared with parental and vector-transfected PC-3 cells.

efficient than that of the later by MR. Of three double RZs examined, RR was more active than RM and MR. RR was also 3-fold more efficient in cleaving a substrate IGF-II RNA than R as judged by kinetic analysis under single-turnover conditions. Both RM and R were equally active despite the difference in the length of antisense arms, 29 and 17 nt, respectively. These results suggest that the tandem repeat of two catalytic domains enhances the catalytic efficiency of the RZ rather than the longer antisense arms. When a longer RNA substrate was used, RR was much more effective in cleaving the substrate than R. However, the cleavage of the longer substrate (1157 nt) required a much higher concentration of RR than that of the shorter substrate (147 nt). These observations are generally in good agreement with the results of previous studies that systematically analyzed the effects of catalytic core tandem repeats (42) or antisense arm lengths on RZ cleavage reactions *in vitro* (43).

Single and double RZs were stably expressed in human prostate cancer PC-3 cells under the control of RNA pol III or pol II promoter. Stable transfectants were isolated and used to determine the efficacy of the RZ activity in cells and effects of active RZs on cell growth. Establishment of quantitative assays for the target RNA was necessary for the detection of RZ cleavage reactions *in vivo* (in cell line). The QC-PCR method was used in this study because it is very sensitive, specific, and quantitative (44). In contrast to most of the RT-PCR methods that use two pairs of primers, the competitor IGF-II RNA shares the same sequences for primer binding as the target endogenous IGF-II mRNA. But, it contains an additional 110-base long insert that will give a PCR product larger than the PCR product generated from the target endogenous IGF-II mRNA. This 110-base difference in size was sufficient for easy separation of the two PCR products on denaturing polyacrylamide gels and for quantitation of the radioactive bands with a PhosphorImager (Fig. 6A). Using QC-PCR, we have clearly demonstrated that the intracellularly expressed RZs cleaved endogenous IGF-II mRNA.

Interestingly, in our study, single and double RZs showed almost the same level of efficacy in reduction of IGF-II mRNA in PC-3 cells. This observation can be explained in the fol-

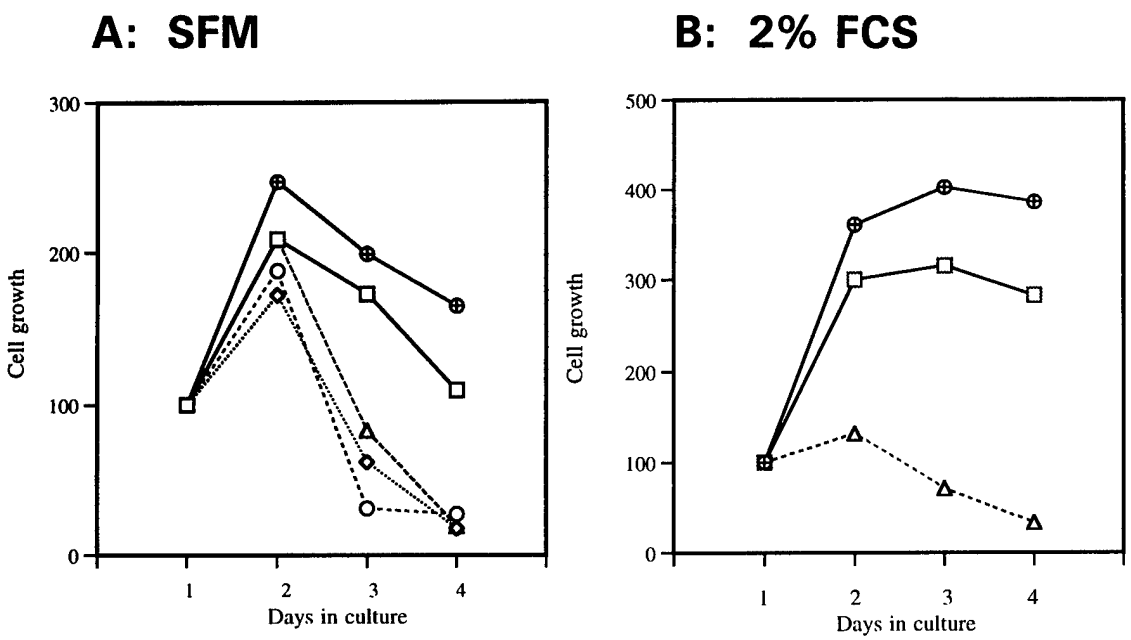

FIG. 8. Effect of RZ expression on PC-3 cell growth as measured by the MTT method. Cell growth under serum-free conditions (A) or in the presence of 2% FCS (B). Parental PC-3 cells (⊕), vector-control PC-3 cells (V37; □), R-expressing PC-3 cells (R4; ◇, R6; ○, and R39; △) were cultured either in serum-free medium (SFM) or in the presence of 2% FCS. Cell growth was determined for 4 days in triplicate by the MTT method. Growth curves are normalized by setting the OD value of day 1 as 100% for each transfectant. Shown are the representative results from three independent experiments.

TABLE 3. Effect of RZ expression on PC-3 cell growth as measured by time-lapse microscopy

	PC-3 cells	R-expressing transfectants			Vector transfectant V37
		R4	R6	R39	
Doubling time ± SEM (h)	28.3 ± 0.39	37 ± 1.1	38.6 ± 2.3	42.5 ± 2.8	32.3 ± 1.0
Doubling time (-fold) relative to parental PC-3 cells	1.00	1.31	1.36	1.50	1.14
		$P < 0.01$	$P < 0.001$	$P < 0.001$	$P > 0.05$

Cell division of parental PC-3 cells and transfectants in RPMI1640 in the presence of 10% FCS was recorded. Doubling time for each clone was calculated from five to eight divisions.

lowing ways: 1) due to unique secondary or tertiary structure caused by other cellular factors, interaction of IGF-II mRNA with the double RZ may make one of the cleavage domains unable to anneal with the substrate (second cleavage site); thus there is no cleavage reaction for that domain; or 2) the RZ-expressing clones selected may be only those that are able to moderately reduce IGF-II to a point that does not cause cell death.

Although *in vitro* studies of RZs are essential steps for quantitating their catalytic efficiencies, they cannot be used to predict the efficiency of the RZs when expressed in cells. Due to the complexity of eukaryotic gene expression, and also multiple factors involved, the RZ action in the cell is heavily influenced by the cellular environment. Factors that may interfere with RZ action in the cell include RZ expression level, colocalization of RZs with the target RNAs, location of the RZ gene relative to the target gene in the host genome, target sites at which the RZ functions, secondary structure of the target RNA or RZs, and cofactors or inhibitors such as proteins, Mg^{2+} concentration, and pH. For example, if RZ expression is not highly efficient, the level of RZs may be too low to cleave the target RNA. Even though RZs are efficiently expressed, if RZs are not in the same cell compartment with the target RNA, RZ activity would be dramatically decreased.

The secondary structure of the target RNA or RZs is also very important. Since RZs cleave the target RNA by first complementary binding to the target RNA, if the secondary structure of target RNA or RZs interferes with the binding of RZ and target, RZ activity will be reduced. Also, proteins may bind to portions of the RNA substrate or to the RZ itself and may facilitate or interfere with the catalysis. For example, previous studies demonstrated an enhancement of RZ cleavage reactions by RNA-binding proteins such as heterogeneous nuclear ribonucleoprotein A1 and the capsid protein NC7 of human immunodeficiency virus type 1 (HIV-1) (37, 45, 46). In our study, pTZU6 + 27 and pcDNA 3 vectors were used to express IGF-II RZs intracellularly under the control of RNA pol III and II, respectively. The RZ transcripts from pTZU6+27/RZ should be relatively stable and expressed in both nucleus and cytoplasm, but mainly in the nucleus (36, 47, 48). Pol III promoters, which naturally drive transfer RNA and small nuclear RNA synthesis, are good for high-level, non-tissue-specific expression of short RNAs. For example, Thompson *et al.* (41) used a transfer RNA-based RNA pol III promoter-driven RZ and found high accumulation of recom-

binant pol III RZ transcripts in all cell lines tested. The RZ activity was readily detectable in total RNA extracted from stably transformed human T cell lines. Michienzi *et al.* (48) used U1 small nuclear RNA chimeric RZs with substrate specificity for the Rev pre-mRNA of HIV and showed that this construct caused more efficient reduction in the Rev pre-mRNA level *in vivo*. Kawasaki *et al.* (49) reported that by using a pol III-driven vector, the adenoviral-E1A-associated 300-kDa protein expression in HeLa cells was inhibited. In contrast, the RZ transcripts from pcDNA3/RZ can be ubiquitously expressed in the cytoplasm under the control of RNA pol II. Pol II promoters, including viral promoters, which are used naturally for mRNA synthesis, can allow tissue-specific expression of RZs. A disadvantage of Pol II promoters is their requirement for long coding sequences, so that the RZ sequence may be placed in long RNA molecules. This can interfere with RZ conformation.

In the present study, both pol II and pol III promoter-driven vectors similarly expressed RZs and suppressed IGF-II mRNA levels in PC-3 cells, which resulted in cell growth inhibition. It should be noted that the growth of M-expressing PC-3 cells was not affected although the M RZ could have an antisense effect. Since the *in vitro* experiments revealed formation of a stable IGF-II RNA substrate/M RZ as seen in Fig. 2, formation of the complex in cells might also take place. Our results, however, indicate that if such a complex formed in PC-3 cells, it was not sufficiently stable to inhibit cell growth. It is possible that short RNA hybrids may be destroyed by ribosome translocation or heterogeneous nuclear ribonucleoproteins (37). The different results in the growth effects observed between R and M RZs thus support the notion that the catalytic activity of R RZ is required to significantly inhibit cell growth under our experimental conditions.

Suppression of IGF-II mRNA levels by the RZs was associated with reduced IGF-II protein levels. The reduction of protein levels was, however, not as significant as that of mRNA levels. This suggests that there may be a possible difference in the regulation of two IGF-II forms, the regular 7.5-kDa form and the incompletely processed 15-kDa form. The IGF-II protein levels measured in this study reflect those of both 7.5- and 15-kDa IGF-II since the RIA used an anti-IGF-II antibody that binds both forms of IGF-II. It is possible that the expression of the 15-kDa IGF-II, which is commonly expressed in cancerous tissues, is more affected by IGF-II RZ actions while the 7.5-kDa IGF-II level may not be affected. Further analysis of the expressed IGF-II protein by immunoblotting is necessary to substantiate this possibility. It is also necessary to examine whether expression of other IGF system components including IGF-binding proteins has been changed when an active RZ is intracellularly expressed.

RZ-expressing PC-3 cells did not grow well but rather die under serum-starved conditions while they grew in the medium supplemented by 10% FCS, which was the condition used for isolation of the RZ-expressing clones. It has been shown that PC-3 cells undergo apoptosis under serum-free conditions (50), and that IGFs are antiapoptotic (15–17). Consistent with those previous studies, the results shown in Fig. 8 show that PC-3 cell and vector-control cells seem to undergo apoptosis in SFM, and that the reduction of IGF-II levels by intracellular expression of IGF-II RZs seem to stimulate apoptosis of PC-3 cells in SFM and low serum medium. Investigation on mitogenic and apoptotic pathways of R-expressing PC-3 cells are now in progress.

In conclusion, the present study demonstrated that IGF-II RZs were active at least in one cell line and were able to lower endogenous IGF-II mRNA and protein levels, and that blockage of IGF-II/IGFIR signaling by IGF-II RZs inhibited cell growth. The IGF-II RZ can thus be used as a tool to investigate the role of IGF-II in other physiological systems. The study also provided the basis for the development of IGF-II RZs as future cancer therapeutics.

References

1. **Daughaday WH** 1990 The possible autocrine/paracrine and endocrine roles of insulin-like growth factors of human tumors. Endocrinology 127:1–4
2. **LeRoith D, Werner H, Beitner-Johnson D, Roberts Jr CT** 1995 Molecular and cellular aspects of the insulin-like growth factor I receptor. Endocr Rev 16:143–163
3. **Casella SJ, Han VK, D'Ercole AJ, Svoboda ME, van Wyk JJ** 1986 Insulin-like growth factor II binding to the type I somatomedin receptor. Evidence for two high affinity binding sites. J Biol Chem 261:9268–9273
4. **Sakano K, Enjoh T, Numata F, Fujiwara H, Marumoto Y, Higashihashi N, Sato Y, Perdue JF, Fujita-Yamaguchi Y** 1991 The design, expression, and characterization of human insulin-like growth factor II (IGF-II) mutants specific for either the IGF-II/cation-independent mannose 6-phosphate receptor or IGF-I receptor. J Biol Chem 266:20626–20635
5. **Bach LA, Hsieh S, Sakano K, Fujiwara H, Perdue JF, Rechler MM** 1993 Binding of mutant of human insulin-like growth factor II to insulin-like growth factor binding proteins 1–6. J Biol Chem 268:9246–9254
6. **Daughaday W, Rotwein P** 1989 Insulin-like growth factors 1 and 2, peptide messenger ribonucleic acid, gene structures and serum and tissue concentrations. Endocr Rev 10:68–91
7. **Daughaday WH, Trivedi B** 1992 Measurement of derivative of proinsulin-like growth factor-II in serum by a radioimmunoassay directed against the E-domain in normal subjects and patients with nonislet cell tumor hypoglycemia. J Clin Endocrinol Metab 75:110–115
8. **Enjoh T, Hizuka N, Perdue JF, Takano K, Fujiwara H, Higashihashi N, Marumoto Y, Fukuda I, Sakano K** 1993 Characterization of new monoclonal antibodies to human insulin-like growth factor-II and their application in Western immunoblot analysis. J Clin Endocrinol Metab 77:510–517
9. **Li SL, Goko H, Xu ZD, Kimura G, Sun Y, Kawachi MH, Wilson TG, Wilczynski S, Fujita-Yamaguchi Y** 1998 Expression of insulin-like growth factor (IGF)-II in human prostate, breast, bladder, and paraganglioma tumors. Cell Tissue Res 291:469–479
10. **Gowan LK, Hampton B, Hill JD, Shlueter RI, Perdue JF** 1987 Purification and characterization of a unique high molecular weight form of insulin-like growth factor II. Endocrinology 121:449–458
11. **Baserga R** 1995 The insulin-like growth factor-1 receptor: a key to tumor growth? Cancer Res 55:249–252
12. **Werner H, Le Roith D** 1997 The insulin-like growth factor-I receptor signaling pathways are important for tumorigenesis and inhibition of apoptosis. Crit Rev Oncog 8:71–92
13. **Kaleko M, Rutter WG, Miller AD** 1990 Overexpression of the human insulin-like growth factor I receptor promotes ligand-dependent neoplastic transformation. Mol Cell Biol 10:464–473
14. **Prager D, Li H-L, Asa S, Melmed S** 1994 Dominant negative inhibition of tumorigenesis in vivo by human insulin-like growth factor I receptor mutant. Proc Natl Acad Sci USA 91:2181–2185
15. **Harrington EA, Bennett MR, Fanidi A, Evan GI** 1994 c-Myc-induced apoptosis in fibroblasts is inhibited by specific cytokines. EMBO J 13:3286–3295
16. **Resnicoff M, Abraham D, Yutanawiboonchai W, Rotman HL, Kajstura J, Rubin R, Zoltick P, Baserga R** 1995 The insulin-like growth factor I receptor protects tumor cells from apoptosis *in vivo*. Cancer Res 55:2463–2469
17. **Sell C, Baserga R, Rubin R** 1995 Insulin-like growth factor (IGF-1) and the IGF-1 receptor prevent etoposide-induced apoptosis. Cancer Res 55:303–306
18. **Dunn SE, Hardman RA, Kari FW, Barrett JC** 1997 Insulin-like growth factor 1 (IGF-1) alters drug sensitivity of HBL100 human breast cancer cells by inhibition of apoptosis induced by diverse anticancer drugs. Cancer Res 57:2687–2693
19. **Pietrzkowski Z, Mulholland G, Gomella L, Jameson BA, Wernicke D, Baserga R** 1993 Inhibition of growth of prostatic cancer cell lines by peptide analogues of insulin-like growth factor I. Cancer Res 53:1102–1106
20. **Figueroa JA, Lee AV, Jackson J, Yee D** 1995 Proliferation of cultured human prostate cancer cells is inhibited by insulin-like growth factor (IGF) binding

protein-1: evidence for an IGF-II autocrine growth loop. J Clin Endocrinol Metab 80:3476–3482
21. **Angelloz-Nicoud P, Binoux M** 1995 Autocrine regulation of cell proliferation by the insulin-like growth factor (IGF) and IGF binding protein-3 protease system in a human prostate carcinoma cell line (PC-3). Endocrinology 136:5485–5492
22. **Kimura G, Kasuya J, Giannini S, Honda Y, Mohan S, Kawachi MH, Akimoto M, Fujita-Yamaguchi Y** 1996 Insulin-like growth factor (IGF) system components in human prostatic cancer cell-lines: LNCaP, DU145, and PC-3 cells. Int J Urol 3:39–46
23. **Tennant MK, Thrasher JB, Twomey PA, Drivdahl RH, Birnbaum RS, Plymate SR** 1996 Protein and messenger ribonucleic acid (mRNA) for the type I insulin-like growth factor (IGF) receptor is decreased and IGF-II mRNA is increased in human prostate carcinoma compared to benign prostate epithelium. J Clin Endocrinol Metab 81:3774–3782
24. **Christofori G, Naik P, Hanahan D** 1994 A second signal supplied by insulin-like growth factor II in oncogene-induced tumorigenesis. Nature 369:414–418
25. **Florini JR, Magri KA, Ewton DZ, James PL, Grindstaff K, Rotwein PS** 1991 "Spontaneous" differentiation of skeletal myoblasts is dependent upon autocrine secretion of insulin-like growth factor-II. J Biol Chem 266:15917–15923
26. **Lin S-B, Hsieh S-H, Hsu H-L, Lai M-Y, Kan L-S, Au L-C** 1997 Antisense oligodeoxynucleotides of IGF-II selectively inhibit growth of human hepatoma cells overproducing IGF-II. J Biochem (Tokyo) 122:717–722
27. **Neuenschwander S, Roberts Jr CT, LeRoith D** 1995 Growth inhibition of MCF-7 breast cancer cells by stable expression of an insulin-like growth factor I receptor antisense ribonucleic acid. Endocrinology 136:4298–4303
28. **Resnicoff M, Coppola D, Sell C, Rubin R, Ferrone S, Baserga R** 1994 Growth inhibition of human melanoma cells in nude mice by antisense strategies to the type 1 insulin-like growth factor receptor. Cancer Res 54:4848–4850
29. **Osborne CK, Coronado EB, Kitten LJ, Arteaga CI, Fuqua SAW, Rasmasharma K, Marchall M, Li CH** 1989 Insulin-like growth factor-II (IGF-II): a potential autocrine/paracrine growth factor for human breast cancer acting via the IGF-I receptor. Mol Endocrinol 3:1701–1709
30. **Furlanetto RW, Harwell SE, Baggs RB** 1993 Effects of insulin-like growth factor receptor inhibition on human melanomas in culture and in athymic mice. Cancer Res 53:2522–2526
31. **Damon SE, Maddison L, Ware JL, Plymate SR** 1998 Overexpression of an inhibitory insulin-like growth factor binding protein (IGFBP), IGFBP-4, delays onset of prostate tumor formation. Endocrinology 139:3456–3464
32. **Miglietta L, Barreca A, Reppetto L, Constantini M, Rosso R, Boccardo F** 1993 Suramin and serum insulin-like growth factor levels in metastatic cancer patients. Anticancer Res 13:2473–2476
33. **Guvakova MA, Surmacz E** 1997 Tamoxifen interferes with the insulin-like growth factor I receptor (IGF-IR) signaling pathway in breast cancer cells. Cancer Res 57:2606–2610
34. **Rossi JJ** 1998 Therapeutic ribozymes, principles and applications. BioDrugs 9:1–10
35. **Bell GI, Merryweather JP, Sanchez-Pescador R, Stempien MM, Priestley L, Scott J, Rall LB** 1984 Sequence of a cDNA clone encoding human preproinsulin-like growth factor II. Nature 310:775–779
36. **Good PD, Krikos AJ, Li SX, Bertrand E, Lee NS, Giver L, Ellington A, Zaia JA, Rossi JJ, Engelke DR** 1997 Expression of small, therapeutic RNAs in human cell nuclei. Gene Ther 4:45–54
37. **Bertrand EL, Rossi JJ** 1994 Facilitation of hammerhead ribozyme catalysis by the nucleocapsid protein of HIV-1 and the heterogeneous nuclear ribonucleoprotein A1. EMBO J 13:2904–2912
38. **Hertel KJ, Hershlag D, Ulenbeck OC** 1994 A kinetic and thermodynamic framework for the hammerhead ribozyme reaction. Biochemistry 33:3373–3385
39. **Heidenreich O, Eckstein F** 1992 Hammerhead ribozyme-mediated cleavage of the long terminal repeat RNA of human immunodeficiency virus type 1. J Biol Chem 267:1904–1909
40. **Chen C, Okayama H** 1987 High-efficiency transformation of mammalian cells by plasmid DNA. Mol Cell Biol 7:2745–2752
41. **Thompson JD, Ayers DF, Malmstrom TA, Mckenzie TL, Ganousis L, Chowrira BM, Couture L, Stinchcomb DT** 1995 Improved accumulation and activity of ribozymes expressed from a tRNA-based RNA polymerase III promoter. Nucleic Acids Res 23:2259–2268
42. **Ohkawa J, Yuyama N, Takebe Y, Nishikawa S, Taira K** 1993 Importance of independence in ribozyme reactions: kinetic behavior of trimmed and of simply connected multiple ribozymes with potential activity against human immunodeficiency virus. Proc Natl Acad Sci USA 90:11302–11306
43. **Sioud M** 1997 Effects of variations in length of hammerhead ribozyme antisense arms upon the cleavage of longer RNA substrates. Nucleic Acids Res 25:333–338
44. **Beaudry AA, McSwiggen JA** 1995 Quantitation of ribozyme target abundance by QCPCR. Methods Mol Biol 74:1357–1364
45. **Tsuchihashi Z, Kholsla M, Herschlag D** 1993 Protein enhancement of hammerhead ribozyme catalysis. Science 262:99–102
46. **Herschlag D, Khosla M, Tsuchihashi Z, Karpel RL** 1994 An RNA chaperone activity of non-specific RNA binding proteins in hammerhead ribozyme catalysis. EMBO J 13:2913–2924
47. **Bertrand E, Castanotto D, Zhou C, Carnbonnelle C, Lee NS, Good P, Chatterjee S, Grange T, Pictet R, Kohn D, Engelke D, Rossi JJ** 1997 The expression cassette determines the functional activity of ribozymes in mammalian cells by controlling their intracellular localization. RNA 3:75–88
48. **Michienzi A, Prislei S, Bozzoni I** 1996 U1 small nuclear RNA chimeric ribozymes with substrate specificity for the Rev pre-mRNA of human immunodeficiency virus. Proc Natl Acad Sci USA 93:7219–7224
49. **Kawasaki H, Ohkawa J, Tanishige N, Yoshinari K, Murata T, Yokoyama K, Traira K** 1996 Selection of the best target site for ribozyme-mediated cleavage within a fusion gene for adenovirus E1A-associated 300 kDa protein (p300) and luciferase. Nucleic Acids Res 24:3010–3016
50. **Rajah R, Valentinis B, Cohen P** 1997 Insulin-like growth factor (IGF)-binding protein-3 induces apoptosis and mediates the effects of transforming growth factor beta1 on programmed cell death through a p53- and IGF-independent mechanism. J Biol Chem 272:12181–12188

Cancer Immunol Immunother (2000) 49:243–252

© Springer-Verlag 2000

ORIGINAL ARTICLE

Shu-Lian Li · Shu-Jian Liang · Ning Guo
Anna M. Wu · Yoko Fujita-Yamaguchi

Single-chain antibodies against human insulin-like growth factor I receptor: expression, purification, and effect on tumor growth

Received: 21 January 2000 / Accepted: 7 March 2000

Abstract Insulin-like growth factors (IGF) I and II are potent mitogens for a variety of cancer cells. The proliferative and anti-apoptotic actions of IGF are mediated by the IGF-I receptor (IGF-IR), to which both IGF-I and IGF-II bind with high affinity. To investigate the mitogenic and anti-apoptotic activities of IGF-IR and to achieve better inhibition of IGF-IR function, single-chain antibodies against human IGF-IR (αIGF-IR scFvs) were constructed and expressed. IgG cDNA encoding variable regions of light and heavy chains (V_L and V_H) from mouse IgG were cloned from a hybridoma producing the 1H7 αIGF-IR monoclonal antibody [Li et al., Biochem Biophys Res Commun 196: 92–98 (1993)]. The splice-overlap extension polymerase chain reaction was used to assemble a gene encoding the αIGF-IR scFv, including the N-terminal signal peptide, V_L, linker peptide, V_H, and C-terminal DYKD tag. Two types of soluble αIGF-IR scFvs, a prototype αIGF-IR scFv and its alternative type αIGF-IR scFv-Fc, were constructed and expressed in murine myeloma cells. αIGF-IR scFv-Fc, containing the human IgG1 Fc domain, was stably expressed in NS0 myeloma cells, using a glutamine synthase selection system, and purified from the conditioned medium of stable clones by protein-A–agarose chromatography. Levels of αIGF-IR scFv-Fc expression ranged from 40 mg/l to 100 mg/l conditioned medium. Sodium dodecyl sulfate/polyacrylamide gel electrophoresis analysis under reducing and nonreducing conditions indicated that αIGF-IR scFv-Fc is a dimeric antibody. αIGF-IR scFv-Fc retained general characteristics of the parental 1H7 monoclonal antibody except that its binding affinity for IGF-IR was estimated to be approximately $10^8\ M^{-1}$, which was one-order of magnitude lower than that of 1H7 monoclonal antibody. Injection of αIGF-IR scFv-Fc (500 μg/mouse, twice a week) significantly suppressed MCF-7 tumor growth in athymic mice. These results suggest that the αIGF-IR scFv-Fc is a first-generation recombinant αIGF-IR for the potential development of future αIGF-IR therapeutics.

Key words IGF · Recombinant antibody · Single-chain antibody · Tumor growth inhibition

S.-L. Li · S.-J. Liang · N. Guo
A. M. Wu · Y. Fujita-Yamaguchi (✉)
Department of Molecular Biology,
Beckman Research Institute of the City of Hope,
1450 East Duarte Road, Duarte, CA 91010, USA
e-mail: yyamaguchi@coh.org
Tel.: +1-626-301-8247
Fax: +1-626-301-8280

Introduction

Insulin-like growth factor I receptor (IGF-IR) belongs to the family of transmembrane protein tyrosine kinases [19, 39]. The biological actions of IGF-I and IGF-II are mediated by IGF-IR, to which both IGF-I and IGF-II bind with high affinity [32]. Triggering of IGF-IR protein tyrosine kinase by these specific ligands results in subsequent activation of signaling pathways, which lead to the proliferative and anti-apoptotic action of IGF in cells. IGF-IR plays an important role in transformation and tumorigenesis, as shown by experiments demonstrating that overexpression of IGF-IR promotes ligand-induced neoplastic transformation and tumorigenesis in the presence of an active PTK [3, 16, 29]. Conversely, it has been shown that cells lacking IGF-IR cannot be transformed by oncogenes and overexpression of other growth factors [1, 7].

Inhibition of IGF-IR function in cancer cells has been actively studied. For example, suppression of mitogenic activity of IGF and cancer cell growth inhibition have been demonstrated by either inhibition of IGF binding by the anti-IGF-IR monoclonal antibody (mAb) αIR-3 [1, 10], or inhibition of IGF-IR (or IGF-I) expression by introduction of antisense IGF-IR (or IGF-I) cDNA [23, 30, 36]. Furthermore, recent studies suggested that an increased IGF-IR function protects breast cancer cell growth from chemotherapy [9], and

that high levels of IGF-IR in breast tumors were highly correlated with local breast cancer recurrence following lumpectomy and radiation therapy [37]. Thus, development of new strategies that inhibit IGF-IR function may lead to alternative treatments in combination with chemotherapy or radiotherapy, which should effectively induce cancer growth inhibition and cancer cell death.

We have produced single-chain antibodies against human IGF-IR by using the mouse IgG cDNA cloned from a hybridoma producing 1H7 mAb [20]. In this study, two types of soluble αIGF-IR scFvs, a prototype αIGF-IR scFv and its alternative type αIGF-IR scFv-Fc, were constructed and expressed in murine myeloma cells. The second construct was prepared because we experienced an extremely low level of expression of the prototype scFv. We show that the humanized construct of αIGF-IR scFv, αIGF-IR scFv-Fc, which can be produced on a large scale, retained characteristics similar to those of the parental 1H7 mAb, and that the αIGF-IR scFv-Fc is a first-generation recombinant anti-IGF-IR for the potential development of future anti-IGF-IR therapeutics.

Materials and methods

Cloning of 1H7 variable domains by RT-PCR

Heavy and light chains of 1H7 [20] were separated by sodium dodecyl sulfate/polyacrylamide gel electrophoresis (SDS-PAGE; 12.5% polyacrylamide gel) under reducing conditions, blotted onto a polyvinylidene difluoride membrane, and subjected to N-terminal amino acid sequence determination by Edman degradation as described [42]. Degenerate oligonucleotides, used as upstream primers, were synthesized on the basis of the N-terminal amino acid sequences of heavy and light chains of 1H7 while the constant-region oligonucleotides for downstream primers were designed and synthesized according to the published nucleotide sequences [12, 13]. Primers (Table 1) containing the *Eco*RI site were used to amplify the heavy- and light-chain variable regions (V_H and V_L, respectively) from 1H7 poly(A)-rich mRNA by the reverse transcriptase/polymerase chain reaction (RT-PCR). PCR products were ligated into the *Eco*RI site of pBluescriptII SK. *Escherichia coli* XL1-Blue was transformed with the vectors encoding PCR-generated V_H and V_L sequences.

In order to verify that the variable-region genes isolated from corresponding plasmids were indeed derived from the 1H7 mAb gene, molecular masses of tryptic fragments derived from the heavy and light chains of reduced and alkylated 1H7 (20 μg) were analyzed by liquid chromatography/mass spectrometry [45].

Design of αIGF-IR antibodies

This study describes two soluble forms of 1H7-based αIGF-IR antibodies, scFv and scFv-Fc, which are schematically presented in Fig. 1. ScFv is a monovalent antibody, and has an expected M_r of 27 kDa. ScFv-Fc is a divalent antibody that contains the human IgG1 Fc domain and has an expected M_r of 120 kDa.

The gene encoding the αIGF-IR scFv was constructed using the N-terminal signal peptide derived from the mT84.66 light chain [24, 40], V_L DNA, an oligonucleotide encoding the linker peptide $(GGGGSGGGS)_2$,V_H DNA, and a C-terminal tag (including DYKD) as described [5, 6]. Figure 2 summarizes the assembly of the αIGF-IR scFv gene by splice-overlap extension PCR. The DYKD sequence (FLAG epitope tag) allowed affinity purification of recombinant proteins using the M2 anti-FLAG mAb (Eastman Kodak Co., Rochester, N.Y.). Following confirmation of the

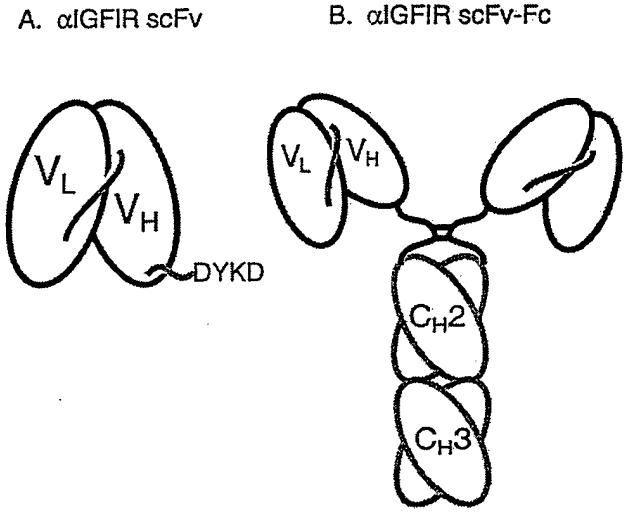

Fig. 1A, B Schematic representation of soluble forms of anti-(human insulin-like growth factor I receptor) single-chain antibodies (*αIGF-IR scFvs*). **A** Single-chain antibody (αIGF-IR scFv). **B** Chimeric αIGF-IR scFv-Fc

Table 1 Primers for polymerase chain reaction amplification of variable regions of heavy and light chains of 1H7

Light-chain primers							
Amino acid		1	2	3	4	5	6
		Asp	Ile	Val	Met	Thr	Gln
5′End primer	5′gggaattc	GAC	ATT	GTG	ATG	ACC	CAA3′
		T	C	C		A	G
						T	
C-region amino acid		Ser	Ile	Phe	Pro	Pro	Ser
		(5′ TCC	ATC	TTC	CCA	CCA	TCC3′)
C-region primer		3′ AGG	TAG	AAG	GGT	GGT	AGG cttaaggc5′
Heavy-chain primers							
Amino acid		1	2	3	4	5	6
		Glu	Val	Lys	Val	Val	Glu
5′End primer	5′gggaattc	GAA	GTA	AAA	GTA	GTA	GAA3′
		G	C	G	C	C	G
			G		G	G	
C-region amino acid		Val	Tyr	Pro	Leu	Ala	Pro
		(5′ GTC	TAT	CCA	CTG	GCC	CCT3′)
C-region primer		3′ CAG	ATA	GGT	GAC	CGG	GGA cttaaggc5′

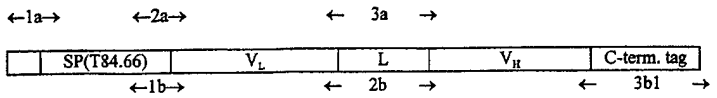

PCR primer	Sequence
1a	5'CGGGATCCAAGCTTGCCGCCACCATGGAGACAGACACACTCCTGCTA3'
1b	3'TCCACTGTAACACTACTGGGTCAGAGTGTTT5'
2a	5'GACATTGTGATGACCCAGTCTCACAAATTCATGT3'
2b	3'TGGTTAGACCTTTATTTTCCGCCTCCGCCATCGCCGCCACCAAGTCCTC CACCGCCGTCA5'
3a	5'AGCGGCGGTGGTTCAGGAGGTGGCGGCAGTGGTGGAGGATCTGAAGT AAAAGTGGTGGAATCT3'
3b1	3'AGCCAGTGGCAGAGGAGTGAGCTCCTGATGTTCCTGATTATCCTTAAG CG5'

Fig. 2 Assembly of the gene for the soluble form of αIGF-IR scFv by splice-overlap extension polymerase chain reaction (*PCR*). The gene encoding the αIGF-IR scFv was constructed using an N-terminal signal peptide (*SP*) derived from mT84.66 light chain [24, 40], 1H7 V_L DNA, an oligonucleotide encoding the linker peptide (*L*) $(GGGGSGGGS)_2$, 1H7 V_H DNA, and a C-terminal tag (including DYKD) as described [5, 6]. The assembled αIGF-IR scFv gene and locations of PCR primers used are schematically presented

αIGF-IR scFv construct by DNA sequence analysis, the scFv was cloned into pcDNA3 (Invitrogen, San Diego, Calif.), containing the cytomegalovirus promoter and *neo*^{r} selection marker (called pcDNA/αIGF-IR scFv).

To produce the gene encoding αIGF-IR scFv-Fc, a *Sal*I fragment containing the human IgG1 Fc (cDNA clone from Dr. J. Schlom, Laboratory of Tumor Immunology and Biology, Division of Cancer Biology and Diagnosis, NCI, Bethesda, Md.) was inserted into the unique *Xho*I site of pcDNA/αIGF-IR scFv. The *Hin*dIII fragment encoding αIGF-IR scFv-Fc, isolated from the pcDNA/αIGF-IR scFv-Fc plasmid, was inserted into the *Hin*dIII site of pEE12-1 [4]. This plasmid encodes a glutamine synthase gene that provides a selection system for myeloma NS0 cells in the L-glutamine-deficient selection medium, since NS0 cells require L-glutamine for growth. Plasmids were isolated from the transformants, and the correct orientation of the inserts was determined by restriction enzyme analysis using *Not*I.

Cell culture, transfection and screening

Murine myeloma Sp2/0 and NS0 cells were grown as described [41, 4]. Selective medium for NS0 cells consisted of L-glutamine-free Celltech DME (JRH Biosciences, Lenexa, KS), dialysed fetal calf serum (Gibco/BRL, Gaithersburg, Md.), and glutamine synthase supplement (JRH Biosciences, Lenexa, kan.).

Myeloma Sp2/0 cells were transfected with pcDNA/αIGF-IR scFv by electroporation [38], and incubated at 37 °C for 3 days in a humidified 5% CO_2 atmosphere. On day 4, cells were collected, counted, and placed in 24-well plates (10^5 cells/well) in regular medium containing 400 μg/ml G418. RNA was isolated from each stable transfectant and analyzed for expression of αIGF-IR scFv mRNA by RT-PCR.

Murine myeloma NS0 cells were stably transfected with pEE12-1/αIGF-IR scFv-Fc by the electroporation method, transferred to non-selective culture medium in a 96-well plate (50 μl/well), and incubated overnight. The next day, 150 μl selection medium was added to each well, and cells were incubated for 3 weeks until discrete surviving colonies appeared. Positive colonies were identified by detecting αIGF-IR scFv-Fc in the medium, using alkaline-phosphatase-conjugated affinity-purified rabbit anti-(human IgG), Fc-fragment-specific antibody (Jackson Immuno-Research Laboratories Inc., West Grove, Pa.) by the enzyme-linked immunosorbent assay (ELISA) method.

Purification of αIGF-IR scFv or scFv-Fc

A 150-ml sample of conditioned medium (CM) collected from Sp2/0 clone 45 was applied to 6 ml αFLAG M2 mAb conjugated to Sepharose 4B (0.2 mg/ml gel). The column was washed with 20 mM TRIS/HCl, pH 7.4, containing 0.3 M NaCl, 0.2 mM EDTA, 0.2 mM dithiothreitol, and 0.5 mM phenylmethylsulfonyl fluoride, and eluted with 5 ml wash buffer containing FLAG peptide (0.2 mg/ml) twice. Eluates 1 and 2 were concentrated and dialyzed, using an Ultrafree-4 spin column (Millipore, Bedford, Mass.).

Approximately 40 ml cell culture supernatants collected from αIGF-IR-scFv-Fc-expressing NS0 transfectants, clone 1F12 or 1B8, was adjusted to pH 8.0 by adding 1/20 volume 1.0 M TRIS (pH 8.0), and passed through a protein-A–Sepharose CL 4B column (1 ml column). The column was washed with ten column volumes of 100 mM TRIS/HCl buffer, pH 8.0, 10 column volumes of 10 mM TRIS/HCl pH 8.0. αIGF-IR scFv-Fc was eluted from the column with 100 mM glycine buffer pH 3.0, and collected in 1.5-ml conical tubes containing 1/10 volume 1 M TRIS (pH 8.0). In order to carry out in vivo experiments, approximately 400 mg αIGF-IR scFv-Fc was purified from approximately 10 l cell culture supernatants.

Determination of binding affinity of αIGF-IR for IGF-IR by surface plasmon resonance

The affinity constants of 1H7 and αIGF-IR scFv-Fc were determined using a BIAcore instrument (BIAcore Inc., Piscataway, N.J.) as previously described [22, 26]. Analytes such as 1H7 (10, 33, 133, and 200 nM) and αIGF-IR scFv-Fc (33, 66, 166, and 400 nM) were passed over the IGF-IR-immobilized chips (0.3 μg/chip) at a flow rate of 5 μl/min. The rates of association (k_a) and dissociation (k_d) were determined, using the kinetics evaluation software package (BIAcore, Inc.), and the thermodynamic association constant (K_A) was derived by dividing (k_a) by (k_d).

In vivo experiments

Human prostate PC-3 and human breast MCF-7 cell lines were obtained from American Type Culture Collection (Rockville, Md.). MCF-7 cells were cultured in Dulbecco's modified Eagle's medium supplemented with 5% fetal calf serum. PC-3 cells were cultured in RPMI-1640 supplemented with 10% fetal calf serum, 2 mM L-glutamine, and 1 mM sodium pyruvate.

Female athymic mice (BALB/C nude, Charles River Facility for NCI, Fredrick, Md.), 4 weeks old, that had received a 0.25-mg 17β-estradiol pellet 1 week previously [2] were inoculated in the flank with 10^7 MCF-7 cells (day 0). On day 3, intraperitoneal or subcutaneous injections near the tumor sites of αIGF-IR scFv-Fc into each of three mice (500 μg/0.1 ml phosphate-buffered saline, PBS/mouse, twice a week) started, and continued for 2 weeks. Control mice received PBS. Tumor sizes were measured at regular intervals. Tumor volumes (mm^3) were calculated by the formula $(\text{width})^2 \times \text{length}/2$.

Effects of αIGF-IR scFv-Fc administration on prostate cancer PC-3 tumor growth in vivo were examined in male athymic mice.

Athymic mice, 3 weeks old, were inoculated in the flank s.c. with 2×10^6 PC-3 cells on day 0. On day 5, αIGF-IR scFv-Fc treatment started; intraperitoneal injections of αIGF-IR scFv-Fc were given to six mice (500 μg/0.1 ml of PBS/mouse) twice weekly while six control mice received PBS. Tumor growth was measured as described above.

Other methods

Cell growth was measured by the 3-(4,5-dimethylthiazol-2-yl)-2, 5-diphenyltetrazolium bromide methods using NIH3T3 cells expressing human IGF-IR as previously described [41, 44]. Purification of the IGF-IR was carried out as previously published [18]. Binding and autophosphorylation activities of the purified IGF-I receptor in the presence of different concentrations of mAb or αIGF-IR scFv-Fc were measured as previously described [20, 41, 43]. Results of cell or tumor growth are expressed as means ± SE from five or six experiments. An unpaired Student's *t*-test was used to compare the growth between two groups of experiments.

Results

Cloning of the variable domains of 1H7 and verification of the amino acid sequences

The N-terminal amino acid sequences of the heavy and light chains of 1H7 were determined to be EVKVVESGGGLVKPG and DIVMTQSHKFMSTSV respectively. Degenerate oligonucleotides used as 5′PCR primers were synthesized on the basis of the N-terminal sequences of heavy and light chains of 1H7 whereas conserved amino acid sequences in the constant regions of murine IgG1 heavy and light chains were used to design 3′PCR primers (Table 1).

DNA sequences of the 400-bp insert from four independent V_H DNA clones matched each other and the deduced amino acid sequence (133 amino acids) was closely related to published IgG heavy-chain subgroup IIID sequences [15]. DNA sequences of the 360-bp insert from three independently amplified V_L DNA clones matched each other completely. Its deduced amino acid sequence (121 amino acids) was very similar to the κ light-chain V sequences [15]. Cloned V_H and V_L regions of 1H7 were consistent with the respective N-terminal amino acid sequences as determined by Edman degradation as well as the masses of and/or amino acid sequences of tryptic peptides derived from 1H7 mAb.

Assembly of V_H and V_L into a single-chain antibody; transfection, expression, and detection of αIGF-IR scFv

The αIGF-IR scFv gene was assembled by splice-overlap extension PCR as summarized in Fig. 2, and subcloned into pcDNA3. Murine myeloma Sp2/0 cells were transfected with pcDNA/αIGF-IR scFv. Culture media of the G418-resistant transfectants were first examined by dot-blot analysis using anti-FLAG antibody. Some of the 23 positive clones identifed were further analyzed for expression of αIGF-IR scFv mRNA by RT-PCR. Two clones were found to express αIGF-IR scFv mRNA.

Purification of soluble αIGF-IR scFvs

αIGF-IR scFv was purified by anti-FLAG M2 immunoaffinity chromatography from 150 ml CM from Sp2/0 clone 45. Figure 3A shows silver-staining and immunoblotting analysis of 1 μl each from the concentrated eluates 1 and 2, which comprised 80 μl and 180 μl respectively. The silver-stained protein band of 27 kDa was immunostained with anti-FLAG antibody, indicating that this protein is a soluble form of αIGF-IR scFv secreted from clone 45. In eluate 2, the scFv was purified to about 20% homogeneity, with bovine serum albumin (57%) as a major contaminant (Fig. 3A, lane 3). The total αIGF-IR scFv protein in eluates 1 and 2 was estimated to be approximately 1.4 μg in each case, suggesting that 2.8 μg αIGF-IR scFv protein was recovered from 150 ml CM. From this purification, the level of αIGF-IR scFv expression was estimated to be approximately 20 ng/ml CM.

To improve the level of αIGF-IR scFv expression and also to produce a humanized anti-IGF-IR antibody, another soluble form of αIGF-IR scFv containing the human IgG1 Fc domain was constructed and stably expressed in NS0 cells. Of 16 stable clones examined, 6 were positive for Fc production by ELISA. αIGF-IR scFv-Fc was purified to homogeneity from about 40 ml culture medium from two independent clones, 1F12 and 1B8, by protein-A–Sepharose CL 4B chromatography (Fig. 3B). From the culture medium of 1F12 (40 ml) and 1B8 (38 ml), 1.8 mg and 3.2 mg αIGF-IR scFv-Fc, respectively, were purified. The level of αIGF-IR scFv-Fc expression was thus calculated to be 45 μg/ml and 85 μg/ml for 1F12 and 1B8 respectively. The purified αIGF-IR scFv-Fc was used for biochemical and activity analyses of the engineered αIGF-IR scFvs as well as in vivo experiments.

Structural and functional analysis αIGF-IR scFv-Fc

SDS-PAGE analysis (7.5% gel) under reducing conditions revealed a single protein band of 53 kDa (Fig. 3B, lanes 2 and 3), which showed immunoreactivity with anti-1H7 antibody (Fig. 3B, lane 5). A single disulfide-linked protein of 120 kDa was detected by SDS-PAGE analysis (5% gel) under nonreducing conditions (Fig. 3C lane 1 & 2), indicating that αIGF-IR scFv-Fc is a disulfide-linked dimer. Gel filtration showed that a single protein peak eluted at the position expected for the size of dimer, indicating that αIGF-IR scFv-Fc does not form aggregates larger than a dimer in solution (data not shown).

The first 15 N-terminal amino acids of the purified αIGF-IR scFv-Fc were sequenced, which confirmed the

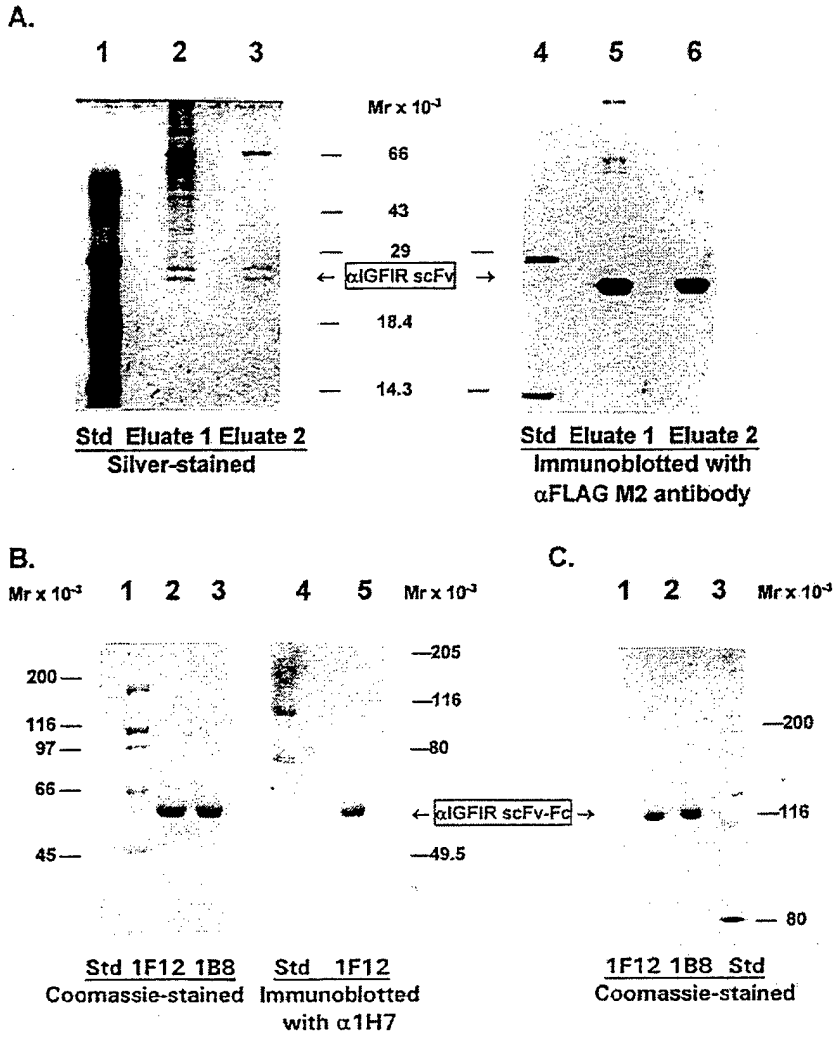

Fig. 3A–C Purification of soluble forms αIGF-IR scFvs. **A** Silver staining (*lanes 1–3*) and immunoblotting (*lanes 4–6*) of partially purified αIGF-IR scFv. Shown are standard proteins (*1*, *4*), M2 antibody column eluates 1 (*2*, *5*) and eluate 2 (*3*, *6*). **B** Sodium dodecyl sulfate/polyacrylamide gel electrophoresis (SDS-PAGE) under reducing conditions followed by Coomassie staining (*lanes 1–3*) and immunoblotting (*lanes 4*, *5*) of the purified αIGF-IR scFv-Fc. Shown are αIGF-IR scFv-Fc purified from conditioned medium of two independent stable clones, 1F12 and 1B8, as indicated. **C** SDS-PAGE under nonreducing conditions, followed by Coomassie staining of the purified αIGF-IR scFv-Fc

authenticity of this recombinant antibody and the proper removal of the signal peptide. The binding constants of 1H7 and αIGF-IR scFv-Fc for IGF-IR determined by BIAcore were 1×10^9 M^{-1} and 1×10^8 M^{-1} respectively.

Inhibition of IGF-I or IGF-II binding to the purified IGF-IR by 1H7 or αIGF-IR scFv-Fc

Effects of αIGF-IR mAb and αIGF-IR scFv-Fc on IGF-I and IGF-II binding to the purified IGF-IR are shown in Fig. 4. αIGF-IR scFv-Fc inhibited IGF-II binding to the IGF-IR more potently than IGF-I binding, which is consistent with the previous observations of 1H7 [20]. The potency of inhibition by αIGF-IR scFv-Fc was, however, ten times less than that by 1H7, which could be explained by the difference in their binding affinity. A control 2C8 mAb did not inhibit IGF-I or IGF-II binding to IGF-IR (Fig. 4).

Stimulation of autophosphorylation of the purified IGF-IR by αIGF-IR scFv-Fc

Autophosphorylation of purified IGF-IR was compared in the absence and presence of IGF-I, αIGF-IR scFv-Fc, 1H7, and poly L-lysine as a positive control. Both antibodies similarly stimulated the β-subunit phosphorylation (Fig. 5). Stimulation was the highest with poly (L-Lys) (12.8-fold) followed by IGF-I (3.8-fold), 1H7 (2.3-fold), and αIGF-IR scFv-Fc (1.8-fold).

Effect of αIGF-IR scFv-Fc on cell growth

The effect of extracellular addition of αIGF-IR scFv-Fc or 1H7 on cell growth was determined by the MTT method using NIH3T3 cells overexpressing IGF-IR. The average results of four independent experiments are shown in Fig. 6. Cell growth was significantly inhibited after 4 days of treatment with 10 nM or 100 nM 1H7 mAb (Fig. 6A) ($P < 0.05$). This result is consistent with

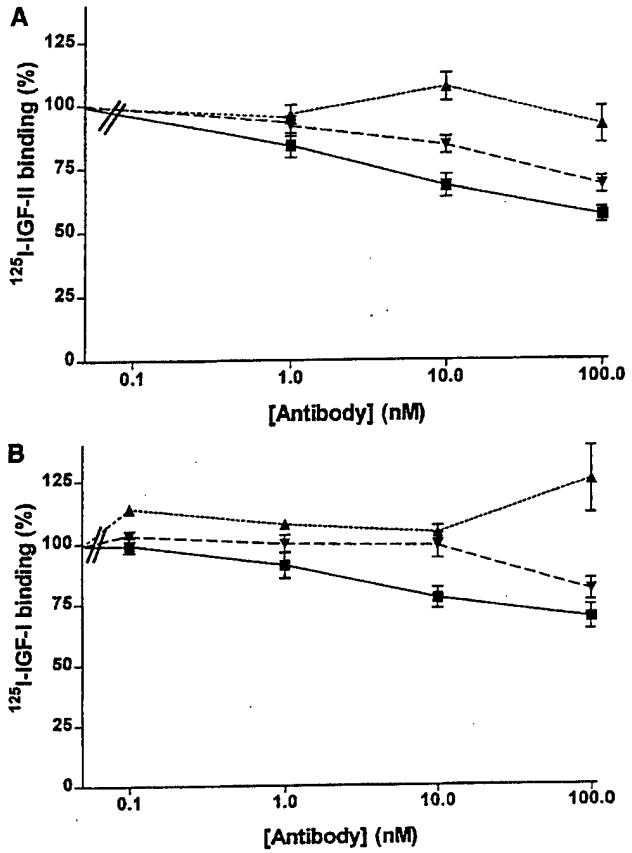

Fig. 4A, B Effects of αIGF-IR scFv-Fc and mAb on ^{125}I-IGF-II (A) and ^{125}I-IGF-I (B) binding to the purified human IGF-I receptor. The binding activity is calculated as the percentage IGF binding in the absence of antibodies, and expressed as average ± SD of four independent experiments for A or seven independent experiments for B, except that two control experiments with the 2C8 mAb were performed for B. Antibodies used are αIGF-IR scFv-Fc (▼), 1H7 (■), and control 2C8 (▲)

our previous observation, in which the growth-inhibitory effect of 1H7 was seen, as judged by [^{3}H]thymidine incorporation into DNA, while 2C8 had no effect on either IGF binding or cell growth, and 3B7 showed stimulation of both IGF binding and cell growth [20]. In contrast, αIGF-IR scFv-Fc was not as effective as 1H7 in inhibiting cell growth (Fig. 6B). After 4 days of treatment with αIGF-IR scFv-Fc, however, cell growth appeared to be inhibited in a dose-dependent manner. The highest dose used, 1000 nM αIGF-IR scFv-Fc, was required to inhibit cell growth to a level similar to that achieved by 100 nM 1H7. This variation is presumably due to the difference in their affinity for the IGF-IR.

Effect of αIGF-IR scFv-Fc on tumor growth in vivo

The aforementioned results suggest that the recombinantly engineered αIGF-IR scFv-Fc retained characteristics similar to those of the parental 1H7 mAb and has a sufficiently high affinity for IGF-IR, although it is

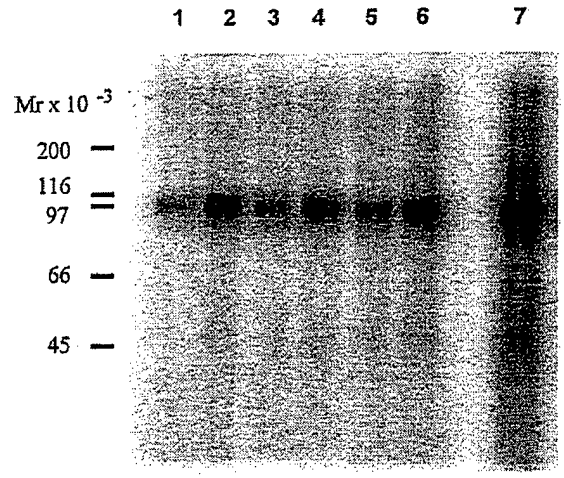

Fig. 5 Effects of αIGF-IR scFv-Fc and 1H7 on β subunit phosphorylation of the purified IGF-IR. IGF-IR was autophosphorylated in the presence of IGF-I and/or antibodies as indicated. Samples were analyzed by SDS-PAGE under reducing conditions. Shown is a phosphoimage of the gel. Stimulation for the samples (*lanes 2–7*) is calculated by dividing by the basal level phosphorylation (*lane 1*)

apparently less than that of the parental 1H7 mAb. Therefore, the effect of αIGF-IR scFv-Fc on cancer cell growth in vivo was determined. In the group treated with αIGF-IR scFv-Fc, three mice received the antibody intraperitoneally whereas the other three mice received it around the MCF-7 tumor site. The results derived from the two injection methods indicated no significant advantage of one group over the other. Thus, results obtained from the two groups were combined as one αIGF-IR-scFv-Fc-treated mouse group. Figure 7, summarizing the in vivo experiment, shows that αIGF-IR scFv-Fc inhibited MCF-7 tumor growth in athymic mice. Although the inhibition was statistically significant only on day 13 ($P < 0.05$), individual tumor growth curves indicated that, in four out of six mice, MCF-7 tumor growth was completely suppressed from day 3 to day 17 (in one case the tumor disappeared), whereas in two mice the tumor growth increased after day 13. In the control group, MCF-7 tumor grew steadily from day 3 to day 20 except in a single mouse. We did not find a significant effect of αIGF-IR scFv-Fc on PC-3 tumor growth in athymic mice (Fig. 8) under the same conditions in which breast cancer MCF-7 tumor growth was significantly inhibited in vivo.

Discussion

IGF-IR is a rational target for potential cancer therapeutics since growing evidence supports a critical role

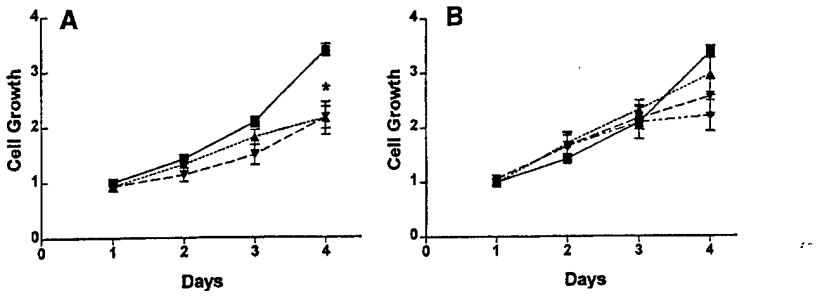

Fig. 6A, B Effects of αIGF-IR scFv-Fc and 1H7 on cell growth. NIH3T3 cells overexpressing IGF-IR were cultured in Dulbecco's modified Eagle's medium supplemented with 2% fetal calf serum in the absence (■) or presence of 10 nM (▲), 100 nM (▼), or 1000 nM (◆) 1H7 (A) or αIGF-IR scFv-Fc (B). Cell growth was determined by the 3-(4,5-dimethylthiazol-2-yl)-2,5-diphenyltetrazolium bromide method. Statistically significant difference between control and 10 nM or 100 nM 1H7 addition is indicated (*$P < 0.05$)

for IGF-IR in the pathogenesis of various malignancies, including breast and prostate cancers [8, 11, 21, 25, 27, 31]. Genetically engineered antibody against a target protein would not only allow high-level production of the antibody, but also provide a valuable resource from which we could further design and develop second-generation recombinant antibodies such as tissue-specific and toxin-conjugated antibodies [33, 35]. Of the two single-chain antibodies against the human IGF-I receptor constructed, the expression level of our first construct, αIGF-IR scFv, in murine myeloma SP 2/0 cells was extremely low. In contrast, high production of the alternative type, αIGF-IR scFv-Fc, was achieved by expressing it in murine myeloma NS0 cells. In other studies on the expression of engineered single-chain antibodies directed against carcinoembryonic antigen, high expression levels have consistently been obtained by using the NS0/pEE12 system, as compared to Sp2/0 myeloma cells or bacterial expression [13] (and Wu et al., unpublished). Thus, favorable expression appears to be a function of the expression system used rather than of the construct. αIGF-IR scFv-Fc was thus used to confirm the authenticity of the genetically engineered anti-IGF-IR by comparison with the parental 1H7 mAb, and for determination of the effect of the anti-IGF-IR antibody on tumor growth in vivo.

Two independent stable clones expressed αIGF-IR scFv-Fc in conditioned medium at concentrations of 40–100 mg/l. αIGF-IR scFv-Fc was purified from the conditioned medium of the two stable clones by one-step purification on a protein-A–agarose column. SDS-PAGE and gel filtration analyses indicated that αIGF-IR scFv-Fc is a dimeric antibody. As judged by

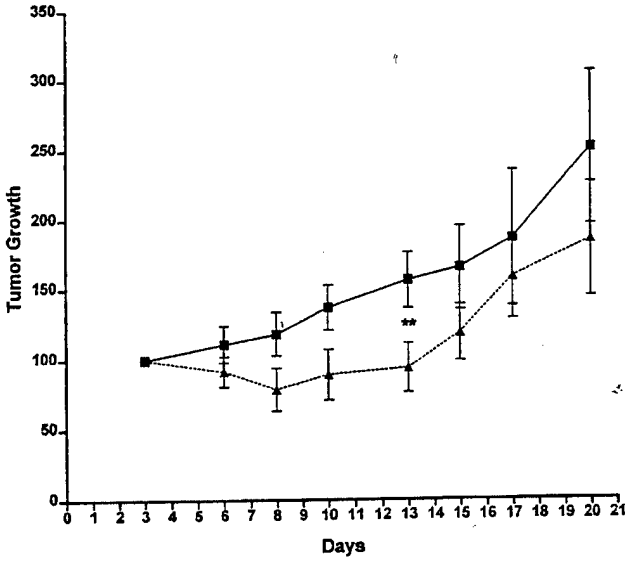

Fig. 7 Breast cancer MCF-7 tumor growth in nude mice with or without αIGF-IR scFv-Fc treatment. Athymic mice, 3 weeks old, that had received a 0.25-mg 17β-estradiol pellet, were inoculated in the flank s.c. with 5×10^5 MCF-7 cells on day 0. On day 3, αIGF-IR scFv-Fc treatment started: intraperitoneal or local injections of αIGF-IR scFv-Fc into three mice each (0.5 mg/mouse) twice weekly while control mice received phosphate-buffered saline (PBS). Tumor growth was measured as described in Materials and methods, normalized by the size on day 3 and expressed as the means ± SE [$n = 5$ and 6 for the PBS (■) and αIGF-IR scFv-Fc (▲) groups respectively]. Inhibition of tumor growth by αIGF-IR scFv-Fc on day 13 was statistically significant ($P < 0.05$)

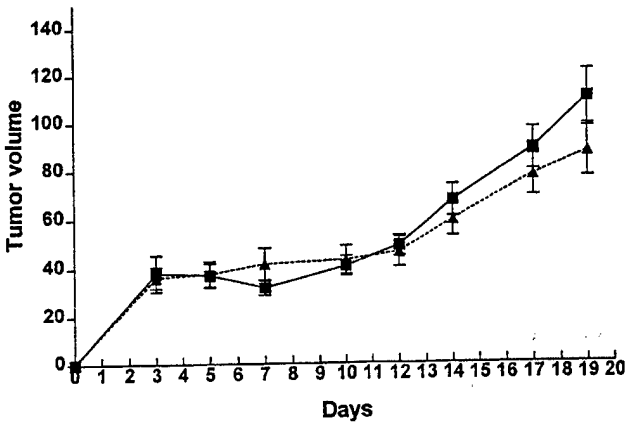

Fig. 8 Effects of αIGF-IR scFv-Fc administration on prostate cancer PC-3 tumor growth in vivo in athymic mice. Athymic mice, 3 weeks old, were inoculated in the flank s.c. with 2×10^6 PC-3 cells on day 0. On day 5, αIGF-IR scFv-Fc treatment started: intraperitoneal injections of αIGF-IR scFv-Fc into each of six mice (0.5 mg/mouse) twice weekly, while control mice received PBS. Tumor growth was measured as described in Materials and methods, and expressed as means ± SE [$n = 6$ for both the PBS (■) and αIGF-IR scFv-Fc (▲) groups]

its effect on the inhibition of IGF binding to IGF-IR, IGF-IR β subunit autophosphorylation, and cell growth in vitro, αIGF-IR scFv-Fc retained the overall characteristics of the parental 1H7 monoclonal antibody. The observed differences between αIGF-IR scFv-Fc and 1H7 can be attributed to the binding affinity of the former for IGF-IR, which was estimated to be approximately $10^8\ M^{-1}$ and was one order of magnitude lower than that of 1H7 monoclonal antibody. Of the two stable clones we originally characterized, the 1B8 clone has been used to purify about 400 mg αIGF-IR scFv-Fc to date.

In this study, autophosphorylation of IGF-IR in vitro and inhibition of IGF-dependent cell growth by the parental 1H7 mAb and αIGF-IR scFv-Fc were measured to verify the authenticity of the recombinant antibody. It should be noted that the antibodies against IGF-IR, which can stimulate IGF-IR autophosphorylation, inhibited cell growth. These two events are apparently contradictory. Although the inhibitory effect of 1H7 on monolayer cell growth was observed with NIH 3T3 cells overexpressing IGF-IR, inhibition of the growth of cancer cells including MCF-7 cells was not significantly seen (data not shown). The fact that MCF-7 tumor growth was inhibited by αIGF-IR scFv-Fc in vivo supports the notion that IGF-IR is not required for monolayer cell growth, but is necessary for anchorage-independent growth.

Injection of αIGF-IR scFv-Fc (500 μg/mouse, twice a week) significantly suppressed MCF-7 tumor growth in athymic mice. Similar in vivo experiments have been repeated four times with reproducible results. Arteaga et al. previously reported that αIR-3 did not inhibit MCF-7 tumor growth while it inhibited MDA-231 tumor growth effectively in athymic mice [1]. In the same report, they showed that αIR-3 significantly inhibited anchorage-independent growth of both MCF-7 and MDA231 cells in vitro. In contrast to the results reported by Arteaga et al., we found that MCF-7 cell growth was inhibited in vivo. The difference between their results for MCF-7 tumor growth inhibition and ours may be due to the clonal difference between the two MCF-7 clones. The MCF-7 clone we used was originally derived from ATCC. Although the original clone does not produce a detectable level of IGF-II, the MCF-7 clone used in this study produces IGF-II at approximately one-tenth the level reached by PC-3 cells [44]. This clone is estrogen-receptor-positive and does not grow without estrogen supplementation. Thus, the inhibitory effect of αIGF-IR scFv-Fc on MCF-7 tumor growth cannot be observed in the absence of 17β-estradiol. We previously determined IGF-IR numbers in breast cancer cell lines by radioimmunoassay, which indicated that MCF-7 cells express 110 ng receptors/10^6 cells whereas MDA231 cells express a very low level of IGF-IR, 1.8 ng receptors/10^6 cells [28]. In contrast to the inhibition of MCF-7 tumor growth, we found that growth of PC-3 tumor was not significantly inhibited by αIGF-IR scFv-Fc in athymic mice. It is known that the response of MCF-7 cells to IGF is much more sensitive than that of PC-3 cells [25, 17]. Our in vivo experiments are consistent with the notion that the number of IGF-IR determines IGF responsiveness and also sensitivity to the inhibition of tumor growth mediated by anti-IGF-IR antibody.

In this study, we have shown the initial characterization of recombinant anti-IGF-I receptor single-chain antibodies. The major advantage of single-chain antibodies over the parental 1H7 mAb is that we can readily design and produce recombinant antibodies with additional functions such as enzyme- or toxin-conjugated antibodies. The αIGF-IR scFv-Fc is one such example: a chimeric antibody incoporating the human IgG1 Fc domain. As described for αIGF-IR scFv-Fc, the advantages of this format include humanization of the murine mAb, improved levels of expression, and ease of purification via protein A affinity chromatography. One disadvantage we found is that the αIGF-IR scFv-Fc shows a lower affinity than that of the parental mAb, as often seen with recombinant scFv. In conclusion, this study suggests that αIGF-IR scFv-Fc is a first-generation recombinant αIGF-IR that is useful for the potential development of future αIGF-IR therapeutics. Mechanisms of MCF-7 tumor growth inhibition and effects of αIGF-IR scFv-Fc immunotherapy in conjunction with chemotherapy are currently under investigation.

Acknowledgements We thank Giselle Tan for helpful suggestions, and Jingjing Ye for her excellent technical assistance. This work was supported in part by the California Breast Cancer Research Program (3CB-0186), the US Army Prostate Cancer Research Program (DAMD17-98-1-8579), and an NIH grant (CA65767).

References

1. Arteaga CL, Osborne CK (1989) Growth inhibition of human breast cancer cells in vitro with an antibody against the type I somatomedin receptor. Cancer Res 49: 6237
2. Arteaga CL, Kitten L-J, Coronado EB, Jacobs S, Kull FC Jr, Allred DC, Osborne CK (1989) Blockade of the type I somatomedin receptor inhibits growth of human breast cancer cells in athymic mice. J Clin Invest 84: 1418
3. Baserga R, Hongo A, Rubini M, Prisco M, Valentinis B (1997) The IGF-I receptor in cell growth, transformation and apoptosis. Biochim Biophys Acta 1332: F105
4. Bebbington CR, Renner G, Thomson S, King D, Abrams D, Yarranton GT (1992) High-level expression of a recombinant antibody from myeloma cells using a glutamine synthetase gene as an amplifiable selectable marker. Biotechnology 10: 169
5. Beerli RR, Wels W, Hynes NE (1994) Autocrine inhibition of the epidermal growth factor receptor by intracellular expression of a single-chain antibody. Biochem Biophys Res Commun 204: 666
6. Beerli RR, Wels W, Hynes NE (1994) Intracellular expression of single chain antibodies reverts ErbB-2 transformation. J Biol Chem 269: 23 931
7. Coppola D, Ferber A, Miura M, Sell C, D'Ambrosio C, Rubin R, Baserga R (1994) A functional insulin-like growth factor I receptor is required for the mitogenic and transforming activities of the epidermal growth factor receptor. Mol Cell Biol 14: 4588

8. Damon SE, Maddison L, Ware JL, Plymate SR (1998) Overexpression of an inhibitory insulin-like growth factor binding protein (IGFBP), IGFBP-4, delays onset of prostate tumor formation. Endocrinology 139: 3456
9. Dunn SE, Hardman RA, Kari FW, Barrett JC (1997) Insulin-like growth factor 1 (IGF-1) alters drug sensitivity of HBL100 human breast cancer cells by inhibition of apoptosis induced by diverse anticancer drugs. Cancer Res 57: 2687
10. Furlanetto RW, Harwell SE, Baggs RB (1993) Effects of insulin-like growth factor receptor inhibition on human melanomas in culture and in athymic mice. Cancer Res 53: 2522
11. Guvakova MA, Surmacz E (1997) Tamoxifen interferes with the insulin-like growth factor I receptor (IGF-IR) signaling pathway in breast cancer cells. Cancer Res 57: 2606
12. Hieter PA, Max EE, Seidman JG, Maizel JV Jr, Leder P (1980) Cloned human and mouse kappa immunoglobulin constant and J region genes conserve homology in functional segments. Cell 22: 197
13. Honjo T, Obata M, Yamawaki-Kataoka Y, Kataoka T, Kawakami T, Takahashi N, Mano Y (1979) Cloning and complete nucleotide sequence of mouse immunoglobulin gamma 1 chain gene. Cell 18: 559
14. Hu S, Shively L, Raubitschek AA, Sherman M, Williams L, Wong JYC, Shively JE, Wu AM (1996) Minibody: a novel engineered anti-carcinoembryonic antigen antibody fragment (single-chain Fv-CH3) which exhibits rapid, high-level targeting of xenografts. Cancer Res 56: 3055
15. Kabat EA, Wu TT, Perry HM, Gottesman KS, Foeller C (1991) Sequences of proteins of immunological interest, 15th edn. US Department of Health and Human Services, NIH, Bethesda, Md
16. Kaleko M, Rutter WJ, Miller AD (1990) Overexpression of the human insulin-like growth factor I receptor promotes ligand-dependent neoplastic transformation. Mol Cell Biol 10: 464
17. Kimura G, Kasuya J, Giannini S, Honda Y, Mohan S, Kawachi MH, Akimoto M, Fujita-Yamaguchi Y (1996) Insulin-like growth factor (IGF) system components in human prostate cancer cell lines, LNCaP, DU145 and PC-3. Int J Urol 3: 39
18. LeBon TR, Jacobs S, Cuatrecasas P, Kathuria S, Fujita-Yamaguchi Y (1986) Purification of insulin-like growth factor I receptor from human placental membranes. J Biol Chem 261: 7685
19. LeRoith D, Werner H, Beitner-Johnson D, Roberts CT Jr (1995) Molecular and cellular aspects of the insulin-like growth factor I receptor. Endocrine Rev 16: 143
20. Li SL, Kato J, Paz IB, Kasuya J, Fujita-Yamaguchi Y (1993) Two new monoclonal antibodies against the alpha subunit of the human insulin-like growth factor-I receptor. Biochem Biophys Res Commun 196: 92
21. Li SL, Goko H, Xu ZD, Kimura G, Sun Y, Kawachi MH, Wilson TG, Wilczynski S, Fujita-Yamaguchi Y (1998) Expression of insulin-like growth factor (IGF)-II in human prostate, breast, bladder, and paraganglioma tumors. Cell Tissue Res 291: 469
22. Li SL, Termini J, Hayward A, Siddle K, Zick Y, Koval A, LeRoith D, Fujita-Yamaguchi Y (1998) The carboxyl-terminal domain of insulin-like growth factor-I receptor interacts with the insulin receptor and activates its protein tyrosine kinase. FEBS Lett 421: 45
23. Neuenschwander S, Roberts CT Jr, LeRoith D (1995) Growth inhibition of MCF-7 breast cancer cells by stable expression of an insulin-like growth factor I receptor antisense ribonucleic acid. Endocrinology 136: 4298
24. Neumaier M, Shively L, Chen FS, Gaida FJ, Ilgen C, Paxton RJ, Shively JE, Riggs AD (1990) Cloning of the genes for T84.66, an antibody that has a high specificity and affinity for carcinoembryonic antigen, and expression of chimeric human/mouse T84.66 genes in myeloma and Chinese hamster ovary cells. Cancer Res 50: 2128
25. Osborne CK, Coronado EB, Kitten LJ, Arteaga CI, Fuqua SA, Ramasharma K, Marshall M, Li CH (1989) Insulin-like growth factor-II (IGF-II): a potential autocrine/paracrine growth factor for human breast cancer acting via the IGF-I receptor. Mol Endocrinol 3: 1701
26. O'Shannessy DJ, Brigham-Burke M, Soneson KK, Hensley P, Brooks I (1994) Determination of rate and equilibrium binding constants for macromolecular interactions by surface plasmon resonance. Methods Enzymol 240: 323
27. Papa V, Gliozzo B, Clark GM, McGuire WL, Moore D, Fujita-Yamaguchi Y, Vigneri R, Goldfine ID, Pezzino V (1993) Insulin-like growth factor-I receptors are overexpressed and predict a low risk in human breast cancer. Cancer Res 53: 3736
28. Pezzino V, Milazzo G, Frittitta L, Vigneri R, Ezaki O, Kasahara M, Le Bon TR, Goldfine ID, Fujita-Yamaguchi Y (1991) Radioimmunoassay for human insulin-like growth factor-I receptor: Applicability to breast carcinoma specimens and cell lines. Metabolism 40: 861
29. Prager D, Li HL, Asa S, Melmed S (1994) Dominant negative inhibition of tumorigenesis in vivo by human insulin-like growth factor I receptor mutant. Proc Natl Acad Sci USA 91: 2181
30. Resnicoff M, Coppola D, Sell C, Rubin R, Ferrone S, Baserga R (1994) Growth inhibition of human melanoma cells in nude mice by antisense strategies to the type 1 insulin-like growth factor receptor. Cancer Res 54: 4848
31. Resnik JL, Reichart DB, Huey K, Webster NJ, Seely BL (1998) Elevated insulin-like growth factor I receptor autophosphorylation and kinase activity in human breast cancer. Cancer Res 58: 1159
32. Sakano K, Enjoh T, Numata F, Fujiwara H, Marumoto Y, Higashihashi N, Sato Y, Perdue JF, Fujita-Yamaguchi Y (1992) The design, expression, and characterization of human insulin-like growth factor II mutants specific for either the IGF-II/cation independent mannose 6-phosphate receptor or IGF-I receptor. J Biol Chem 266: 20 626
33. Schmidt M, Maurer-Gebhard M, Groner B, Koehler G, Brochmann-Santos G, Wels W (1999) Suppression of metastasis formation by a recombinant single chain antibody-toxin targeted to full-length and oncogenic variant EGF receptors. Oncogene 18: 1711
34. Sell C, Dumenil G, Deveaud C, Miura M, Coppola D, DeAngelis T, Rubin R, Efstratiadis A, Baserga R (1994) Effect of a null mutation of the insulin-like growth factor I receptor gene on growth and transformation of mouse embryo fibroblasts. Mol Cell Biol 14: 3604
35. Skrepnik N, Zieske AW, Bravo JC, Gillespie AT, Hunt JD (1999) Recombinant oncotoxin AR209 (anti-P185 erbB-2) diminishes human prostate carcinoma xenografts. J Urol 161: 984
36. Trojan J, Blossey BK, Johnson TR, Rudin SD, Tykocinski M, Ilan J (1992) Loss of tumorigenicity of rat glioblastoma directed by episome-based antisense cDNA transcription of insulin-like growth factor I. Proc Natl Acad Sci USA 89: 4874
37. Turner BC, Haffty BG, Narayanan L, Yuan J, Havre PA, Gumbs AA, Kaplan L, Burgaud JL, Carter D, Baserga R, Glazer PM (1997) Insulin-like growth factor-I receptor overexpression mediates cellular radioresistance and local breast cancer recurrence after lumpectomy and radiation. Cancer Res 57: 3079
38. Ullrich MJ, Ley TJ (1990) Function of normal and mutated gamma-globin gene promoters in electroporated K562 erythroleukemia cells. Blood 75: 990
39. Ullrich A, Gray A, Tam AW, Yang-Feng T, Tsubokawa M, Collins C, Henzel W, LeBon TR, Kathuria S, Chen E, Jacobs S, Franke U, Ramachandran J, Fujita-Yamaguchi Y (1986) Insulin-like growth factor I receptor primary structure: comparison with insulin receptor suggests structural determinants that define functional specificity. EMBO J 5: 2503
40. Wu AM, Chen W, Raubitschek A, Williams LE, Neumaier M, Fischer R, Hu SZ, Odom-Maryon T, Wong Y, Shively JE (1996) Tumor localization of anti-CEA single-chain Fvs: improved targeting by non-covalent dimers. Immunotechnology 2: 21
41. Xiong L, Kasuya J, Li SL, Kato J, Fujita-Yamaguchi Y (1992) Growth-stimulatory monoclonal antibodies against human

insulin-like growth factor I receptor. Proc Natl Acad Sci USA 89: 5356
42. Xu QY, Paxton RJ, Fujita-Yamaguchi Y (1990) Substructural analysis of the insulin receptor by microsequence analyses of limited tryptic fragments isolated by sodium dodecyl sulfate-polyacrylamide gel electrophoresis in the absence or presence of dithiothreitol. J Biol Chem 265: 18 673
43. Xu QY, Li SL, LeBon TR, Fujita-Yamaguchi Y (1991) Aggregation of IGF-I receptors or insulin receptors and activation of their kinase activity are simultaneously caused by the presence of polycations or K-ras basic peptides. Biochemistry 30: 11 811
44. Xu ZD, Oey L, Mohan S, Kawachi MH, Lee NS, Rossi JJ, Fujita-Yamaguchi Y (1999) Hammerhead ribozyme-mediated cleavage of the human insulin-like growth factor-II ribonucleic acid in vitro and in prostate cancer cells. Endocrinology 140: 2134
45. Yates JR 3rd, Eng JK, McCormack AL, Schieltz D (1995) Method to correlate tandem mass spectra of modified peptides to amino acid sequences in the protein database. Anal Chem 67: 1426

Growth Hormone & IGF Research 2000, **10**, 61–70
doi:10.1054/ghir.2000.0141, available online at http://www.idealibrary.com on IDEAL®

Original articles

A quantitative reverse transcription and polymerase chain reaction assay for human IGF-II allows direct comparison of IGF-II mRNA levels in cancerous breast, bladder, and prostate tissues

E. Fichera, S. Liang, Z. Xu, N. Guo, R. Mineo and Y. Fujita-Yamaguchi

Department of Molecular Biology, Beckman Research Institute of the City of Hope, Duarte, California 91010, USA

Summary Previously, we showed by *in situ* hybridization that insulin-like growth factor (IGF)-II is upregulated in approximately 50% of prostate, breast, and bladder tumours. In this study, a quantitative competitive reverse transcription and polymerase chain reaction (QC RT-PCR) assay was established and used to quantify human IGF-II mRNA levels in cells and tissues. In this QC RT-PCR assay, a competitor IGF-II RNA, prepared from a newly constructed plasmid encoding the human IGF-II sequence with a 110-bp fragment inserted, was added to RNA samples prior to RT-PCR. The human IGF-II specific QC RT-PCR assay has allowed us to readily compare the levels of IGF-II mRNA in human tissues and cultured cells. Consistent with our previous observations by *in situ* hybridization, IGF-II mRNA was up-regulated in 50% of cancerous breast tissues examined as compared to the matching benign tissues, and IGF-II mRNA levels were higher in bladder tumours than breast and prostate tumours. In summary, we present here quantitative data confirming that a subclass of breast cancer samples has elevated levels of IGF-II transcripts by the new competitive RT-PCR assay.
© 2000 Harcourt Publishers Ltd

Key words: insulin-like growth factor, competitive RT-PCR, gene expression, human, breast cancer, prostate, bladder.

INTRODUCTION

Insulin-like growth factor (IGF)[1]-II is a single chain polypeptide of 67 amino acid residues, that has amino acid homology with IGF-I and proinsulin[1]. Both IGF-I and IGF-II bind to the IGF-I receptor with high affinity, which initiates mitogenic and anti-apoptotic responses in the cell[2–5]. Increased expression of IGFs in a variety of cancer cells and various tumours has been reported[6]. Experimental evidence suggests that IGF-II may act as an autocrine growth factor in the pathogenesis not only of childhood cancers but also of several types of adult cancers[2,6–10]. It has been reported by *in situ* hybridization (ISH) and immunohistochemisry (IHC) that IGF-II mRNA is highly expressed in adult cancers including cancerous breast and prostate tissues[11–13]. In addition, we have shown that IGF-II is up-regulated in cancerous cells of more than 50% of prostate, breast, and bladder tumours by ISH, IHC, and immunoblotting[14]. In this study, in

Received 16 January 2000
Revised 20 February 2000
Accepted 20 February 2000

Correspondence to: Yoko Fujita-Yamaguchi, Department of Molecular Biology, Beckman Research Institute of the City of Hope, 1450 East Duarte Road, Duarte, California 91010, USA. Tel: 626-301-8249; Fax: 626-301-8280; E-mail: yyamaguchi@coh.org

1096–6374/00/020061+10 $35.00/0

© 2000 Harcourt Publishers Ltd

order to quantitatively compare IGF-II mRNA levels between benign and cancerous tissues and among different tissues, we developed a quantitative, competitive (QC) reverse transcription and polymerase chain reaction (RT-PCR) assay. RT-PCR provides a simple and sensitive method as an alternative to Northern blot and RNase protection assay[15]. Other groups have reported various quantitative RT-PCR assays to measure human IGFs, IGF-I receptor, IGF binding proteins, and GH receptor[16–20]. Although QC RT-PCR for IGF-I has been reported[19], such a method is not readily available for human IGF-II. A major advantage of this method over existing methods is its sensitivity for quantitative measurement, which allows us to determine the IGF-II mRNA levels in tissues with limited availability.

Here, we present the first quantitative data comparing IGF-II transcripts in benign and cancerous tissues and cultured cells using the QC RT-PCR assay.

MATERIALS AND METHODS

Construction of plasmids

pBluescriptII KS(+) (Stratagene, La Jolla, California) containing an approximately 1 kb EcoRI fragment encoding the human precursor IGF-II (911 to 2067 nucleotide)[21] (pBS KS/IGF2), was used to generate a plasmid which encodes a competitor IGF-II DNA sequence as schematically summarized in Fig. 1. pBS KS/IGF2 was digested by EcoRI and the EcoRI fragment was ligated into the EcoRI-digested pBS SK vector. *Escherichia coli* transformants containing the insert with the opposite direction to the original IGF-II clone were selected by restriction enzyme analysis using XhoI and PvuII. Since the EcoRI/EcoRI insert as well as multi-cloning sites contained unique SalI and XhoI sites, the pBS SK/IGF2 plasmid was digested by XhoI, from which the small XhoI/XhoI fragment was removed. Ligation of the remaining XhoI fragment resulted in pBS SK/IGF2S encoding the shortened IGF-II sequence which contained a unique SalI site. To this SalI site, a 110 bp SalI-SalI DNA was inserted. The new plasmid, pBS SK/IGF2C, yielded restriction enzyme maps of 1506, 683 and 463 bp, whereas the original pBS SK/IGF2S revealed restriction enzyme maps of 1506, 683 and 353 bp with PvuII digestion. Since the 110 bp SalI/SalI fragment was inserted into the site between the two PCR primers, RT-PCR of the competitor RNA and

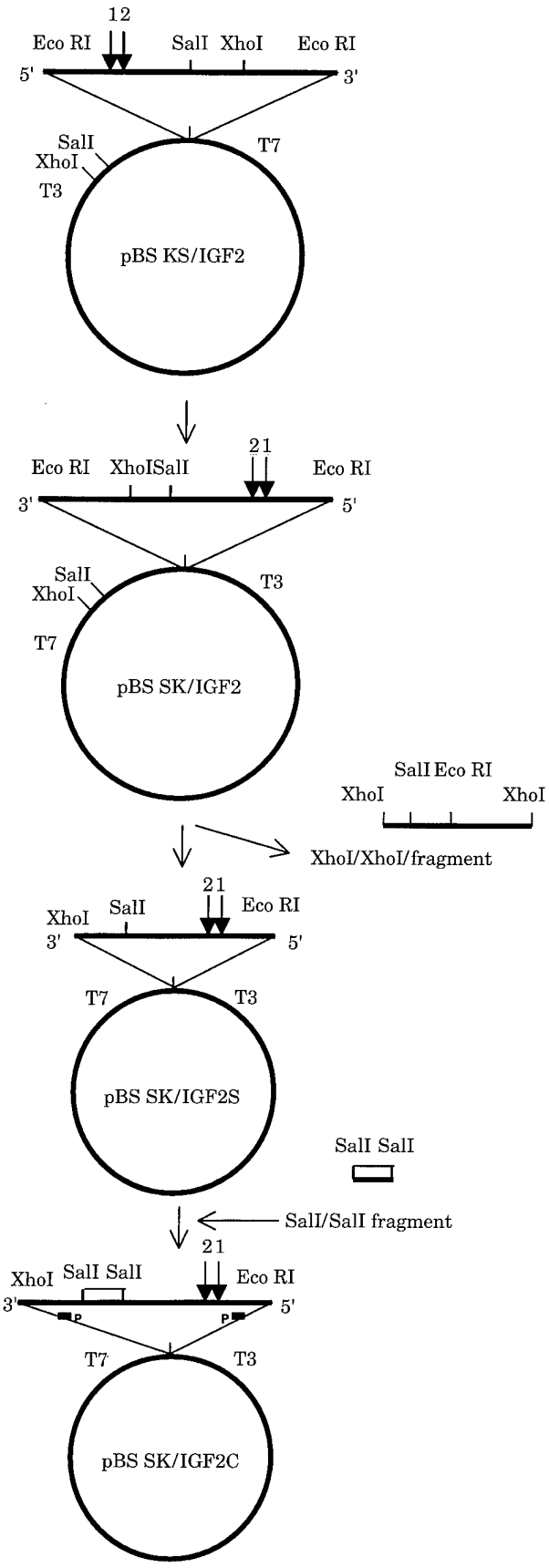

Fig. 1 Construction of the competitor IGF-II plasmid. pBluescript KS containing approximately 1 kb EcoRI fragment encoding the human precursor IGF-II (pBS KS/IGF2) was modified to construct pBS SK/IGF2S and pBS SK/IGF2C, which were used to transcribe authentic IGF-II RNA and control competitor IGF-II RNA, respectively. The arrow (↓) and P ■ indicate the sites for ribozyme-cleavage and PCR primers, respectively.

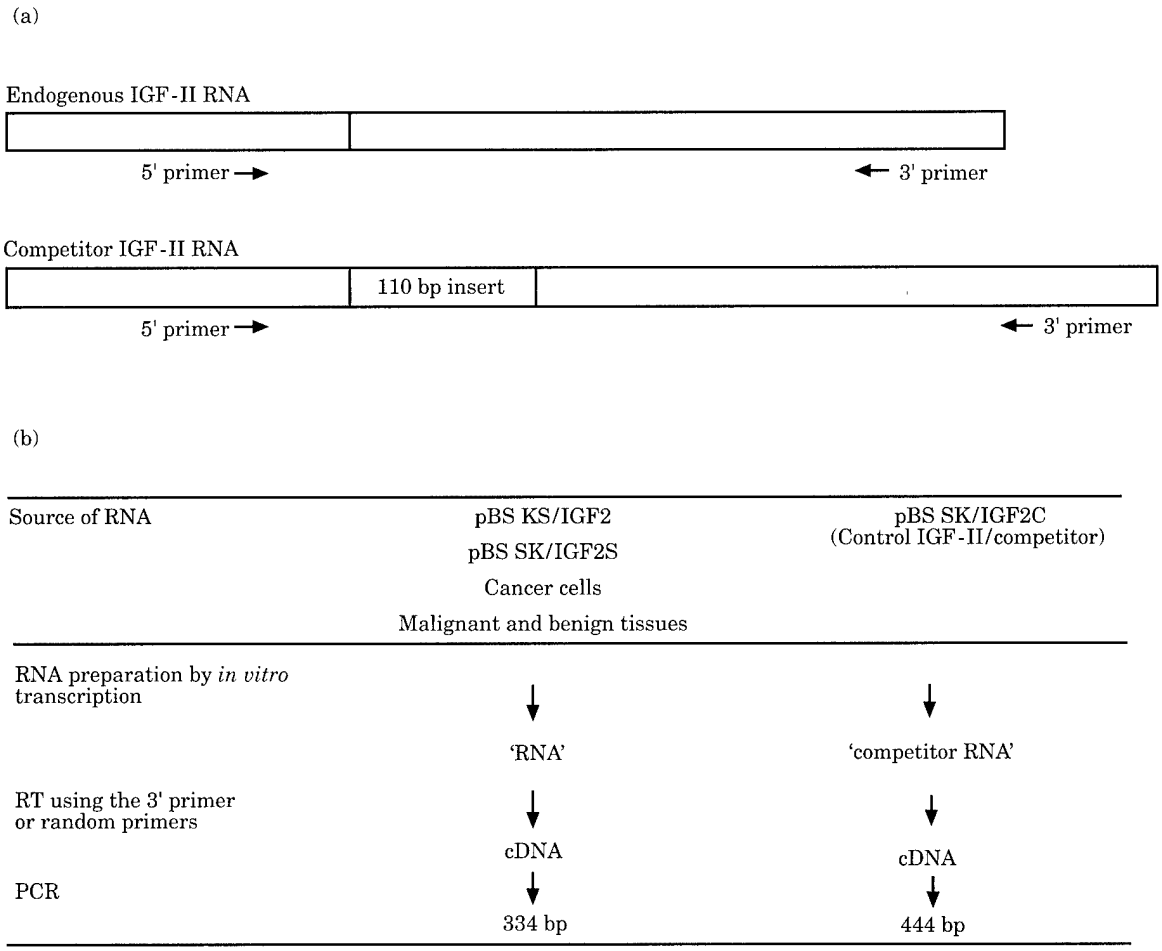

Fig. 2 Summary of IGF-II quantitative RT-PCR. (a) Endogenous IGF-II RNA and competitor IGF-II RNA which share the same PCR primers are illustrated. (b) Sources of IGF-II RNA and corresponding RT-PCR products, 334 bp or 444 bp, are schematically presented.

cellular RNA should produce a 444 bp band and a 334 bp band, respectively (Fig. 2).

Synthesis of short authentic and control (competitor) IGF-II RNAs *in vitro*

The pBS SK/IGF2S and pBS SK/IGF2C (Fig. 1) were linearized by BamHI and XhoI digestion, respectively, and used as templates for *in vitro* transcription. Transcription reaction was carried out at 37°C for 1 h in 20 µl of 40 mM Tris-HCl buffer, pH 7.9, containing 0.4 µg DNA template, 10 units of T3 RNA polymerase (Promega, Madison, Wisconsin), 20 mM $MgCl_2$, 10 mM NaCl, 10 mM DTT, 0.5 mM each of ATP, GTP, CTP, and UTP, and 40 units of RNasin (Promega, Madison, Wisconsin). After transcription, RNA was treated with 5 units of RNase-free DNase I (Promega, Madison, Wisconsin) for 30 min, and with phenol/chloroform/isoamyl alcohol (25/24/1). RNA was precipitated with ethanol, dissolved in 20 µl diethylpyrocarbonate-treated water and stored at −75°C.

RNA isolation from tissues and cells

Total RNA was prepared from frozen tissues (20–30 mg) or freshly harvested cells (10^7 cells) using TRIzol Reagent (GIBCO BRL, Gaithersburg, Maryland) according to the manufacturer's protocol. Prostate cancer PC-3 cell clones, which had been stably transfected with pcDNA/ribozyme (R) or pcDNA (V; vector-control) were previously described[22].

Quantification of IGF-II mRNA in cancer cells or tissues

In this report, two RT-PCR methods were described. The first method, used for the experiments shown in Figs. 3 and 8, was done with only one concentration of the competitor (0.1 ng), which allows semiquantitative determination of relative IGF-II mRNA levels within the same experiments such as Figs. 3 and 8. For this set of experiments, either Northern blot analysis or measurement of 28S RNA level were used for normalization of the RNA samples. The second method was then developed after

we produced and confirmed the result shown in Figs. 4 and 5. The experiments shown in Figs. 4, 5, and 7 were carried out using random primers for reverse transcription and four competitor amounts (0.05, 0.1, 1 and 2 ng). For this assay, β-actin PCR was used for normalization of the RNA samples.

Reverse transcription was performed at 42°C for 50 min in 20 µl of reaction mixture in the presence of 2 µg of total cellular RNA mixed with a set of 0.05, 0.1, 0.5, or 1 ng of the control competitor and 150 ng of Random Primers (GIBCO BRL, Gaithersburg, Maryland). The reaction mixture consisted of 50 mM Tris-HCl, pH 7.5, 10 mM DTT, 75 mM KCl, 3 mM $MgCl_2$, 1 mM of each deoxynucleoside triphosphate (dNTP), 200 units of SuperScript II (GIBCO BRL, Gaithersburg, Maryland), and 40 units of RNasin (Promega, Madison, Wisconsin). The reaction was terminated by incubation at 70°C for 15 min. Alternatively, RT was performed at 47°C for 30 min in a reaction volume of 25 µl in the presence of 2 µg of total cellular RNA mixed with 0.1 ng of the control competitor RNA and 10 pmol of the 3′ primer (5′TTGTCCGGAAGCACGGTCGGA3′), which is complementary to IGF-II mRNA.

One tenth or 2 µl of the cDNA obtained by RT reaction was incubated in the presence of 0.63 units of Takara Taq (Fischer Scientific, Pittsburgh, Pennsylvania) in 25 µl of 10 mM Tris-HCl, pH 7.5, containing 0.2 mM of each dNTP, 2.5 pmol each of ^{32}P-labelled and unlabelled 5′ primer (5′CAATGGGAATCCCAATGGGGAA3′) and 5 pmol of the 3′ primer, 50 mM KCl, 1.5 mM $MgCl_2$ and 0.1% Triton-X-100. Reaction mixtures were placed in a DNA thermal cycler at 94°C for 2 min, 25 cycles at 94°C for 1 min, 60°C for 1 min, and 72°C for 1 min, followed by 72°C for 10 min. The PCR-amplified products were analysed by electrophoresis in a 3.5% polyacrylamide gel in Tris-borate-EDTA (TBE) buffer in the absence or presence of 8 M urea. Regular size gels (15 × 12 cm) as well as mini gels (8 × 6 cm) were used. After electrophoresis, the gel was dried on Whatman 3 MM paper. The PCR products were visualized and quantitated using a PhosphorImager (Molecular Dynamics Inc., Sunnyvale, CA). Pixel volumes were calculated using Image Quant Software.

For normalization of various RNA samples, β-actin content in each sample was measured by RT-PCR. PCR conditions used for β-actin measurement were the same as above, with the exception of the use of 1/20 of cDNA, 0.4 µM PCR primers (Actin5′, 5′-TCATCACCATTGGCAATGAG-3′; Actin3′, 5′-CACTGTGTTGGCGTACAGGT-3′), and a thermocycle program of 94°C for 2 min, 27 cycles of 94°C for 1 min, 58°C for 1 min, 72°C for 1 min, and then at 72°C for 10 min. Alternatively, 28S RNA content in total RNA was measured for normalization of the samples. Briefly, RNA samples were run on 2.2 M formaldehyde agarose gel and stained with ethidium bromide (0.5 µg/ml). Intensity of the bands was quantitated by AlphaImager 2000 (Alpha Innotech Co., San Leandro, CA).

RESULTS AND DISCUSSION

Determination of optimal conditions for RT-PCR

The competitor IGF-II RNA prepared by *in vitro* transcription was used to determine optimum PCR conditions for quantitation of IGF-II mRNA. Linearity of the PCR products was observed up until 28 PCR cycles under the conditions used (Fig. 3a). The results shown in Fig. 3b indicate that 0.01 to 100 ng of IGF-II RNA per assay is in the optimum range for this assay. The optimum ratio of the competitor and authentic IGF-II RNA was next determined by employing RT-PCR on sets of different ratios (from 20 to 0.05). A typical result is summarized in Fig. 4, which clearly indicates that 10-fold differences in the ratio still result in quantitative measurements. It should be noted that the one-to-one mixture did not give an expected result. When control IGF-II and authentic IGF-II were each subjected to RT-PCR (Fig. 4A lane 11 and 12, respectively), PCR of the latter resulted in only marginally more products than those

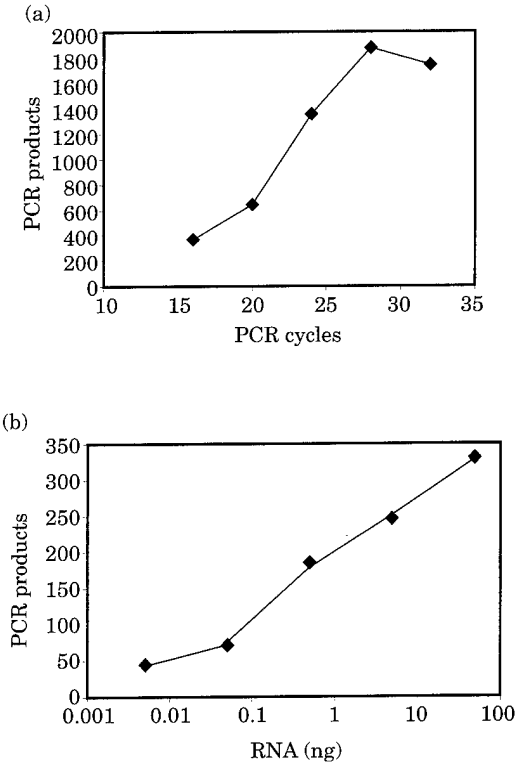

Fig. 3 Optimal conditions for RT-PCR. (a) Determination of optimal PCR cycles. (b) Optimal range of IGF-II RNA amounts for the assay.

(a)

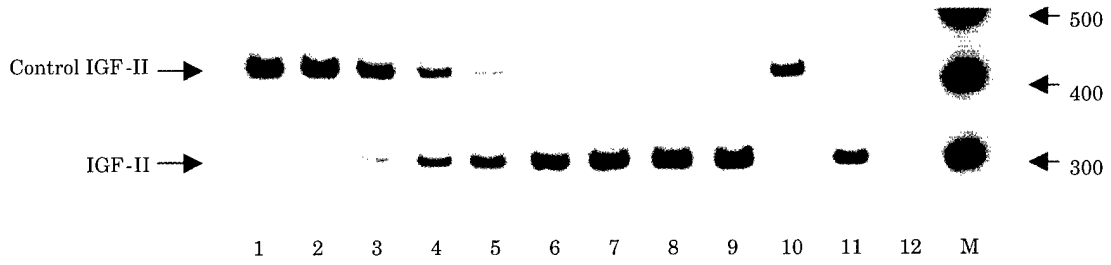

(b)

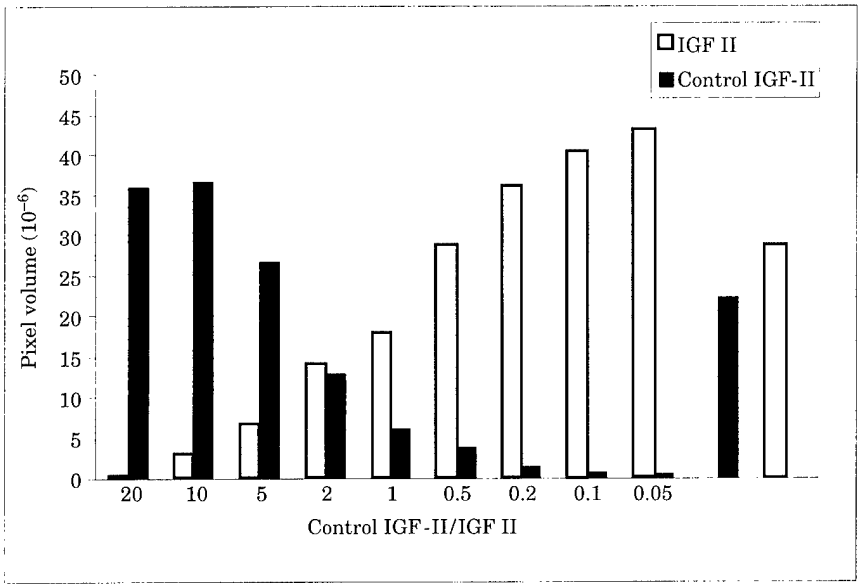

Lane in Fig. 4A	Theoretical values: RNA added, Control IGF-II (C) ng	Theoretical values: RNA added, IGF II	Theoretical values: Ratio, C/IGF II	Observed values: Pixel volume $\times 10^{-6}$, Control IGF°II	Observed values: Pixel volume $\times 10^{-6}$, IGF II	Observed values: Ratio, C/IGF II
1	2.0	0.1	20	35.81	0.51	70.566
2	1.0	0.1	10	36.56	2.71	13.502
3	1.0	0.2	5	26.52	6.54	4.057
4	0.2	0.1	2	12.89	13.98	0.922
5	0.1	0.1	1	6.16	17.63	0.349
6	0.1	0.2	0.5	3.63	28.45	0.128
7	0.2	1.0	0.2	1.35	35.72	0.038
8	0.1	1.0	0.1	0.69	40.32	0.017
9	0.1	2.0	0.05	0.54	43.06	0.012
10	0.1	0		22.10	28.43	
11	0	0.1				

Fig. 4 Determination of optimal control IGF-II/authentic IGF-II ratios. The optimum ratio of the competitor and authentic IGF-II RNA was determined by employing RT-PCR on sets of different ratios of the competitor IGF-II RNA and IGF-II RNA, from the ratio of 20 to 0.05. (a) PhosphoImage of a polyacrylamide gel. Lanes 1–9 contained the control IGF-II/IGF-II ratios of 20 to 0.05 whereas lanes 10–12 contained control IGF-II alone, authentic IGF-II alone, and water, respectively. Lane M contained marker DNAs. (b) Quantitation of radioactivity in (a) and comparison of theoretical and observed values. The results shown in figures are summarized in a table by comparing theoretical values and observed values.

derived from the former. When equal amounts of control IGF-II and authentic IGF-II were mixed and subjected to PT-PCR, however, the product from authentic IGF-II was about twice that derived from control competitor IGF-II (Fig. 4a lane 5). A similar two-fold shift was often observed in several independent experiments, which suggests that this may be the limitation of this assay. It is plausible that the lower yield of PCR products from the competitor IGF-II RNA template as compared to that of the authentic IGF-II RNA template is due to the greater length of competitor RNA. Within the same set of experiments, however, excellent reproducibility was achieved.

Quantitation of IGF-II mRNA in cells and tissues

Based on the above results, total cellular RNA was used to measure IGF-II mRNA content. Aliquots of 0.05, 0.1, 0.5, and 1 ng of control competitor IGF-II RNA were added to 2 μg of total RNA isolated from tissues, and subjected to RT-PCR. Fig. 5 shows the results of competitive RT-PCR using total RNA isolated from prostate cancer PC-3 cells. The same sets of control competitor RNA, 0.05–1 ng, as above were mixed with either 1 μg or 0.2 μg of total PC-3 cell RNA, and subjected to RT-PCR. Fig. 5a, lanes 5–8 clearly show that all four measurements in the

(a)

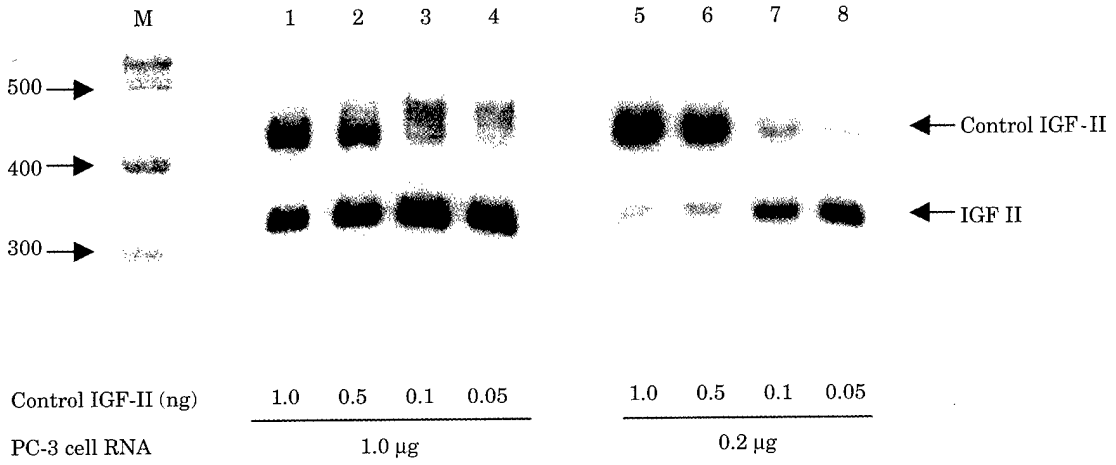

(b)

Fig. 5A Lane	Control IGF-II added in tube (ng)	Quantitation of PhosphoImage (Pixel volume)			IGF-II content	
		Control IGF-II (I)	Endogenous IGF-II (II)	II/I	Control IGF-II (ng) x II/I	Average ± SD (n)
PC-3 RNA 1 μg						
1	1.00	992216	790177	0.79	0.79*	*0.81 ± 0.02 (2)
2	0.50	740882	1228151	1.65	0.83*	
3	0.10	485264	2109714	4.34	0.43	
4	0.05	349806	1840048	5.26	0.26	
PC-3 RNA 0.2 μg						
5	1.00	2388486	415309	0.17	0.17*	*0.16 ± 0.02 (4)
6	0.50	2147058	558852	0.26	0.13*	
7	0.10	691357	1104195	1.59	0.16*	
8	0.05	417005	1406912	3.37	0.17*	

Fig. 5 Quantitative RT-PCR with cellular RNA prepared from prostate cancer PC-3 cells. Aliquots of 0.05, 0.1, 0.5, and 1 ng of control competitor IGF-II RNA were mixed with either 1 μg or 0.2 μg of total PC-3 cellular RNA, and subjected to RT-PCR. In (a), lanes 5–8 clearly show that all four measurements in the 0.2 μg group are in the optimum range, which provided an average of 0.16 ng ± 0.02 (n=4) (b). In contrast, two out of four measurements were not in the range for the 1 μg group as seen in (a) & (b) lanes 3 and 4. This deviation can be detected from the appearance of a smear in the control IGF-II in (a) lanes 3 and 4, which obviously contributed to the inaccuracy of measurements. Lane M shows marker DNAs.

0.2 μg group were in the optimum range, which provided an average of 0.16 ng ± 0.02 (n=4). In contrast, two out of four measurements were not in the range for the 1 μg group as seen in Fig. 5a & b lanes 3 and 4. This deviation can be predicted from a broad appearance of the control IGF-II band, which obviously contributed to the inaccuracy of measurements. The estimates from two assays (1.0 and 0.5 ng of control IGF-II) revealed the IGF-II mRNA content of 0.81 ng in 1 μg RNA, which is 5.1 times the value obtained from the 0.2 μg RNA group, indicating that the values nearly matched with the expected difference, five times. These results suggest that our new competitive RT-PCR assay is applicable to the measurement of IGF-II mRNA amounts in cellular RNA.

Endogenous IGF-II mRNA levels in PC-3 cells, and IGF-II ribozyme-expressing PC-3 cells

The competitive RT-PCR assay was carried out to measure IGF-II mRNA levels in parental and ribozyme(R)- or vector(V)-transfected PC-3 cells (Fig. 6). In this experiment, 0.1 ng of control IGF-II RNA was added to 1 μg of each cellular RNA sample. When endogenous IGF-II levels were quantified and compared with that of parental PC-3 cells, the IGF-II level in IGF-II R-expressing clones was on average reduced to approximately 40% of that in six V-transfectants that do not express the ribozyme. Since ribozyme-cleavage sites are between the PCR primers (see Fig. 1), the reduction of the PCR products in ribozyme-expressing cells indicates the presence of active IGF-II ribozymes.

IGF-II mRNA levels in prostate cancer, BPH, and bladder cancer

The competitive RT-PCR assay was performed, in the presence of four different amounts of control IGF-II (0.05–1 ng) for each sample, to determine IGF-II mRNA contents in 2 μg of total RNA prepared from breast, prostate, and bladder tissues. Unlike cultured cells, however, the quality of RNA prepared from patient tissues is expected to be variable due to the different condition of the tissues. It is therefore necessary to normalize the data by the amount of ubiquitous RNA such as β-actin and 28S RNA in each sample. The normalized values of the results are shown in Fig. 7. Although sample numbers are limited, bladder cancer tissues apparently expressed IGF-II mRNA more abundantly than breast and prostate cancer tissues, which is in agreement with our previous observation[14]. IGF-II expression in breast tissues was generally low except for two cases (N2 and C7). N2 and C7 represent normal and cancerous areas of the breast tissue from one patient with breast cancer, which indicates that this particular breast expresses an unusually high level of IGF-II mRNA. In this case, the IGF-II mRNA level in the cancerous area was lower than that of the benign area. It is interesting to note that IGF-II mRNA levels were similarly high in four out of six breast tissue-derived RNA shown in Fig. 8. (Note that the results obtained in this experiment cannot readily be compared to the results in Fig. 8 because the latter was done using semi-quantitative RT-PCR.) Our recent analysis of IGF-II mRNA levels in T61 tumour, which expresses IGF-II and grows in an IGF-II dependent manner[23], by the multiple competitor method revealed 0.20–0.22 ng IGF-II mRNA. This value is comparable to the high levels seen in one breast cancer patient (N2 and C7).

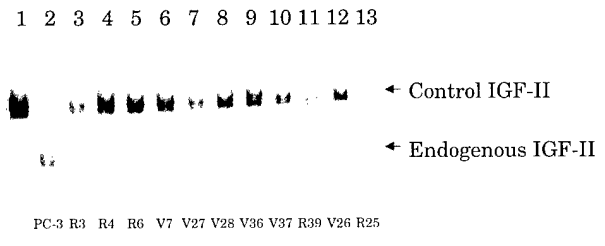

Fig. 6 Determination of endogenous IGF-II mRNA levels in parental and IGF-II ribozyme-expressing PC-3 cells by IGF-II semi-quantitative RT-PCR. One μg of total RNA prepared from parental PC-3 cells (lane 2) or IGF-II ribozyme-(R) or vector-(V) transfectants (lanes 3–13) was subjected to RT-PCR in the presence of 0.1 ng control competitor IGF-II RNA (lanes 3–13) (22). Lane 1 shows a RT-PCR product derived from 0.1 ng control competitor IGF-II RNA alone.

IGF-II mRNA levels in pairs of cancerous and normal areas from breast cancer

IGF-II expression in three pairs of benign and cancerous breast tissues was determined by the competitive RT-PCR in the presence of 0.1 ng of control IGF-II (Fig. 8a). Cellular IGF-II RNA levels were normalized by the amount of 28S RNA in each RNA preparation (Fig. 8b). In cases 2 and 3, much higher expression of IGF-II mRNA was apparent in cancerous breast than benign breast, whereas no significant difference was observed with case 1. The results of four cases are consistent with our previous ISH studies in that an elevated IGF-II mRNA expression was observed in approximately 50% of breast cancer samples examined[14].

In summary, we presented for the first time quantitative data confirming that a subclass of breast cancer samples has elevated levels of IGF-II transcripts by the new competitive RT-PCR assay.

ACKNOWLEDGEMENTS

We thank Dr J. Singer-Sam for helpful suggestions. This work was supported in part by California Breast Cancer

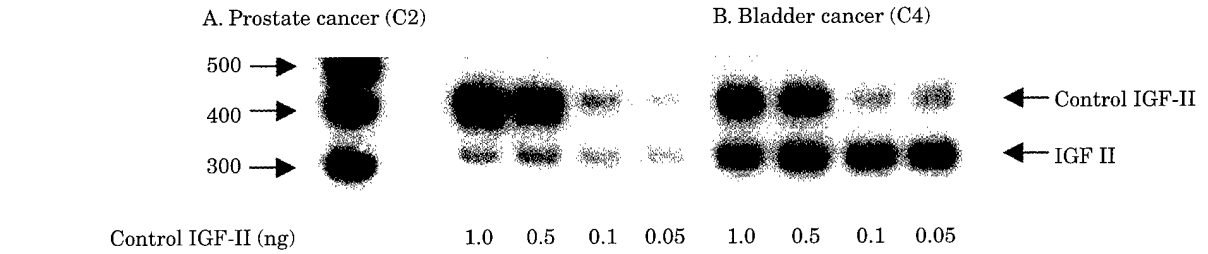

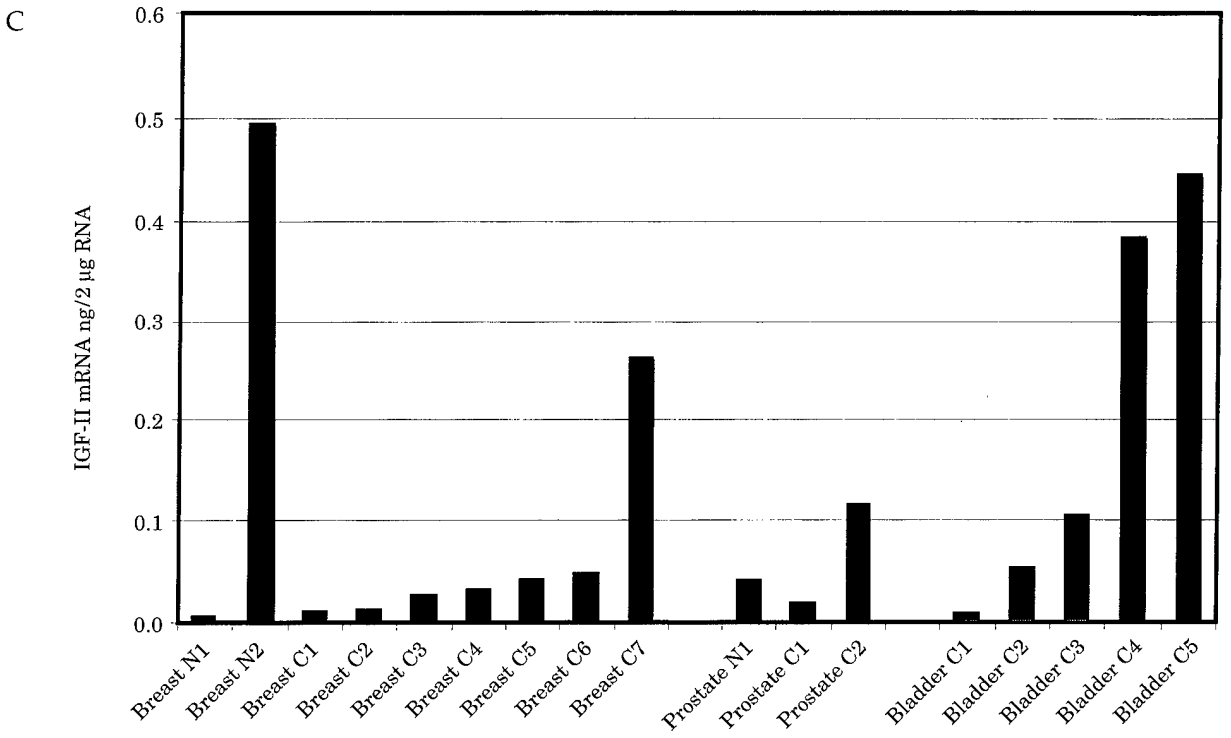

Fig. 7 IGF-II mRNA levels in breast, prostate, and bladder tissues as determined by quantitative RT-PCR. Competitive RT-PCR assay was performed in the presence of four combinations of control IGF-II (0.05–1 ng) for each sample as described in Fig. 5 to determine IGF-II mRNA amounts in 2 µg of total RNA prepared from breast, prostate, and bladder tissues. Two examples are shown in A and B, which correspond to prostate cancer (C2) and bladder cancer (C4), respectively in C. The values are normalized by the β-actin content; that is, by multiplying by a correction factor calculated from [β-actin content in each RNA sample]/[average β-actin content in all the samples].

Research Program (3CB-0186), US Army Prostate Cancer Research Program (DAMD17-98-1-8579), and NIH grant (CA65767). The initial part of this work was included in the PhD dissertation of Loma Linda University graduate school for Zhao-Dong Xu.

REFERENCES

1. Humbel RE. Insulin-like growth factors I and II. Eur J Biochem 1990; 190: 445–462.
2. Osborne CK, Coronado EB, Kitten LJ, Arteaga CI, Fuqua SAW, Ramasharma K, Marshall M, Li CH. Insulin-like growth factor-II

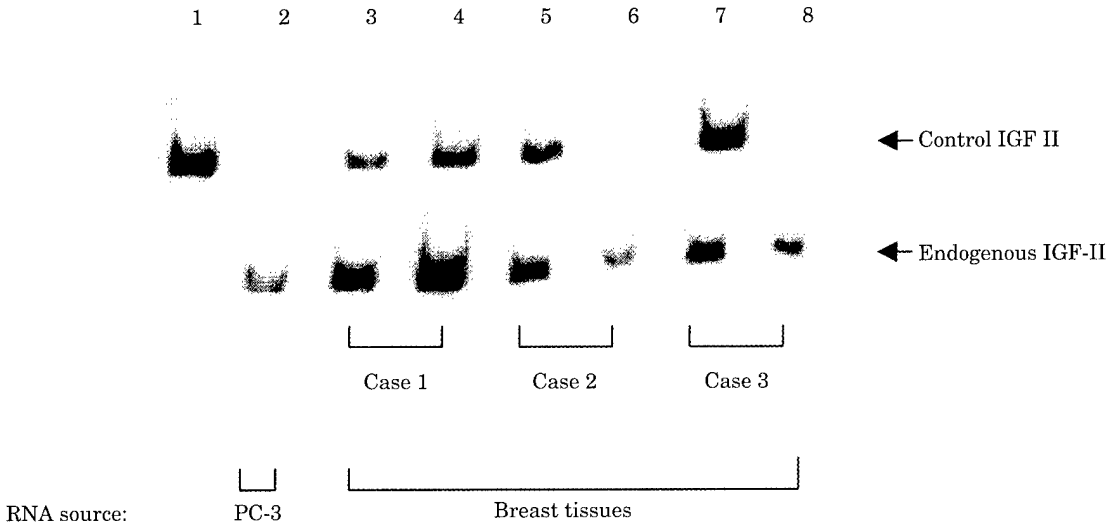

Case	Source of RNA	IGF-II mRNA ng/2 μg RNA observed	Correction factor based on 28S RNA content	IGF-II mRNA ng/2 μg RNA normalized	Ratio of Cancerous/ Benign
1	Benign breast	0.275	0.73	0.38	0.82
	Cancerous	0.396	1.26	0.31	
2	Benign breast	0.131	1.0	0.13	4.23
	Cancerous	0.77	1.4	0.55	
3	Benign breast	0.0416	0.8	0.05	11.6
	Cancerous	0.465	0.8	0.58	

Fig. 8 Determination of endogenous IGF-II mRNA levels in three pairs of benign and cancerous breast tissues by IGF-II semi-quantitative RT-PCR. IGF-II expression in three pairs of benign and cancerous breast tissues was determined by competitive RT-PCR in the presence of 0.1 ng of control IGF-II. Cellular IGF-II RNA levels are normalized by a correction factor calculated from [the amount of 28S RNA in each RNA sample]/[average of 28S RNA content in all six samples].

(IGF-II): a potential autocrine/paracrine growth factor for human breast cancer acting via the IGF-I receptor. Mol Endocrinol 1989; 3: 1701–1709.
3. Daughaday WH, Rotwein P. Insulin-like growth factors 1 and 2, peptide messenger ribonucleic acid, gene structures and serum and tissue concentrations. Endocrinol Rev 1989; 10: 68–91.
4. Perdue JF, LeBon TR, Kato J, Hampton B, Fujita-Yamaguchi Y. Binding specificities and transducing function of the different molecular weight forms of insulin-like growth factor-II (IGF-II) on IGF-I receptors. Endocrinology 1991; 129: 3101–3108.
5. Baserga R. The insulin-like growth factor-I receptor: a key to tumor growth. Cancer Res 1995; 55: 249–252.
6. Daughaday WH. The possible autocrine/paracrine and endocrine roles of insulin-like growth factors of human tumors. Endocrinology 1990; 127: 1–4.
7. Cullen KJ, Lippman ME, Chow D, Hill S, Rosen N, Zwiebel JA. Insulin-like growth factor-II overexpression in MCF-7 cells induces phenotypic changes associated with malignant progression. Mol Endocrinol 1992; 6: 91–100.
8. Christofori G, Naik P, Hanahan D. A second signal supplied by insulin-like growth factor II in oncogene-induced tumorigenesis. Nature 1994; 369: 414–418.
9. Rogler CE, Yang D, Rossetti L, Donohoe J, Alt E, Chang CJ, Rosenfeld R, Neely K, Hintz R. Altered body composition and increased frequency of diverse malignancies in insulin-like growth factor-II transgenic mice. J Biol Chem 1994; 269: 13779–13784.
10. Bates P, Fisher R, Ward A, Richardson L, Hill DJ, Graham CF. Mammary cancer in transgenic mice expressing insulin-like growth factor II (IGF-II). Br J Cancer 1995; 72: 1189–1193.

11. Giani C, Cullen KJ, Campani D, Rasmussen A. IGF-II mRNA and protein are expressed in the stroma of invasive breast cancers: an *in situ* hybridization and immunohistochemistry study. Breast Cancer Res Treat 1996; 41: 43–50.
12. Jarrard DF, Bussemakers MJG, Bova GS, Isaacs WB. Regional loss of imprinting of the insulin-like growth factor II gene occurs in human prostate tissues. Clin Cancer Res 1995; 1: 1471–1478.
13. Tennant MK, Thrasher JB, Twomey PA, Drivdahl RH, Birnbaum RS, Plymate SR. Protein and messenger ribonucleic acid (mRNA) for the Type 1 insulin-like growth factor (IGF) receptor is decreased and IGF-II mRNA is increased in human prostate carcinoma compared to benign prostate epithelium. J Clin Endocrinol Metab 1996; 81: 3774–3782.
14. Li S-L, Goko H, Xu Z-D, Kimura G, Sun Y, Kawachi MH, Wilson TG, Wilczynski S, Fujita-Yamaguchi Y. Expression of insulin-like growth factor (IGF)-II in human prostate, breast, bladder, and paraganglioma tumors. Tissue Cell Res 1998; 291: 469–479.
15. Gilliland DG, Blanchard KL, Levy J, Perrin S, Bunn HF. Clonality in myeloproliferative disorders: analysis by means of the polymerase chain reaction. Proc Natl Acad Sci USA 1991; 88: 6848–6852.
16. Coenen Schimke JM, Ljungqvist OH, Sarkar G, Conover CA, Nair S. A quantitative PCR measurement of messenger RNA expression of IGF-I, IGF-II, and IGFBP-5 in human skeletal muscle. Growth Horm IGF Res 1999; 9: 179–186.
17. Clarke RB, Howell A, Anderson E. Type I insulin-like growth factor receptor gene expression in normal human breast tissue treated with oestrogen and progesterone. Br J Cancer 1997; 75: 251–257.
18. Zenilman ME, Graham W. Insulin-like growth factor I receptor messenger RNA in the colon is unchanged during neoplasia. Cancer Invest 1997; 15: 1–7.
19. Pfaffl M, Meyer HH, Sauerwein H. Quantification of insulin-like growth factor-I (IGF-1) mRNA: development and validation of an internally standardised competitive reverse transcription-polymerase chain reaction. Exp Clin Endocrinol Diabetes 1998; 106: 506–513.
20. Holt RI, Crossey PA, Jones JS, Baker AJ, Portmann B, Miell JP. Gene expression of the insulin-like growth factor system during mouse kidney development. Mol Cell Endocrinol. 1997; 132: 81–91.
21. Dull TJ, Gray A, Hayflick JS, Ullrich A. Insulin-like growth factor II precursor gene organization in relation to insulin gene family. Nature 1984; 310: 777–781.
22. Xu ZD, Oey L, Mohan S, Kawachi MH, Lee NS, Rossi JJ, Fujita-Yamaguchi Y. Hammerhead ribozyme-mediated cleavage of the human insulin-like growth factor-II ribonucleic acid in vitro and in prostate cancer cells. Endocrinology 1999; 140: 2134–2144.
23. Brünner N, Yee D, Kern FG, Spang-Thomsen M, Lippman ME, Cullen KJ. Effect of endocrine therapy on growth of T61 human breast cancer xenografts is directly correlated to a specific down-regulation of insulin-like growth factor II (IGF-II). Eur J Cancer 1993; 29A: 562–569.

Biochemical and Biophysical Research Communications **268,** 886–892 (2000)
doi:10.1006/bbrc.2000.2225, available online at http://www.idealibrary.com on IDEAL®

Promoter Usage for Insulin-like Growth Factor-II in Cancerous and Benign Human Breast, Prostate, and Bladder Tissues, and Confirmation of a 10th Exon

Rossana Mineo,[1] Epifanio Fichera,[1] Shu-Jian Liang, and Yoko Fujita-Yamaguchi
Department of Molecular Biology, Beckman Research Institute of the City of Hope, Duarte, California 91010

Received January 7, 2000

Upregulation of insulin-like growth factor (IGF)-II expression has been reported for a variety of childhood and adulthood tumors. We determined IGF-II gene promoter usage in human cancerous and benign tissues by semiquantitative RT-PCR using P1–P4-specific primers. Although the human IGF-II gene structure is commonly thought to consist of nine exons and four promoters, we detected substantial utilization of a previously reported exon 4b, which is downstream of exon 4. Thus, exon 4b was intensively studied using 4b-specific primers. IGF-II gene promoter usage is highly variable in malignant and benign breast, prostate, and bladder tissues. While a majority of samples utilized P2–P4 promoters in a variety of combinations, when quantitated, P3 and P4 promoters were much more active than P2 promoter. This study not only demonstrated that IGF-II gene promoter usage is highly variable in malignant and benign tissues, but suggested that alternatively spliced exon 4b should be recognized as a 10th exon. © 2000 Academic Press

Insulin-like growth factor (IGF)-II is a single chain polypeptide of 67 amino acid residues, that has amino acid homology with IGF-I and proinsulin (1). Both IGF-I and IGF-II bind to the IGF-I receptor with high affinity, which initiates mitogenic responses in the cell (2–5). Experimental and pathological evidence suggests that IGF-II may act as an autocrine growth factor in the pathogenesis not only of childhood cancers but also of several types of adulthood cancers (2, 6–10). We also reported that over 50% of breast, prostate, and bladder cancers contain malignant cells expressing IGF-II by *in situ* hybridization (ISH) and/or immunohistochemistry (IHC) (11).

Abbreviations used: IGF, insulin-like growth factor; ISH, *in situ* hybridization; IHC, immunohistochemistry; RT-PCR, reverse transcription and polymerase chain reaction; P1–4, promoter 1–4; E, exon; E4b, exon 4b; dNTP, deoxynucleoside triphosphate.

[1] These two authors equally contributed to this work.

IGF-II gene expression is regulated in a complex manner, involving developmentally regulated use of four different promoters (P1–P4) as well as transcriptional repression of the maternal allele due to genomic imprinting (12–17). For example, while only three promoters (P2–P4) are used in fetal liver, in which P3 and P4 promoters are highly active, all four promoters are used from the age of 2 months after birth (13, 15). In adult liver, IGF-II transcription from P1 and P4 are equally active (15). In other tissues, however, P3 and P4 predominate during adult life. Enhanced levels of P3- and P4-driven IGF-II mRNA have been detected in many human tumors of different origin (6). Potential mechanisms for IGF-II upregulation thus far proposed include biallelic expression of IGF-II in tumors with loss of imprinting caused by biallelic activation of P2-P4 (14), and IGF-II overexpression or reexpression from P3 promoter caused by inactivation of wild-type p53 which normally suppresses P3 activity (17).

In order to gain insight into transcriptional regulation of the human IGF-II gene in cancer, we asked whether a specific promoter such as P3 or P4 is preferably used in cancerous tissues or particular types of cancer. Although the human IGF-II gene structure consisting of nine exons is widely accepted (18) and commonly used (13–16), in this study, we detected substantial utilization of previously reported but overlooked exon 4b (19), which is downstream of exon 4.

Qualitative and semiquantitative RT-PCR suggested that IGF-II gene promoter usage is highly variable in malignant and benign breast, prostate, and bladder tissues. While a majority of samples utilized three promoters, P2, P3 and P4, in a variety of combinations, when quantitated, P3 and P4 promoters were much more active than P2. The finding of the exon 4b (E4b) transcript in a significant number of samples; in liver (100%), placenta (100%), cancerous (50%) and benign (50%) breast, bladder cancer (33%) and prostate cancer (17%), indicates that alternative splicing involving this exon generally occurs in human tissues. Thus,

0006-291X/00 $35.00
Copyright © 2000 by Academic Press
All rights of reproduction in any form reserved.

alternatively-spliced exon 4b should be recognized as the 10th exon.

MATERIALS AND METHODS

Tissues and cells. Human cancerous and benign tissues were obtained from the Department of Anatomic Pathology, City of Hope Medical Center. Human prostate PC-3, human breast MCF-7, and MDA-157 cell lines were obtained from American Type Culture Collection (Rockville, MD). PC-3 cells were cultured in RPMI1640 supplemented with 10% fetal calf serum, 2 mM L-glutamine, and 1 mM sodium pyruvate. MCF-7 and MDA-157 cells were cultured in DMEM supplemented with 5% fetal calf serum. Human neuroblastoma cell line, SK-N-AS, which can grow continuously in serum-free medium by autocrine growth stimulation by IGF-II, was kindly provided by Dr. Carol Thiele, Pediatric Branch, NCI, and were grown as described (20).

RNA preparation. Total RNA was prepared from frozen tissues (20–30 mg) or freshly harvested cells (10^7 cells) using TRIzol Reagent (GIBCO BRL, Gaithersburg, MD) according to the manufacturer's protocol.

RT-PCR. cDNA was synthesized by reverse transcription (RT) from 2 μg of total RNA in a final reaction volume of 20 μl. RNA and 150 ng of Random Primers (GIBCO BRL, Gaithersburg, MD) in 10 μl of water were placed in a 0.2 ml tube, incubated at 70°C for 10 min, and then quickly chilled on ice. To this mixture, were added 4 μl of 5× First Strand Buffer, 2 μl of 0.1 M DTT, 2 μl of 10 mM dNTP mix, 200 units of SuperScript II (GIBCO BRL, Gaithersburg, MD), and 40 units of RNasin (Promega, Madison, WI) to final concentrations of 50 mM Tris-HCl, pH 8.3, 75 mM KCl, 3 mM $MgCl_2$, 10 mM DTT, and 1 mM dNTP. The reaction mixture was incubated at 25°C for 10 min, and at 42°C for 50 min. The reaction was then terminated by incubation at 72°C for 15 min.

Polymerase chain reaction (PCR) primers used in this study are listed in Table I. PCR conditions used for P2 and P3 promoter usage analysis were as follows: PCR mixtures (50 μl) consisted of 1× Buffer (Qiagen Inc., Chatsworth, CA), 0.2 mM dNTPs, 0.6 μM 5′- and 3′-primers, 2.5 μl cDNA, and 1.25 units of *Taq* polymerase (Qiagen Inc., Chatsworth, CA). PCR was carried out by a programmable thermocycler (Perkin-Elmer Cetus, Norwalk, CT) using a program; at 94°C for 2 min, 35 cycles of denaturation/annealing/extension (94°C for 1 min, 60°C for 1 min, 72°C for 1 min), and then at 72°C for 10 min. Similar PCR conditions were used for P1, P4, and E4b except that 4 μl cDNA and 1.25 units of Takara Taq (Fischer Scientific, Pittsburgh, PA) were used as well as a different thermocycler program of 94°C for 2 min, 26 cycles of denaturation/annealing/extension (94°C for 30 sec, 60°C for 1 min, 72°C for 45 sec), and then at 72°C for 5 min.

For qualitative analysis, 35 cycles of PCR were performed, then 9 μl of the PCR products were analyzed by 2% agarose gel electrophoresis and staining with 0.00005% ethidium bromide for 20 min.

Preparation of standard DNAs and semi-quantitative PCR for P2, P3, and P4. After completion of the initial qualitative analysis which provided information on the existence of transcripts, it was necessary to quantify the levels of P2, P3, and P4 transcripts in order to further evaluate the IGF-II promoter usage in cancerous and benign tissues. Standard DNAs corresponding to P2, P3, and P4 transcripts were generated by RT-PCR from total RNA isolated from SK-N-AS cells. PCR products were separated by 2% agarose gel electrophoresis, and DNA of interest (P2, P3, and P4) was extracted from the gel slice using QIAquick gel extraction kit (Qiagen Inc., Chatsworth, CA). Concentrations of the purified DNA were determined by measuring the optical density at 260 nm.

For quantitative evaluation of the IGF-II promoter usage in various tissues, PCR was carried out in duplicate as described above, together with two sets of known amounts of DNA corresponding to each promoter. Briefly, 5, 25, and 100 fg of P3 DNA or 5, 25, and 75 fg of P4 DNA, respectively, were used as templates for PCR, which provided a standard curve for each experiment. Five μl of PCR products from sample DNA and standard DNA were run on a 2.5% agarose gel side by side, and stained with ethidium bromide. Intensity of the bands was quantitated by AlphaImager 2000 (Alpha Innotech Co., San Leandro, CA). Promoter usage in each sample was then determined from the standard curve.

TABLE I

List of PCR Primers Used in This Study

5′-P1	5′-CCACTCGCACGGGTAGAGACAGG-3′
5′-P2A	5′-GGCCTCTCTGTCTCCTACGAAGTCC-3′
5′-P2B	5′-GAGACCGAACTCGCGTCTATGCAAG-3′
5′-P3	5′-AAAGTACAACATCTGGCCCGCCC-3′
5′-P4	5′-CCTGTGAAAGAGACTTCCAGCTTCCTC-3′
3′-P1R	5′-GAAACTGCCTGGACGATGATCCG-3′
3′-P2AR	5′-AACGCCCAGTCCGTTGGAAGAC-3′
3′-P2BR	5′-TCGGGGGCCACCACGATAATTTG-3′
3′-E7R	5′-GGCCAAGAAGGTGAGAAGCACC-3′
B1	5′-GAAGTGATTGATGGCGGAAGCGGG-3′
B2	5′-CCTTCCCCTTGGCTAGGCTTAGG-3′
Actin5	5′-TCATCACCATTGGCAATGAG-3′
Actin3	5′-CACTGTGTTGGCGTACAGGT-3′

For normalization of various RNA samples, β-actin content in each sample was measured within a linear range of PCR. PCR conditions used were similar to those used for P2 and P3, with the exceptions of using 0.4 μM of actin primers (Table I) and a thermocycle program of 94°C for 2 min, 27 cycles of 94°C for 1 min, 58°C for 1 min, and 72°C for 1 min, and then at 72°C for 10 min.

Analysis of exon 4b by PCR and DNA sequencing. The presence of exon 4b was examined by PCR amplification using 5′-P2B and 3′E7R primers, which produced one 192 bp band. In addition, 5′-P2A and 3′E7R were used for PCR, which produced two major bands of 562 and 398 bp and one minor ~500 bp band. The 562 and 398 bp bands derived from SK-N-AS cells were isolated and subjected to DNA sequencing. The nucleotide sequences were obtained by dideoxy-mediated chain termination method using 3′-E7R as a primer.

Analysis of exon 4b by primer extension. The 3′-P2BR primer was ^{32}P-labeled by T4 kinase (New England BioLab, Beverly, MA) in the presence of γ-^{32}P ATP (6000Ci/mmol) (NEN, Boston MA), and purified by ethanol precipitation. Annealing was carried out by incubating 15 μl of 10 mM Tris-HCl, pH 8.3, containing 0.15 M KCl, 1 mM EDTA, total RNA (50 or 20 μg prepared from SK-N-AS cells or liver, respectively), and ^{32}P-labeled 3′-P2BP primer at 65°C for 90 min, and by cooling to room temperature. Thirty μl of primer extension buffer solution were added to the annealing mixture to final concentrations of 50 mM Tris-HCl, pH 8.3, 50 mM KCl, 3 mM MgCl, 20 mM DTT, and 0.15 mM dNTPs. Primer extension was performed at 42°C for 60 min in the presence of 200 units of SuperScript II (GIBCO BRL, Gaithersburg, MD). The reaction was terminated by adding 105 μl of RNase reaction mixture containing 10 mM Tris-HCl, pH 8.0, 0.1 M NaCl, 1 mM EDTA, 100 μg/ml salmon sperm DNA, and 20 μg/ml RNase A. After phenol/chloroform extraction and ethanol precipitation, primer-extended products were analyzed by 9% polyacrylamide/7 M urea gel electrophoresis together with 5′ end [γ-^{32}P]ATP labeled 100 bp ladder DNA molecular weight markers.

RESULTS AND DISCUSSION

IGF-II gene promoter usage in human benign and cancerous tissues. Figures 1A and B schematically illustrate the locations of promoters as well as sets of

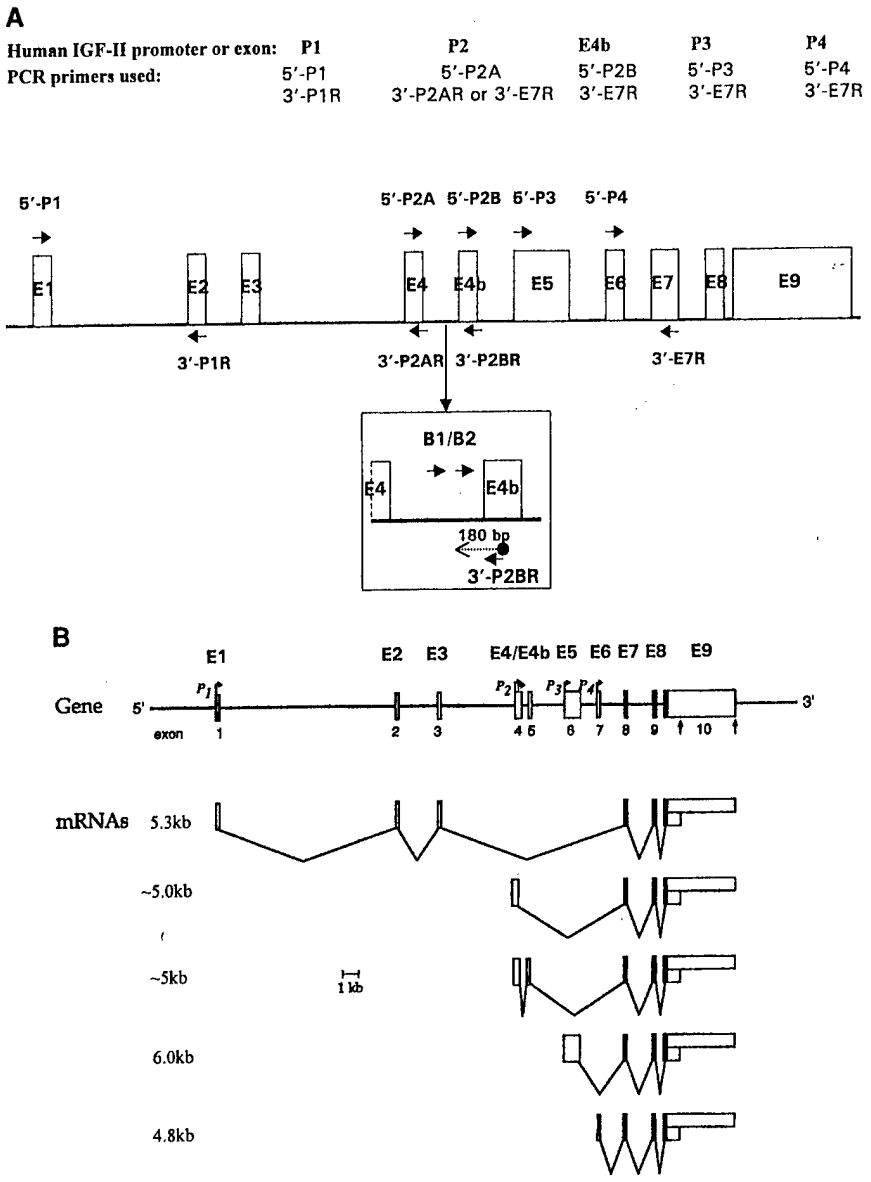

FIG. 1. Human IGF-II gene organization. (A) Sets of PCR primers used for detection of four promoters and exon 4b. Locations of PCR primers in relation to the human IGF-II gene structure are shown. The inset illustrates the details of the exon 4/intron 4/exon 4b region, and the summary of primer extension experiments, from which PCR primers B1 and B2 were chosen. (B) Structure and expression of the human IGF-II gene. A commonly used 9 exon-gene structure is aligned with the 10 exon–gene structure. E4 and E4b described in this study correspond to E4 and E5 in the 10 exon–gene structure (19, 21). Five IGF-II mRNA species are illustrated according to the Rotwein's review (21).

PCR primers used to detect each promoter and exon 4b in the context of the IGF-II gene structure. The results from qualitative analysis are summarized in Table II. Of breast, prostate, bladder, liver, and placenta tissues examined, P1-specific transcript was found only in liver as expected. All other transcripts containing P2, E4b, P3, and P4 were detected in liver and placenta. In cancerous and benign breast, prostate, and bladder tissues, IGF-II gene promoter usage was highly variable. While the majority of samples contained one to three transcripts in a variety of combinations, some samples contained all of P2, E4b, P3, and P4 transcripts but not P1. In breast cancer, P2 and P3 transcripts (77%) were more abundantly found than P4 (58%) transcripts whereas in prostate cancer, P3 (55%), P4 (61%) and P2 (61%) transcripts were equally abundant. At first glance, these results do not appear to support our original hypothesis that certain promoters may be preferably used in cancerous tissues or in a cancer-specific manner. P2 appears to be used in cancer cell lines such as PC-3 and MDA-157 whereas all promoters but P1 were detected in the transcripts from SK-N-AS cells. SK-N-AS cells were thus used to prepare P2-P4 specific DNA for standard curves.

TABLE II

Human IGF-II Gene Promoter Usage in Cancerous and Benign Tissues

Tissues and cell lines	IGF-II promoter usage					Tissues examined
	P1	P2	E4b*	P3	P4	
Breast: Cancer	0/12	10/13	8/13	10/13	8/13	13
Breast: Benign	0/3	4/4	2/4	2/4	4/4	4
Prostate: Cancer	0/7	11/18	3/18	10/18	11/18	18
Prostate: Benign	0/3	4/7	0/7	3/7	5/7	7
Bladder: Cancer	0/6	5/6	2/6	5/6	6/6	6
Bladder: Benign	0/2	2/2	1/2	2/2	2/2	2
Liver	2/2	2/2	2/2	2/2	2/2	2
Placenta	0/2	2/2	2/2	2/2	2/2	2
SK-N-AS	−	+	+	+	+	
PC-3	−	+	−	−	−	
MCF-7	−	−	−	−	−	
MDA-157	−	+	±	−	±	
kb mRNA** (Fig. 1B)	5.3	~5.0	~5	6.0	4.8	

Note. Promoter usage and alternative splicing were qualitatively determined. Promoter usage is expressed as a number of the positive samples (>+)/a number of samples examined. For each cell line, promoter usage is expressed as yes (+) or no (±).

* Alternative splicing.

** Five IGF-II mRNA species are shown in Fig. 1B.

Since cancerous breast or prostate tissues do not contain an homogenous population of cancerous cells, but also contain benign cells as well, differences in IGF-II gene promoter usage between benign and cancerous tissues, if any, depend on the proportion of cancerous cells in total tissues used. This is obviously the major disadvantage of this approach when compared to ISH or IHC. In addition, we have to take into consideration the fact that one half of the cancerous tissues may not express significantly higher levels of IGF-II mRNA than benign tissue (11). Of four, five, and two sets of benign and cancerous areas from the same breast, prostate, and bladder tissues, respectively, analyzed, the promoter usage differences between benign and cancerous tissues were not apparent.

Since the above-mentioned qualitative analysis did not provide us with information on cancer-specific IGF-II gene promoter activation, quantitative analysis was next carried out. P2 promoter usage was below detection levels for all the samples tested except SK-N-AS cells which was ~5 fg/1 μg RNA. P3 and P4 promoter usage was determined from respective standard curves within linear ranges as shown in Fig. 2, which ranged from 0.4–800 and 0.5–19 fg/1 μg RNA, respectively. P3 and P4 promoter usage in breast, prostate, bladder, liver, placenta, and SK-N-AS cells, which was normalized using β-actin content, is shown in Fig. 3. This demonstrates that P3 usage levels generally are higher than P4 usage levels. Of five cases of benign and cancerous areas of the same breast examined, an increase in IGF-II promoter activity in the cancerous area was observed in three cases (Fig. 3A). Cases 2 and 4 clearly show upregulation of P3 and P4 promoter usage in cancerous tissues, respectively. P3 usage in the cancerous area in case 5 appears to be

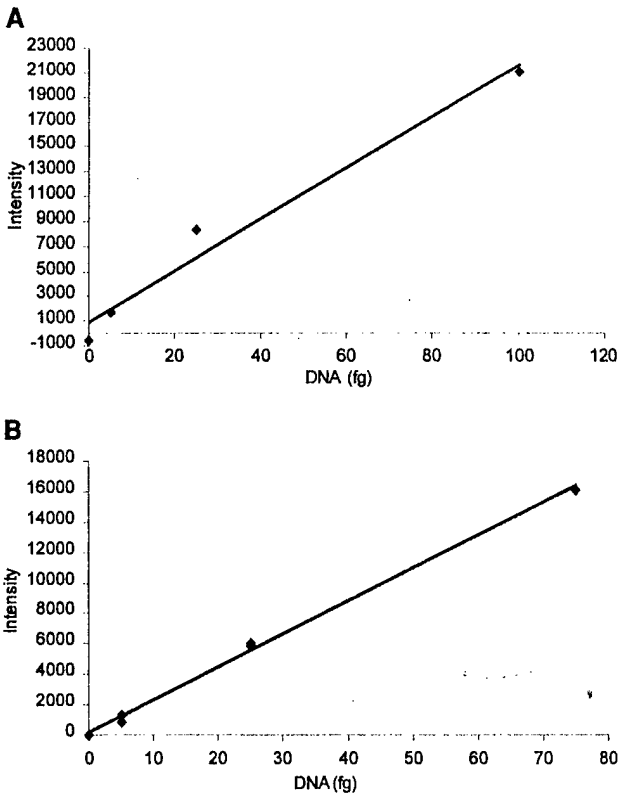

FIG. 2. Standard curves for P3 (A) and P4 (B) promoters. For quantitative evaluation of the IGF-II promoter usage in various tissues, PCR was carried out in duplicate together with two sets of known amounts of DNA corresponding to each promoter. Briefly, 5, 25, and 100 fg of P3 DNA or 5, 25, and 75 fg of P4 DNA, respectively, were used as templates for PCR, which provided a standard curve for each experiment. Shown are typical examples of the standard curves.

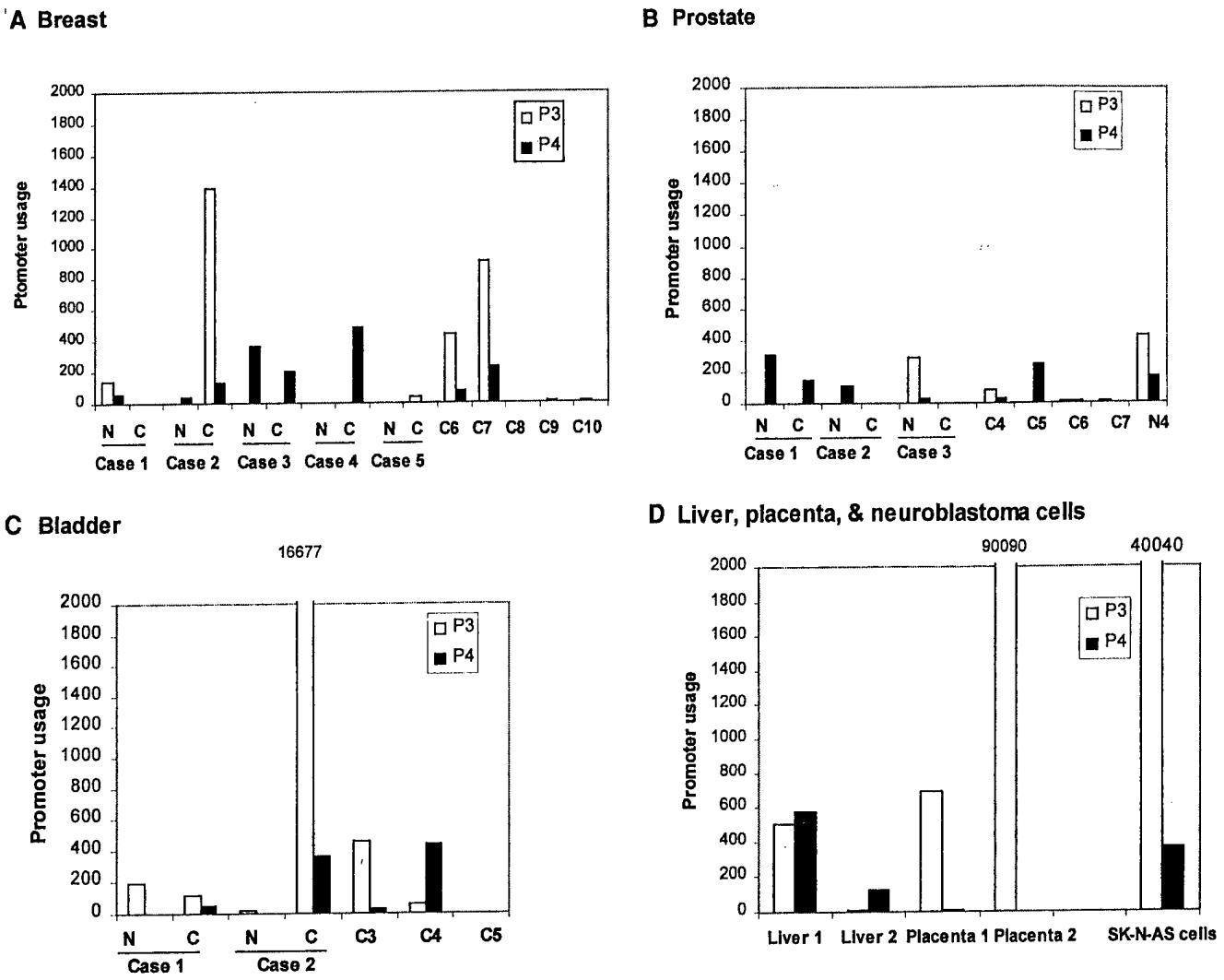

FIG. 3. Qualitative analysis of P3 and P4 promoter usage in human breast (A), prostate (B), bladder (C), liver, placenta, and a cancer cell line (D). Promoter usage is expressed as an arbitrary number calculated by fg/μg RNA/β-actin content in density. Cases 1–5 represent pairs of cancerous (C) and benign (N) tissues from the same patient, whereas the rest of the samples did not have matching paired tissues. Two independent liver or placenta tissues and neuroblastoma cancer cell line, SK-N-AS, were also analyzed. The levels of promoter usage are shown in numbers for three samples (bladder C2, placenta 2, and SK-N-AS cells), which contained exceedingly high concentrations of P3 promoter transcript.

higher than that of the benign area although the expression level is marginal. The other two cases revealed the opposite results. These results are consistent with our previous observation that IGF-II is upregulated in >50% of breast cancer (11). In cases of prostate cancer (Fig. 3B), we did not find upregulation of promoter usage in three cases examined. In bladder cancer (Fig. 3C); however, one of two cases examined (case 2) showed super upregulation of P3 promoter as well as significant up-regulation of P4 promoter in the cancerous area as compared to the benign area. It is interesting to see that the promoter usage which is the reflection of IGF-II mRNA expression was highly variable between two independent liver or placenta samples (Fig. 3D). In placenta 2, P3 usage was the highest level among all the samples examined. In SK-N-AS cells, which express high levels of IGF-II, P3 transcript was found to be ~100 times more abundant than P4 transcript (Fig. 3D). Thus, IGF-II promoter usage in this cell line is P3 $\gg$ P4 > P2.

In summary, IGF-II promoter usage is highly variable in cancerous as well as benign tissues. Semiquantitative analysis, however, revealed that P3 and/or P4 promoter usage are increased in cancerous areas more than benign areas in three of five paired breast tissues and one of two paired bladder tissues examined.

Confirmation of exon 4b as a 10th exon of the human IGF-II gene. Utilization of exon 4b was confirmed by PCR amplification using 5′-P2B and 3′E7R primers, which produced a 192 bp DNA. The E4b transcript was

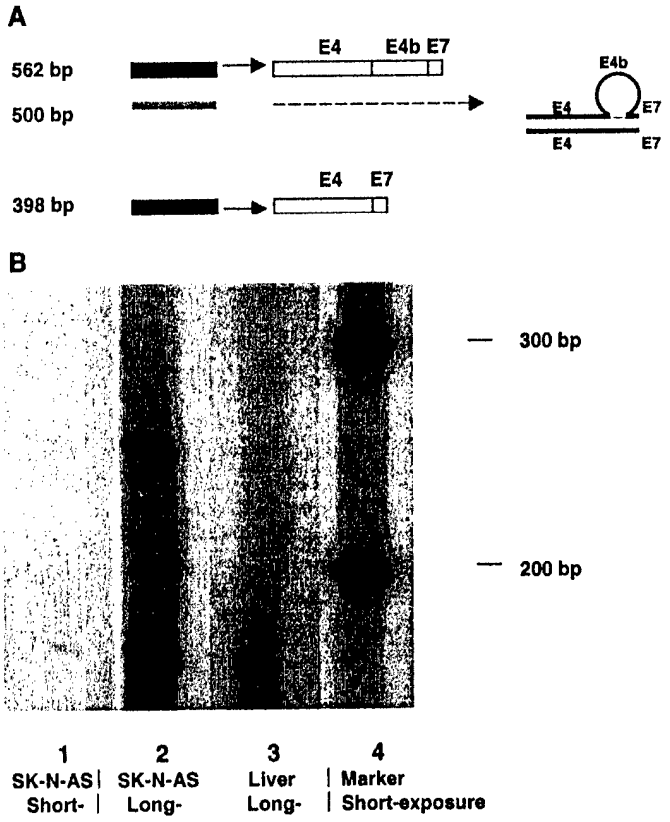

FIG. 4. Alternative splicing involving exon 4b and primer extension from Exon 4b to intron 4. (A) Schematic presentation of three PCR products primed by sets of 5′-P2A, and 3′-E7R. Two major bands with 562 and 398 bp were excised and sequenced, which revealed their sequences of Exon 4–Exon 4b–Exon 7 and Exon 4–Exon 7, respectively. The 500 bp minor band is likely to be a heteroduplex as illustrated. (B) Primer extension. Reverse transcription of SK-N-AS RNA and liver RNA priming with ^{32}P-labeled 3′P2BR resulted in discrete 180 and 250 bp product (lanes 1 and 2) and a 180 bp product (lane 3), respectively. Autoradiograms exposed for 16 hr without intensifying screens (short-exposure; lanes 1 and 4) or for 3 days with 2 intensifying screens (long-exposure; lanes 2 and 3) are shown.

found in a significant number of samples; in liver (100%), placenta (100%), cancerous (50%) and benign (50%) breast, bladder cancer (33%) and prostate cancer (17%) (Table II), indicating that alternative splicing involving this exon generally occurs in human tissues. The finding that exon 4b is alternatively spliced is also supported by the observation that the products generated by PCR using 5′-P2A and 3′E7R from many cDNA samples produced two major bands of 562 and 398 bp and one minor 500 bp band as illustrated in Fig. 4A. The 562 and 398 bp bands derived from SK-N-AS RNA were isolated and subjected to DNA sequencing, which revealed that they consisted of E4-E4b-E7 and E4-E7, respectively (Fig. 4A). This certainly confirmed that exon 4b is alternatively spliced. It should be noted that there is not even one case among the tissues examined that the E4b transcript was present in the absence of P2 transcript. This strongly suggested that transcription of exon 4b is under the control of P2 promoter. The presence of this exon was reported earlier by Ikejiri *et al.* (19). It has not been recognized, however, because it was considered to be a unique event in a human histocytoma cell line. Instead of 10 exons, the 9 exon–gene structure is usually used in studies concerning IGF-II gene regulation (13–16). In the recent review, Rotwein presented the 10 exon–gene structure which was used to draw Fig. 1B (21).

We, however, obtained three lines of experimental evidence to support that the "intron 4" region approximately 100 bp upstream of IGF2 exon 4b is transcribed, implying the presence of transcriptional initiation sites proceeding exon 4b. First, primer extension starting from exon 4b resulted in a ~180 bp product which was detected in total RNA prepared from SK-N-AS cells and liver, and a ~260 bp product which was a minor band and only detected in the former (Fig. 4B). If all the E4b transcripts are the products of P2 promoter as the result of alternative splicing, the expected size for primer extension products would be >446 bp. Thus, the result of primer extension experiments shows that transcriptional start sites may exist in intron 4 between exon 4 and 4b. Second, using total RNA prepared from SK-N-AS cells, RT-PCR with two sets of primers, B2 & 3′-E7R and B2 & 3′-P2BR, resulted in PCR products of expected sizes (338 and 158 bp, respectively). As shown in Fig. 1A, inset, the primer B2 is located 124 bp upstream of exon 4b in the intron 4 region. Since the 3′-E7R is located in exon 7, it is not likely that the PCR product is transcribed from either genomic DNA or unprocessed mRNA. Third, when 5′ primer B1, which is located 180 bp upstream of exon 4b, was used in place of B2, PCR did not result in any products. Again, if genomic DNA or unprocessed mRNA contamination are responsible for those products, PCR with 5′primer B1 and 3′primer 3′-E7R or 3′P2BR should have produced corresponding DNAs. Furthermore, the same results as the second and third lines of evidence were obtained when RT-PCR was performed on poly(A)$^+$ RNA isolated from SK-N-AS RNA in the presence of either B2 or B1 with both 3′ primers. This again confirmed that the E4b transcript is one of the components of mRNA. Finally, of 16 cancerous and benign tissues, two livers, one placenta, and PC-3 and MDA-157 cells examined, we did not find any other tissues or cells from which PCR with B2 & 3′-E7R primers yielded a 338 bp product. It can be thus concluded that the transcript with the intron 4 sequence proceeding exon 4b found in SK-N-AS cells is rarely present in other tissues.

In conclusion, the present study shows that IGF-II gene promoter usage is highly variable in malignant and benign breast, prostate, and bladder tissues. When quantitated, P3 and P4 promoters are much more active than P2 promoter. It was not possible to determine

specific promoter usage associated with breast, prostate, or bladder cancer. The finding of the E4b transcript in a significant number of samples indicates that alternative splicing involving this exon generally occurs in human tissues. Thus, alternatively-spliced exon 4b should be recognized as the 10th exon.

ACKNOWLEDGMENTS

We thank Dr. Elly Holthuizen, University of Utrecht, for providing us with genomic clones encoding exon 1 and 2, and for invaluable discussions. Drs. Sharon Wilczynski and Yansu Sun for providing us with tissues and pathological analysis. This work was supported in part by California Breast Cancer Research Program (3CB-0186), US Army Prostate Cancer Research Program (DAMD17-98-1-8579), and NIH Grant (CA65767).

REFERENCES

1. Humbel, R. E. (1990) *Eur. J. Biochem.* **190,** 445–462.
2. Osborne, C. K., Coronado, E. B., Kitten, L. J., Arteaga, C. I., Fuqua, S. A. W., Ramasharma, K., Marshall, M., and Li, C. H. (1989) *Mol. Endocrinol.* **3,** 1701–1709.
3. Daughaday, W. H., and Rotwein, P. (1989) *Endocrinol. Rev.* **10,** 68–91.
4. Perdue, J. F., LeBon, T. R., Kato, J., Hampton, B., and Fujita-Yamaguchi, Y. (1991) *Endocrinology* **129,** 3101–3108.
5. Baserga, R. (1995) *Cancer Res.* **55,** 249–252.
6. Daughaday, W. H. (1990) *Endocrinology* **127,** 1–4.
7. Cullen, K. J., Lippman, M. E., Chow, D., Hill, S., Rosen, N., and Zwiebel, J. A. (1992) *Mol. Endocrinol.* **6,** 91–100.
8. Christofori, G., Naik, P., and Hanahan, D. (1994) *Nature* **369,** 414–418.
9. Rogler, C. E., Yang, D., Rossetti, L., Donohoe, J., Alt, E., Chang, C. J., Rosenfeld, R., Neely, K., and Hintz, R. (1994) *J. Biol. Chem.* **269,** 13779–13784.
10. Bates, P., Fisher, R., Ward, A., Richardson, L., Hill, D. J., and Graham, C. F. (1995) *Br. J. Cancer* **72,** 1189–1193.
11. Li, S.-L., Goko, H., Xu, Z.-D., Kimura, G., Sun, Y., Kawachi, M. H., Wilson, T. G., Wilczynski, S., Fujita-Yamaguchi, Y. (1998) *Tissue Cell Res.* **291,** 469–479.
12. Drummond, I. A., Madden, S. L., Rohwer-Nutter, P., Bell, G. I., Sukhatme, V. P., and Rauscher, F. J., III (1992) *Science* **257,** 674–678.
13. van Dijik, M. A., van Schaik, F. M. A., Bootsma, H. J., Holthuizen, P., and Sussenbach, J. S. (1991) *Mol. Cell. Endo.* **81,** 81–94.
14. Vu, T. H., and Hoffman, A. R. (1996) *J. Biol. Chem.* **271,** 9014–9023.
15. Li, X., Cui, H., Sandstedt, B., Nordlinder, H., Larsson, E., and Ekstroem, T. J. (1996) *J. Endocrinol.* **149,** 117–124.
16. Wu, H.-K., Squire, J. A., Catzavelos, C. G., and Weksberg, R. (1997) *Biochem. Biophys. Res. Commun.* **235,** 123–129.
17. Zhang, L., Kashanchi, F., Zhan, Q., Zhan, S., Brady, J. N., Fornace, A. J., Seth, P., and Helman, L. J. (1996) *Cancer Res.* **56,** 1367–1373.
18. Holthuizen, E., LeRoith, D., Lund, P. K., Roberts, C. T., Jr., Rotwein, P., Spencer, E. M., and Sussenbach, J. S. (1991) *in* Modern Concepts of Insulin-like Growth Factors (Spencer, E. M., Ed.), pp. 733–336, Elsevier Science Publishing Co., New York, NY.
19. Ikejiri, K., Wasada, T., Haruki, K., Hizuka, N., Hirata, Y., and Yamamoto, M. (1991) *Biochem. J.* **280,** 439–444.
20. El-Badry, O. M., Helman, L. J., Chatten, J., Steinberg, S. M., Evans, A. E., and Israel, M. A. (1991) *J. Clin. Invest.* **87,** 648–657.
21. Rotwein, P. S. (1999) *in* The IGF System: Molecular Biology, Physiology, and Clinical Applications (Rosenfeld, R. G., and Roberts, C. T., Eds.), pp. 19–35, Humana Press, Totowa, NJ.

Best Available Copy
Per PI

Fig. 1

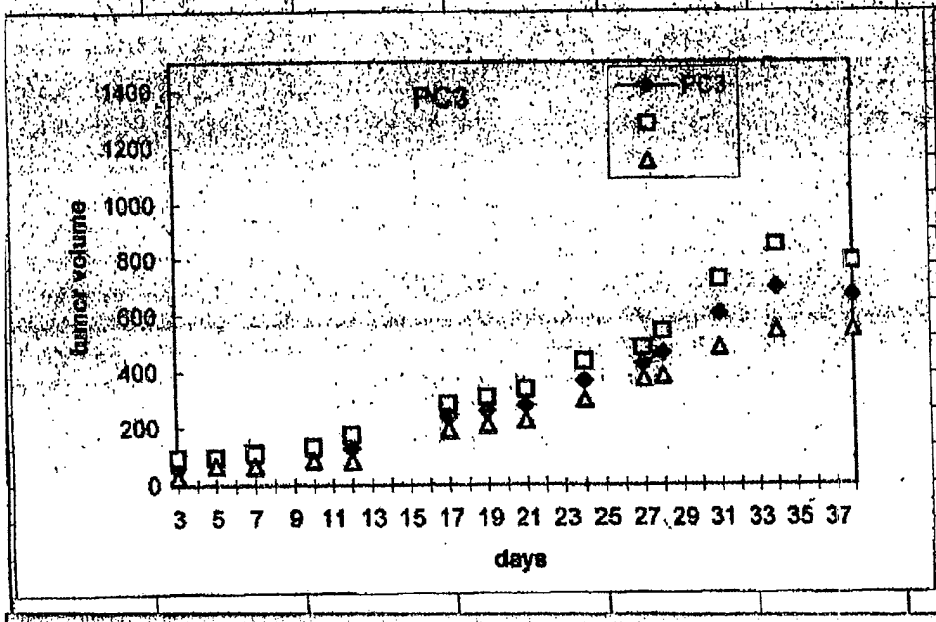

Fig. 2

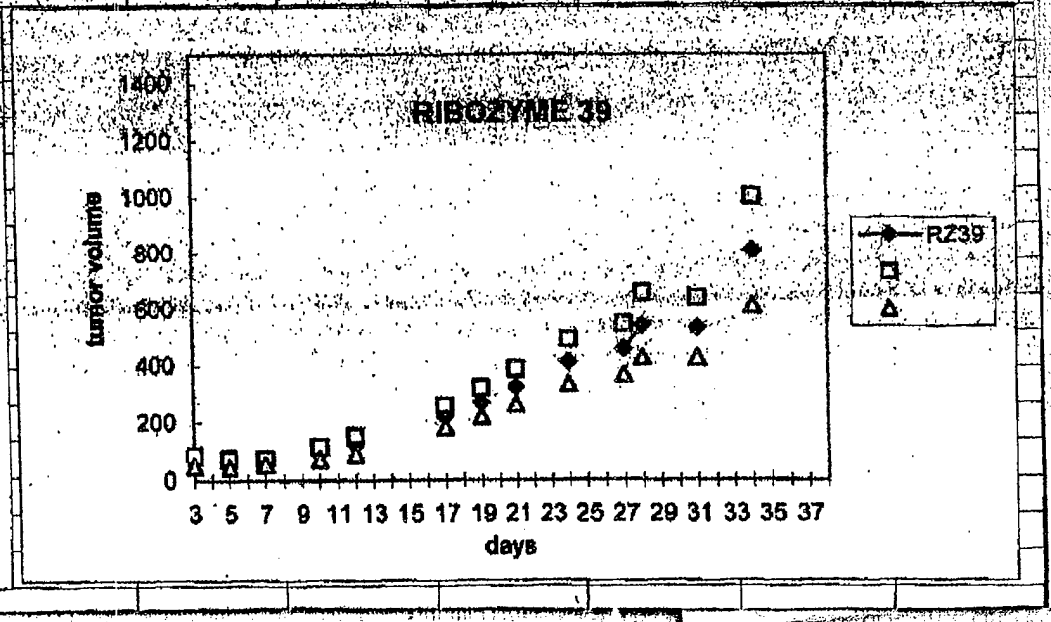

APPENDIX 6

Email received from Robert Sikes to Yoko Fujita-Yamaguchi
Dated Monday, August 28, 2000

From: Robert Sikes <rs3d@virginia.edu> Save Address Block Sender
To: Yoko Fujita-Yamaguchi : Save Address
Subject: retroviruses
Date: Mon, 28 Aug 2000 16:30:38 -0400

Reply Reply All Forward Delete

Dear Yoko,

The selection is over, let the games begin! The following cell lines have been transduced with sk-3b2 and pBABE backbone and selected in Puromycin: LNCaP, C4-2, PC-3, PC-3M, Du145, P69. These represent two lineage-derived sets of cells with increasing malignant potential and a relatively benign cell line P69. We are currently in the process of freezing stocks and characterizing receptor expression and presentation.

Chia-Ling Maieh (recently appointed research instructor) was ultimately responsible for the successful transduction. In an effort coordinated with Meg Shea (my tech.) the cells were transduced with fresh retroviral supernatants. This has taken a little longer than anticipated because I thought we were having a packaging cell line problem. This is still an issue since the efficiency from pa317 packaging line was only about 30% and not the 90% + that we saw with the HER2 construct from AM12. AM12 is not useable due to mycoplasma contamination that seems to be universal (every lab I know has this problem) and hard to remove.

I hope your move is or will go well.

Best wishes
Robert

Robert A. Sikes, Ph.D.
Assistant Professor
University of Virginia Health System
Molecular Urology and Therapeutics Program
Dept. of Urology, Box 800422
Charlottesville VA 22908-0422
804-243-6647/6935 office/lab
804-243-6648 (fax)

Best Available Copy
Per PI